

https://dspace.org/

Adapting the staphylococcus aureus CRISPR/Cas9 gene editing system to target hepatitis B virus

Sibiya, Bongiwe

2020

https://hdl.handle.net/10539/29993

Downloaded from a DSpace repository. https://dspace.org/

Adapting the *Staphylococcus aureus* CRISPR/Cas9 gene editing system to target hepatitis B virus

Bongiwe Sibiya

A dissertation submitted to the Faculty of Health Sciences, University of the Witwatersrand, in fulfilment of the requirements for the degree of

Master of Science in Medicine

Johannesburg, 2020

DECLARATION

I, Bongiwe Sibiya (Student number: 715813) declare that this Dissertation is my own work. It is being submitted for the Degree of Master of Science in Medicine at the University of the Witwatersrand, Johannesburg. It has not been submitted before for any degree or examination at this or any other University.



..…… ……23/06/20202……

Signature Date

DEDICATION

This work is dedicated to my mom and my sisters. Thank you for your continuous love and support. I also dedicate this work to the memory of my dearly departed grandmother who never forgot my dreams and aspirations.

PUBLICATIONS AND PRESENTATIONS

Poster presentations

Sibiya. B, Bloom. K, and Arbuthnot. P., (2018), Adapting the bacterial CRISPR/Cas9 gene editing system to treat chronic hepatitis B virus infection, 26th SASBMB Congress, 8-11 July, Potchefstroom, South Africa.

Sibiya. B, Bloom. K, and Arbuthnot. P., (2018), Adapting the bacterial CRISPR/Cas9 gene editing system to target the basic core promoter and enhancer sequences of the hepatitis B virus, University of the Witwatersrand, Faculty of Health Sciences Research Day, 6th September, Parktown, South Africa.

Sibiya. B, Bloom. K, Ely. A, and Arbuthnot. P., (2018), Targeting essential sequences of the hepatitis B virus with the *Staphylococcus aureus* CRISPR/Cas9 gene editing system, Molecular Biosciences Research Thrust, Postgraduate Research Day, 29th November, Johannesburg, South Africa.

ABSTRACT

Chronic hepatitis B virus (HBV) infection remains a global health burden despite the availability of approved therapeutics and a vaccine. Complications associated with chronic HBV infection include cirrhosis and hepatocellular carcinoma. Current approved therapies are not completely effective for the treatment of chronic HBV infection, as these do not target the covalently closed circular DNA (cccDNA) of the virus. The cccDNA intermediate is required for the transcription of viral RNA resulting in the persistence of the infection. Several designer nucleases have been explored as a promising option to target the cccDNA to achieve a sustainable therapy. This is based on the ability to introduce double stranded breaks (DSBs) at a specific DNA target site. A DSB may lead to the non-homologous end joining (NHEJ) repair pathway which is error-prone and introduces mutations in the target gene. Based on this rationale, this project focused on the adaptation of the *Staphylococcus aureus* CRISPR/Cas9 system to target various regions of the HBV genome with the aim of disrupting the cccDNA. This RNA-guided nuclease system requires the Cas9 nuclease, a single guide RNA (sgRNA) sequence as well as the protospacer adjacent motif (PAM) sequence for target recognition. To achieve targeted disruption, a portion of the sgRNA sequence called the CRISPR RNA (crRNA) was designed using *in silico* tools to target all the open reading frames of the HBV genome. Immunofluorescence staining and RT-qPCR *in vitro* analysis confirmed the successful expression of the Cas9 nuclease and crRNA sequences. However, *in vitro* analysis confirmed the newly designed crRNA sequences did not achieve significant targeted disruption of the cccDNA. *In vitro* studies also confirmed the SaCas9 nuclease did not exhibit any knockdown effect on the HBV replication marker, hepatitis B surface antigen (HBsAg). Although the crRNA sequences were not efficient, these sequences were not associated with any cytotoxicity to the cells.

It was therefore concluded that the CRISPR/Cas9 system depends largely on the design of the crRNA sequences as these are crucial for the Cas9 targeted cleavage abilities. Further improvements in the design of these artificial nuclease systems will be carried out to improve their efficiency to treat HBV.

ACKNOWLEDGEMENTS

I would like to sincerely thank, Dr Kristie Bloom and Prof. Arbuthnot for their unending support and guidance throughout my studies.

My heartfelt appreciation goes to Prof. Abdullah Ely who not only gave his support and guidance throughout my studies, he truly inspired me to be a better student. His genuine kindness and teaching will never be forgotten. He taught me true perseverance and ensured that all students matter.

I would like to acknowledge Dr Tristan Scott for the plasmids used in this study and Prof. Patrick Arbuthnot for the provision of the Cel1 enzyme.

My appreciation also goes to Ms Gladys Gagliardi and Ms Tracy Khorombi for their administrative and technical support throughout my studies.

To the AGTRU family, I thank you for your advice, support and kindness that was freely given.

To my mom Sizakele, my sisters Simphiwe, Ayanda and Zonke I wish to express my utmost appreciation to them. Their hard work and sacrifices have allowed me to be where I am today. They are my biggest supporters not only physically but in prayer they have held me up. I would also like to acknowledge Lwazi and Sebaga for their unending physical and emotional support.

I would like to thank my funders (National Research Foundation, Poliomyelitis Research Foundation, Witwatersrand Postgraduate Merit Award and AGTRU) for the financial support for without it my studies would not be possible.

Most importantly, all glory, honour and praise belong to my Heavenly Father who showers me with His grace and mercy. He gave me strength when I was down. “For I can do all things through Christ, who gives me strength.” -Philippians 4:13

TABLE OF CONTENTS

Contents

ADAPTING THE BACTERIAL CRISPR/CAS9 GENE EDITING SYSTEM TO TARGET THE BASIC CORE PROMOTER AND ENHANCER SEQUENCES OF THE HEPATITIS B VIRUS....1

DECLARATION....II

DEDICATION....III

PUBLICATIONS AND PRESENTATIONS....IV

ABSTRACT....V

ACKNOWLEDGEMENTS....VII

TABLE OF CONTENTS....VIII

LIST OF FIGURES....XII

LIST OF TABLES....XIV

LIST OF ABBREVIATIONS....XV

CHAPTER 1-INTRODUCTION....1

1.1 Epidemiology of the hepatitis B virus....1

1.2 HBV structure and viral replication....3

1.3 Current HBV therapeutics....8

1.4 Sequence-specific designer nucleases....10

1.5 Clustered regularly interspaced short palindromic repeats (CRISPR)/CRISPR-associated (Cas)....13

1.6 Mechanism of action of sequence-specific designer nucleases....19

1.7 Rationale of the study....21

1.8 Research Aims and Objectives 22

CHAPTER 2-MATERIALS AND METHODS 23

2.1 Plasmids 23

2.1.1 HBV target plasmid (pCH-9/3091) 23

2.1.2 Reporter plasmid (pCMV-eGFP) 23

2.1.3 Plasmids encoding SaCas9/dCas9 and HBV target sequences 23

2.2 Large-scale plasmid preparations 32

2.3 Tissue culture conditions 33

2.4 Detection of anti-HBV sgRNAs and SaCas9 proteins 33

2.4.1 Immunofluorescence staining of Cas9 nuclease 33

2.4.2 RNA extraction from transfected Huh7 cells 35

2.4.3 Reverse transcription of RNA for quantification of anti-HBV sgRNA 36

2.5 Assessment of anti-HBV efficacy of newly designed sgRNAs 37

2.6 Evaluation of toxicity associated with gene products of anti-HBV plasmids 38

2.7 Assessment of targeted disruption with anti-HBV sgRNA and Cas9 complex 39

2.7.1 Transfection of HepG2.2.15 cells 39

2.7.2 DNA Extraction from HepG2.2.15 cells 40

2.7.3 Surveyor assay 41

CHAPTER 3-RESULTS 44

3.1 Construction of wild type Cas9 anti-HBV sgRNA plasmids 44

3.2 Construction of inactive Cas9 anti-HBV sgRNA plasmids 46

3.3 Expression of CRISPR/Cas9 system in vitro 48

3.3.1 SaCas9 nucleases are expressed efficiently in liver-derived cells 48

3.3.2 Expression of pAAV-SaCas9 sgRNA sequences in vitro 50

3.4 Surface antigen knockdown assay to assess the efficacy of anti-HBV plasmids 52

3.5 Inactive SaCas9 anti-HBV sgRNA plasmid's effect on HBsAg secretion 57

3.6 Targeted disruption by anti-HBV sgRNA and Cas9 complex in vitro 59

3.7 Anti-HBV sgRNA and Cas9 complex do not exhibit toxicity in vitro 63

3.8 Anti-HBV sgRNA plasmids do not exhibit self-cleavage of plasmid DNA.....65

CHAPTER 4-DISCUSSION 67

4.1 Successful generation of pAAV-SaCas9 and pAAV-dSaCas9 plasmids expressing the newly designed anti-HBV sgRNA sequences.....67

4.2 Targeting of cccDNA of HBV using CRISPR/Cas.....68

4.3 Safety of the gene products from pAAV-SaCas9 plasmids 69

4.4 The design of the sgRNA sequences is important for the efficiency of the CRISPR/Cas9 system.....70

4.5 Future work to address the challenges faced for a successful HBV gene therapy.....72

4.6 Conclusion.....75

CHAPTER 5-APPENDIX.....76

5.1 Bacterial culturing: Preparation and transformation of chemically competent cells 76

5.1.1 Bacterial transformation 77

5.2 Agarose gel electrophoresis 78

5.3 Gel extraction (extraction of DNA from agarose gel).....79

5.4 Plasmid preparations 80

5.4.1 Small-scale plasmid preparation.....80

5.5 Tissue culture (Culturing of mammalian cells).....81

5.5.1 Culturing and passaging of cells.....81

5.5.2 Transfection mixes.....82

5.6 Sequence analysis of the anti-HBV sgRNA plasmids 83

5.7 Transfection efficiency of anti-HBV sgRNA plasmids 86

5.7.1 Huh7 transfection efficiency for RT-qPCR studies.....86

5.7.2 Huh7 transfection efficiency of pSaCas9-sgRNA plasmids.....87

5.7.3 Huh7 transfection efficiency of pdSaCas9-sgRNA plasmids.....89

5.7.4 HepG2.2.15 transfection efficiency for surveyor assay 90

5.8 PCR amplification for Surveyor assays 91

5.8.1 PCR amplification of HepG2.2.15 transfected cells for targeted disruption.....91

5.9 Ethics certificate.....93

REFERENCES.....94

LIST OF FIGURES

Figure 1.1: The HBV genome.....5

Figure 1.2: The HBV replication cycle.....7

Figure 1.3: Schematic of the Staphylococcus aureus CRISPR/Cas9 system.....16

Figure 1. 4: Possible pathways of cellular DNA repair following DSB.....20

Figure 2.1: Oligonucleotide cloning of the crRNA insert into the pAAV expression vector……..25

Figure 2.2: Binding sites of sgRNA sequences in the HBV replication-competent plasmid ..28

Figure 2.3: Cloning strategy for the generation of the pSaCas9-A1 to A20 and pdSaCas9-A1 to 20 plasmids. 31

Figure 3.1: Generation of the wild type SaCas9 pAAV plasmid ……...…… 45

Figure 3.2: Enzymatic digestion of inactive dSaCas9 plasmid.....47

Figure 3.3: Detection of expressed Cas9 nuclease by immunofluorescence staining in Huh7 cells transfected with SaCas9 plasmids 49

Figure 3.4: RNA expression profiles of sgRNAs relative to hGAPDH 51

Figure 3.5: Assessment of core anti-HBV sgRNA-mediated knockdown of HBsAg in liver-derived cells 53

Figure 3.6: Assessment of polymerase anti-HBV sgRNA-mediated knockdown of HBsAg in liver-derived cells.....54

Figure 3.7: Assessment of polymerase/surface anti-HBV sgRNA-mediated knockdown of HBsAg in liver-derived cells 55

Figure 3.8: Assessment of HBx anti-HBV sgRNA-mediated knockdown of HBsAg in liver-derived cells 56

Figure 3.9: Assessment of active and inactive SaCas9-mediated knockdown of HBsAg in liver-derived cells.....58

Figure 3.10: Schematic diagram depicting Cel1-mediated cleavage of heteroduplexes 61

Figure 3.11: sgRNA and Cas9 mediated cleavage of HepG2.2.15 extracted DNA 62

Figure 3.12: In vitro assessment of CRISPR/Cas9 complex mediated cytotoxicity in cultured cells by MTT assay 64

Figure 3.13: Cel1 assay to assess self-cleavage of the SaCas9 plasmid.....66

Figure 5.1: Chromatograms of the cloned crRNA sequences into the SaCas9 plasmids ……... 85

Figure 5.4: Transfection efficiency of pSaCas9-plasmids in Huh7 cells.....86

Figure 5.2: Transfection efficiency of pSaCas9-plasmids in Huh7 cells.....88

Figure 5.3: Transfection efficiency of pSaCas9-plasmids in Huh7 cells.....89

Figure 5.5: Transfection efficiency of pSaCas9-plasmids in HepG2.2.15 cells.....90

Figure 5.6: PCR amplification of the sgRNA target sites.....91

Figure 5.7: PCR amplification of sgRNA target sites from HepG2.2.15 transfections.....92

LIST OF TABLES

Table 2.1: Target sites of the selected sgRNAs from in silico tools.....27

Table 2.2: HBV sequences encoding the crRNA of sgRNA sequences 29

Table 2.3: Primers used for RT-qPCR.....37

Table 2.4: Primers used for Surveyor Assay 43

LIST OF ABBREVIATIONS

bp	-	base pair
BSA	-	bovine serum albumin
Cas9	-	CRISPR associated 9
cccDNA	-	covalently closed circular DNA
Cel1	-	celery endonuclease I
CMV	-	cytomega
CRISPR	-	clustered regularly interspaced short palindromic repeats
crRNA	-	CRISPR RNA
Cys_2His_2	-	cysteine2-histidine2
DAPI	-	4,6-diamidine-2-phenylindole chloride
dCas9	-	dead Cas9
DMEM	-	Dulbecco's Modified Eagle's Medium
DMSO	-	dimethyl sulphoxide
DR1/DR2	-	direct repeats1/2
DSB	-	double-strand breaks
E. coli	-	*Escherichia coli*
EDTA	-	ethylene diamine tetra-acetic acid
eGFP	-	enhanced green fluorescent protein
ELISA	-	enzyme-linked immunosorbent assay
ER	-	endoplasmic reticulum
FBS	-	foetal bovine serum
FITC	-	fluorescein isothiocyanate
HA	-	haemagglutinin
HBsAg	-	hepatitis B virus surface antigen
HBV	-	hepatitis B virus
HB*x*	-	hepatitis B virus X protein
HCC	-	hepatocellular carcinoma
HDR	-	homology directed repair

Hek293	-	human embryonic kidney 293
h*GAPDH*	-	human *glyceraldehydes-3-phosphate dehydrogenase*
HIV	-	human immunodeficiency virus
Huh7	-	human hepatoma 7
IFN-α	-	interferon-α
Indel	-	insertion/deletion
MTT	-	3-(4,5-dimethylthiazol-2-yl)-2,5-diphenyltetrazolium bromide
mTTR	-	modified transthyretin
NAs	-	nucleoside/nucleotide analogues
ng	-	nanograms
NHEJ	-	non-homologous end joining
nm	-	nanometers
NTCP	-	sodium taurocholate co-transporting polypeptide
OD	-	optical density
ORF	-	open reading frame
PAM	-	protospacer adjacent motif
PBS	-	phosphate buffered saline
PCR	-	polymerase chain reaction
PEI	-	polyethyleneimine
PFA	-	paraformaldehyde
PMSF	-	phenylmethylsulphonyl fluoride
pgRNA	-	pregenomic
rcDNA	-	relaxed circular DNA
RT-qPCR	-	reverse transcriptase quantitative PCR
RVDs	-	repeat variable diresidues
sgRNA	-	single guide RNA
Smc	-	structural maintenance of chromosomes
SaCas9	-	*Staphylococcus aureus* Cas9
SpCas9	-	*Staphylococcus pyogenes* Cas9
TALEN	-	transcription activator-like effector nuclease

tracrRNA	-	trans-activating crRNA
WT	-	wild type
ZFN	-	zinc finger nuclease

CHAPTER 1-INTRODUCTION

1.1 Epidemiology of the hepatitis B virus

Hepatitis B virus (HBV) is a virus that causes both chronic and acute infection of the liver. Chronic infections caused by HBV represent a global health concern. According to the WHO, around 257 million people worldwide are chronically infected by the virus and approximately 880 000 people die from liver disease related complications (Smith et al., 2019, WHO, 2017). Chronically infected individuals are at risk to develop liver fibrosis, cirrhosis and hepatocellular carcinoma (HCC) (Stanaway et al., 2016). Eradicating this serious disease remains an international health priority (WHO, 2017). The areas that are mostly affected by the endemic caused by HBV are the African and Western Pacific regions (WHO, 2017). Within the South African context, it is estimated that 3.5 million people are chronically infected with HBV (Schweitzer et al., 2015).

Chronic infection is defined by the presence of HBV surface antigen (HBsAg) remaining in serum for more than 6 months. Acute infections are often characterised by mild symptoms and clearance of infected hepatocytes by the immune system. (Shepard et al., 2006). Symptoms of acute HBV infection include abdominal pain, nausea, vomiting, dark urine and jaundice. The development of these symptoms is age-dependent [reviewed by (Shepard et al., 2006)]. Most perinatal HBV infections are asymptomatic. Symptoms are noticed in 5-15% of young children between the ages of one to five, and in 30-50% of older children including adults[reviewed by (Shepard et al., 2006)]. The likelihood of becoming chronically infected with HBV also depends on the age at which infection occurs. Children below 6 years of age are more likely to develop chronic infection whereas only 5% of otherwise healthy adults develop chronic infection (WHO, 2017).

Individuals who are chronically infected may serve as a source for new infections in susceptible individuals (Seeger and Mason, 2000). In highly endemic areas such as Africa, HBV is commonly transmitted horizontally and in Asia HBV is most commonly transmitted from mother to child at birth (perinatal) (Smith et al., 2019). Other transmissions include exposure to infected blood through blood transfusions, needlestick injuries, tattooing and piercings. The virus can also be sexually transmitted (WHO, 2017). To prevent the spread of HBV, vaccination programmes were introduced. South Africa was one of the first countries to introduce universal vaccination in 1995, however there is no birth dose or catch-up programme in place (Spearman and Sonderup, 2014). It has been recommended that South Africa implements a birth-dose vaccine into the existing schedule to prevent the breakthrough of infections and reduce the risk of perinatal transmission (Spearman and Sonderup, 2014). Infant vaccine programmes have been successful but much attention is needed when screening pregnant women for HBV and people living in rural areas (Spearman and Sonderup, 2014). Despite these challenges the vaccination programmes have drastically reduced the HBV carrier rate in children.

HBV prevalence defined by surface antigen varies between 1% and 10% depending on the geographic region (Kramvis et al., 2008). Based on the genomic sequence, HBV isolates have been identified that exhibit distinct geographic distributions. In total there are ten genotypes of HBV worldwide (A, B, C, D, E, F, G, H, I and J) which have been divided into subgenotypes that have distinct epidemiologies (Paudel and Suvedi, 2019). Each genotype differs from each other by at least 8% whereas the subgenotypes differ by 4% (Schaefer, 2007). The subgenotypes have been given a numerical nomenclature for each identified within the genotype (Kramvis et al., 2005). The most commonly distributed genotype worldwide is D and in South Africa, genotype A1 is the most prevalent (Kramvis and Paraskevis, 2013).

1.2 HBV structure and viral replication

HBV is a small DNA virus belonging to the *Hepadnaviridae* family which is known to infect the liver of mammals (Transy et al., 1992). This spherical enveloped particle has a diameter of approximately 42 nm. The HBV genome is a relaxed partially double-stranded circular DNA (rcDNA)(Cummings et al., 1980). It is composed of a plus (+) and minus (-) strand. The minus strand is the longer of the two and is estimated to be 3.2 kb in length while the plus strand is of variable length. The plus strand serves to maintain the circular structure of the genome via a cohesive overlap at the 5' and 3' ends of the minus strand (Shih et al., 1987). This circular genome is surrounded by a capsid composed of the core antigen (HBcAg) which in turn is enclosed by a lipid envelope with HBsAg embedded (Murray et al., 1984).

HBV has a highly compact genome that comprises four overlapping open reading frames (ORFs) namely *Surface* (*S*), *Core* (*C*), *Polymerase* (*P*), and *HBx* (*X*) (Figure 1.1). The *P* ORF is the largest and it codes for the polymerase protein which can be divided into three domains: the terminal protein (TP) domain, the reverse transcriptase (RT) domain, and the ribonuclease H domain. The TP domain is necessary for protein priming and initiates minus-strand synthesis (i.e. reverse transcription) from the pregenomic RNA (pgRNA) template; the RT domain is responsible for synthesising the plus and minus strand; and the ribonuclease H domain facilitates replication and the degradation of pgRNA as it is reverse transcribed (Liang, 2009). The *S* ORF encoding the viral envelope proteins can be divided into *Pre S1*, *Pre S2* and *S* regions. These regions have in-frame start codons initiating the translation of large, middle and major surface antigens (HBsAg) respectively (Liang, 2009). The *C* ORF is divided into the precore and core regions that code for HBV e antigen (HBeAg) and core protein, respectively. Core proteins form the nucleocapsid while precore proteins are processed to form the secreted HBeAg (Jean-Jean et al., 1989, Liang, 2009).

The *HBx* ORF codes for a protein that has been implicated in the regulation of viral gene transcription, signal transduction, DNA repair, protein degradation and hepatocarcinogenesis (Huang et al., 2013). However, it has recently been discovered that the HBx protein plays a role in the stability of the covalently closed circular DNA (cccDNA) of HBV (Abdul et al., 2018). The HBx protein achieves this by antagonising the restriction of episomal DNA through the Structural Maintenance of Chromosome (SMC) Smc5/6 complex (Decorsière et al., 2016, Murphy et al., 2016). This complex is found in eukaryotes and plays a role in housekeeping functions such as chromosome replication, segregation and repair (Abdul et al., 2018). When HBx protein is absent, the Smc5/6 complex binds to the HBV episomal DNA genome and inhibits viral transcription (Abdul et al., 2018). HBx proteins hijack the hosts E3 ubiquitin ligase complex to target the Smc5/6 complex. This leads to ubiquitin-mediated degradation and enables HBV gene expression (Abdul et al., 2018).

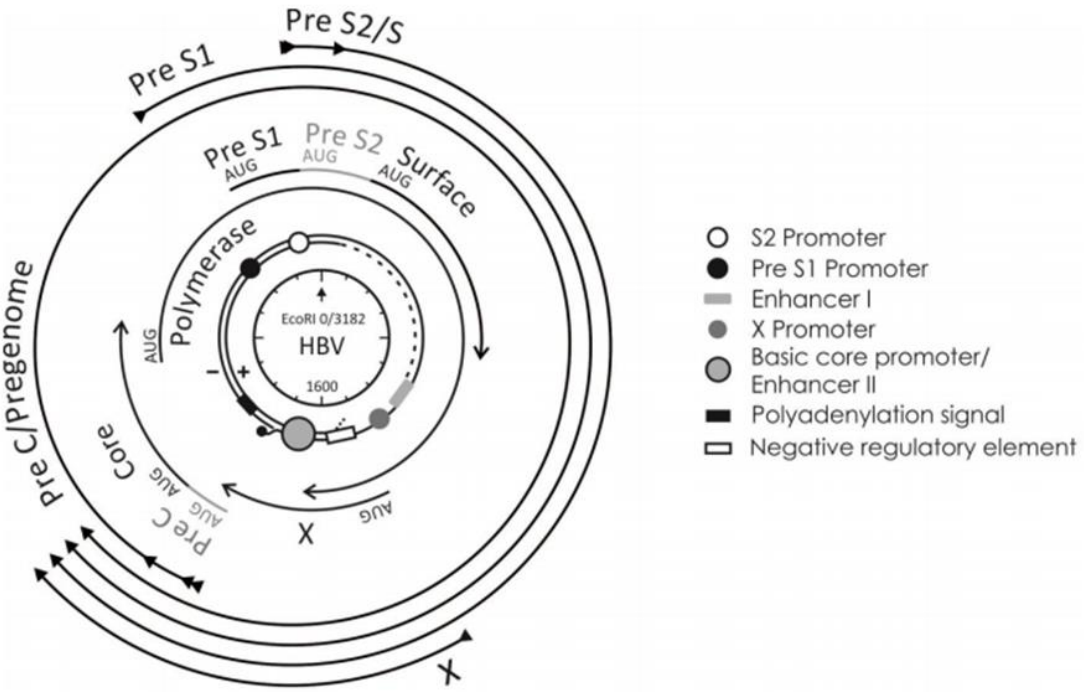


Figure 1.1: The HBV genome

The rcDNA is represented in the centre as the circular genome by the partial positive (+) and full negative (-) sense strands. The four overlapping open reading frames (*surface, polymerase, core* and *X*) are shown as open arrows immediately around the genome. The closed arrows represent the four major viral transcripts. The promoters and other regulatory elements are shown as circles and rectangles respectively. Transcriptional regulatory elements and nucleotide coordinates shown are relative to the *Eco*RI site. From (Passman et al., 2000, Scott et al., 2017)

The HBV genome includes additional important elements. The direct repeats DR1 and DR2 located at the 5' end of the plus strand are required for strand-specific DNA synthesis during replication. Two enhancer elements, Enhancer 1 and 2, are necessary for liver-specific expression of viral gene products (Beck and Nassal, 2007, Grimm et al., 2011). DNA-binding motifs for liver-specific transcription factors have been identified in the enhancer regions, which regulate transcription in a tissue-specific manner. This feature contributes to the hepatotropism of HBV(Antonucci and Rutter, 1989, Shaul et al., 1985).

HBV replicates in the nucleus of hepatocytes. The infectious virion contains the rcDNA in its icosahedral core (Lucifora and Protzer, 2016). Following the binding of the viral envelope proteins to the sodium taurocholate co-transporting polypeptide (NTCP), the virus enters the cell through endocytosis. Once inside the cell the virion is uncoated exposing the nucleocapsid (Beck and Nassal, 2007) (Figure 1.2). The nucleocapsid translocates to the nucleus where the rcDNA is released and repaired to form cccDNA (Beck and Nassal, 2007). This viral replication intermediate is essential for the persistence of HBV and drives viral replication. It is maintained episomally as a minichromosome-like structure and is epigenetically regulated (Bock et al., 1994). Epigenetic regulation mechanisms may include DNA-methylation, chromatin remodelling and histone modifications (Cheung and Lau, 2005). Several viral RNAs are transcribed from the cccDNA and transported to the cytoplasm for translation and virion assembly. Progeny capsids form around the pgRNA which is reverse transcribed to form new rcDNA genomes (Beck and Nassal, 2007, Grimm et al., 2011). Nucleocapsids are enveloped in a lipid bilayer embedded with surface proteins in the endoplasmic reticulum (ER) and infectious virions are subsequently secreted from hepatocytes to infect other cells. Alternatively uncoated nucleocapsids are recycled back to the nucleus for cccDNA amplification (Grimm et al., 2011).

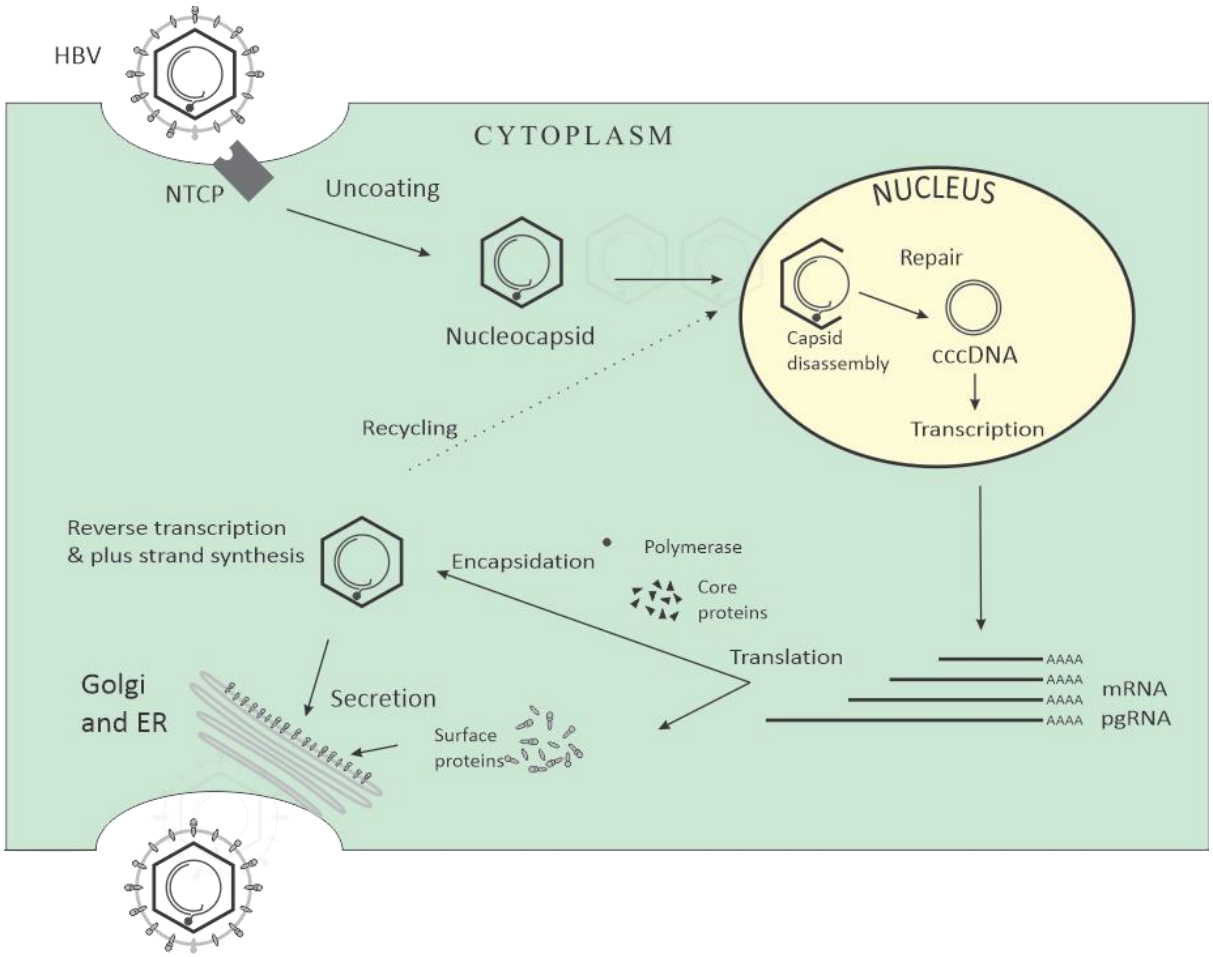


Figure 1.2: The HBV replication cycle

The hepatitis B virion gains entry by binding to the sodium taurocholate co-transporting polypeptide (NTCP) on hepatocytes and is engulfed into the cell via endocytosis. Upon entry into the cell the virion is uncoated and the nucleocapsid is translocated to the nucleus. In the nucleus, the capsid is disassembled allowing rcDNA to be released and repaired by viral and host proteins to form the cccDNA. The cccDNA serves as the template for transcription of pgRNA and viral RNAs. Viral RNAs are translated into polymerase, HBx, surface and core proteins necessary for the assembly of a new infectious virion. Polymerase binds to the pgRNA and initiates its encapsidation. This process then leads to the reverse transcription of pgRNA to minus strand which serves as template for synthesis of the plus strand. A mature nucleocapsid containing the rcDNA genome is produced. The nucleocapsid is transported to the endoplasmic reticulum (ER) and Golgi apparatus where it is enveloped with a lipid bilayer embedded with surface proteins. Progeny virions are secreted out of the cell by exocytosis to infect other cells. Alternatively, the nucleocapsid can be transported back into to the nucleus to replenish the cccDNA pool.

1.3 Current HBV therapeutics

Preventative vaccines against HBV have been available for a number of years and many countries have adopted their use in childhood immunisation programmes (Vitiello et al., 1995). For chronic HBV infection there are several therapeutics that have been approved and are currently in use. Interferon-alpha (IFN-α) and pegylated IFN-α are immunomodulators that function to enhance the immune response to HBV. This is achieved by binding to a type I interferon receptor which activates the Jak-Stat pathway in conjunction with upregulating other interferon cytokines which limit viral replication and dissemination (Saravolatz et al., 2010). Pegylated IFN-α contains an addition of polyethylene glycol which makes its half-life longer than standard IFN-α. However, the adverse side effects from using these drugs include fatigue, arthralgias, anorexia and insomnia. More importantly, only a small proportion of patients respond to treatment. In addition to their immunomodulatory activity, IFN-α and pegylated IFN-α have also been described to have antiviral effects through other mechanisms (Revill et al., 2019). These include the suppression of RNA and protein production in infected cells and the ability to inhibit HBV DNA replication through the blocking of nucleocapsid assembly (Belloni et al., 2012, Wieland et al., 2005).

Other licensed drugs against HBV include nucleoside/nucleotide analogues. These drugs inhibit viral polymerase activity and they block viral DNA synthesis [reviewed by (Zoulim and Locarnini, 2009)]. Depending on the drug, it may affect priming of the reverse transcription, minus strand DNA synthesis (RNA dependent DNA polymerase activity) or plus strand DNA synthesis (DNA dependent DNA polymerase activity) (Zoulim and Perrillo, 2008). Lamivudine is a drug that inhibits reverse transcriptase activity. Clevudine is a drug that affects both plus and minus strand synthesis. Adefovir and Tenofovir are drugs that affect priming polymerisation to prevent reverse transcription and minus strand synthesis (Clark and Hu, 2015).

A number of studies have evaluated the combination of pegylated IFN-α with lamivudine and pegylated IFN-α combined with adefovir (Terrault, 2009). It was found that the combination therapy displayed no advantage over pegylated IFN-α as a monotherapy. With or without lamivudine and adefovir, pegylated IFN-α worked better than monotherapies (Terrault, 2009). *In vitro* studies have shown an additive antiviral effect for some combinations of the nucleoside/nucleotide analogues but has not yet been proven in clinical trials (Clark and Hu, 2015).The effect of nucleoside/nucleotide analogues results in a decrease in the production of infectious viral particles, which in turn may limit the spread to uninfected hepatocytes (Zoulim and Perrillo, 2008). While they may be effective to block DNA synthesis, there are drawbacks associated with the use of nucleoside/nucleotide analogues. Since they resemble naturally occurring nucleosides, the danger is that human polymerases incorporate these into DNA which may lead to adverse side effects (Health, 2017).

Although immunomodulators and nucleoside/nucleotide analogues may effectively inhibit viral replication in the cytoplasm, they do not remove the cccDNA reservoir (Zoulim and Perrillo, 2008). Since nucleoside/nucleotide analogues do not affect cccDNA, patients have to remain on treatment indefinitely. This is the goal of effective HBV therapy, to permanently disable or eliminate the cccDNA. Disabling or eliminating cccDNA would inhibit viral replication as this intermediate is responsible for the persistence of the virus. As the above-mentioned drugs are unable to achieve this goal, gene editing strategies are being explored as alternative therapies. Several definitions of an HBV cure have been described. A complete sterilising cure is defined as the complete eradication of cccDNA with no detection of HBsAg in serum. A functional cure is defined as the clearance of HBsAg and HBV DNA in serum, the resolution of liver injury and a decrease in risk of HCC. Another described as a partial cure is the detection of HBsAg in serum but no detection of HBV DNA in serum (Lok et al., 2017).

Although a sterilising cure would be ideal to avoid reactivation of HBV replication, it is not yet achievable. The alternative functional cure is more likely achievable with the use of designer nucleases (Revill et al., 2019).

1.4 Sequence-specific designer nucleases

As the HBV genome has been studied extensively, designer nuclease technologies have been explored to target specific regions of the viral sequences with the aim of achieving curative treatments for chronic infection. Targeted mutagenesis of cccDNA may be achieved by designer nucleases (Bloom et al., 2018).

Homing Endonucleases (HEs) (Belfort and Roberts, 1997), Zinc finger nucleases (ZFNs) (Miller et al., 1985), transcription activator-like effector nucleases (TALENs) (Boch et al., 2009) and clustered regularly interspaced short palindromic repeats (CRISPR)/CRISPR-associated (Cas) systems (Ran et al., 2013) have been widely used as gene editing tools. These tools create double stranded breaks (DSB) at specific target DNA regions which induces one of two repair mechanisms. These mechanisms are termed homology-directed repair (HDR) and the non-homologous end joining (NHEJ) pathway (Ran et al., 2013).

HEs or meganucleases are microbial derived DNA cleaving enzymes that mobilise their own reading frames by creating a DSB at a homologous site thereby enabling insertion of their sequence by homologous recombination. These proteins are quite small in size, however they target long DNA sequences between 14 and 40 bp to induce DSBs (Stoddard, 2011). Homing is the lateral transfer of introns or inteins to a homologous allele within the host's genome that lacks that sequence. Inteins are intervening sequences that are spliced out and excised from proteins post translation. The process is mediated by an endonuclease that cleaves the target allele (Chevalier and Stoddard, 2001). This leads to a gene conversion and inheritance of the mobile element (Stoddard, 2011).

HEs are found in group I and II introns as well as inteins (Stoddard, 2011). To date there are five known families of HE catalysts with the largest family termed 'LAGLIDADG' endonucleases or meganucleases. These are found in mitochondrial and chloroplast genomes of single cell eukaryotes (Stoddard, 2011). Several studies have shown how HEs are used for meganuclease redesign and specificity towards a chosen DNA sequence (Silva et al., 2011). Although HEs are highly specific DNA cleaving enzymes there are limitations to their use in gene therapy, as their design and assembly is difficult and they can only target certain pre-defined DNA sequences [reviewed in (Bloom et al., 2015)].

The Zinc finger (Cys_2-His_2) was originally discovered in *Xenopus* and it is regarded as the most common DNA binding motif in metazoans (Miller et al., 1985, Urnov et al., 2005). This array of Cys_2-His_2 fingers recognises 3-4 bp of DNA via an α-helix. When linked to other zinc fingers, they have the ability to recognise longer DNA sequences which allows for higher specificity (Urnov et al., 2005). The discovery of zinc fingers has led to their use in genome editing by engineering the zinc finger protein (ZFP) DNA binding domains to various effector domains. The ZFP can be coupled to the cleavage domain of the *Fok*I enzyme, which is a Type IIS restriction enzyme, producing what is called the zinc finger nuclease (ZFN) (Urnov et al., 2005). A pair of ZFNs will then cleave DNA at its target site, which is determined by the arrangement of the ZFP domain. This mechanism requires two *Fok*I nuclease domains to dimerise, which create a DSB in the DNA (Urnov et al., 2005). A study by Cradick et al demonstrated the use of ZFNs for HBV targeted disruption in cell culture (Cradick et al., 2010). Their pair of ZFNs successfully demonstrated a therapeutic use to directly target and inactivate viral DNA (Cradick et al., 2010). Although this naturally occurring protein has proven its capabilities as a gene editing tool, ZFNs are difficult to assemble and they are associated with off-target cleavage [reviewed in (Bloom et al., 2015)].

Transcription activator-like effectors (TALEs) are from the plant pathogenic bacteria *Xanthomonas.* These DNA-binding proteins are important virulence factors as they mimic eukaryotic transcription factors within the plant nucleus (Boch et al., 2009). The translocation of effector proteins via a type III secretion system is how the bacteria achieve pathogenicity during infection. Once the TALEs have gained entry into the plant cell they translocate into the nucleus and bind to effector-specific DNA sequences to activate gene expression (Christian et al., 2010).

The TALE protein is made up of many tandem repeats of a 33-35 amino acid motif. The amino acid sequences of the repeat motif are conserved except for two adjacent amino acids at positions 12 and 13, known as the repeat variable di-residues (RVDs) (Christian et al., 2010). Different RVDs recognise different DNA base pairs with a one-one association between an RVDs and a nucleotide within the target sequences, creating what is known as a cipher. With this cipher, the DNA targets of TALEs can be correctly predicted and TALE DNA-binding domains assembled leading to their application as a gene editing tool (Christian et al., 2010). The effector *Fok*I nuclease domain can be coupled to TALEs to result in transcription activator-like effector nucleases (TALENs). TALENs are capable of achieving directed cleavage of DNA sequences.

The use of TALENs has been successfully demonstrated in many studies including that of Bloom et al (Bloom et al., 2013). Plasmids encoding the monomers of TALENs were delivered to mice by hydrodynamic injection for *in vivo* analysis. This study successfully demonstrated TALENs with sequences targeting the *S* and *C* ORF were able to introduce mutations at the intended sites in the HBV (Bloom et al., 2013). The advantage of using TALEs include its high specificity and ease of assembly. The disadvantages include the limitation for packaging into a single delivery vector due to the size of its heterodimers.

1.5 Clustered regularly interspaced short palindromic repeats (CRISPR)/CRISPR-associated (Cas)

The CRISPR/Cas system was first discovered as an adaptive immune system present in archaeal as well as bacterial species that defends against invading foreign genetic elements (Cong et al., 2013). In prokaryotic genomes there is an array of direct repeats known as clustered regularly interspaced short palindromic repeats (CRISPR) which includes spacers that are unique between the CRISPR repeats (Cong et al., 2013). These CRISPR arrays function with CRISPR-associated (Cas) genes which code for proteins that have cleaving capabilities such as nucleases.

The CRISPR/Cas system can be described as a complex that uses RNA-guided nucleases to cleave genetic elements (Ran et al., 2013). There are three types (I-III) of well characterised CRISPR systems that have been identified across a wide range of bacterial and archaeal species. Each of these systems comprises the non-coding RNAs, the CRISPR-associated genes (Cas) and distinctive direct repeats (Ran et al., 2013).

The distinct arrays with unique spacers discovered in bacterial and archaeal genomes have been known for years however their function was only recently elucidated [reviewed in (Makarova et al., 2011)]. The initial speculation was that CRISPR arrays function as a DNA repair system, however it was observed that unique CRISPR spacers were identical to virus genes which led to the hypothesis that CRISPR systems have a defence function (Mojica et al., 2005, Pourcel et al., 2005). The role of the CRISPR/Cas system in defence against invading DNA was validated in a study that integrated a short phage-specific sequence into the CRISPR locus of the *Staphylococcus thermophilus* bacterium which displayed resistance to the phage (Barrangou et al., 2007). In addition these experiments confirmed that resistance was evaded by as little as single mismatches between the phage target sequence and the CRISPR insert [reviewed in (Makarova et al., 2011)].

Short fragments of foreign DNA are incorporated into the CRISPR locus within the bacterial host (Jinek et al., 2014). The transcription of the newly incorporated fragments yields mature CRISPR RNAs (crRNAs) (Wade, 2015). The bacterial RNA is responsible for the recruitment of the endonucleases that cleave foreign DNA (Wade, 2015). This allows bacteria to have an adaptive immune response so that previously encountered foreign pathogens are targeted and cleared (Wade, 2015).

Staphylococcus pyogenes and many other bacterial species such as the *Staphylococcus aureus* relies on one Cas9 nuclease, the noncoding crRNA and the trans-activating crRNA (tracrRNA) to be able to cleave DNA (Type II system). These noncoding RNAs (crRNA and tracrRNA) can be fused into what is termed the single guide RNA (Wu et al., 2014). The sgRNA together with the Cas9 nuclease forms a complex that binds to DNA, cleaving it and creating the DSBs. The target sequence matches the first 17-20 nucleotides (crRNA portion) of the sgRNA. This naturally occurring system has been exploited for gene editing purposes as it is easy to design and quick to produce [reviewed in (Bloom et al., 2015)]. For gene editing purposes the crRNA can be designed to target any desired sequence. The Cas9 nuclease binds to the target DNA with the assistance of the tracrRNA scaffold of the sgRNA (Figure 1.3).

Another essential component for Cas9 recognition is a protospacer adjacent motif (PAM) which is immediately adjacent to the target sequence (Wu et al., 2014). PAM recognition limits the targeting range for the nucleases. The broadly used Cas9 from *S. pyogenes* recognises a short 5'-NGG-3' PAM sequence in the target strand. This PAM sequence can occur once in every 8 base pairs in random DNA due to its short length. Cas9 orthologues such as *S. aureus* (SaCas9) recognise a longer PAM sequence 5'-NNGRRT-3' which occurs less frequently, one in thirty-two random DNA base pairs, in the target sequence (Kleinstiver et al., 2015).

Lengthening the PAM narrows the target range which is important for various applications such as modifying small genetic elements for performing allele-specific alterations (Kleinstiver et al., 2015). The Cas9 nuclease contains two independent domains, RuvC and HNH, which cleave the target sequence 3 bases upstream of the PAM to create a blunt ended DSB (Kleinstiver et al., 2015).

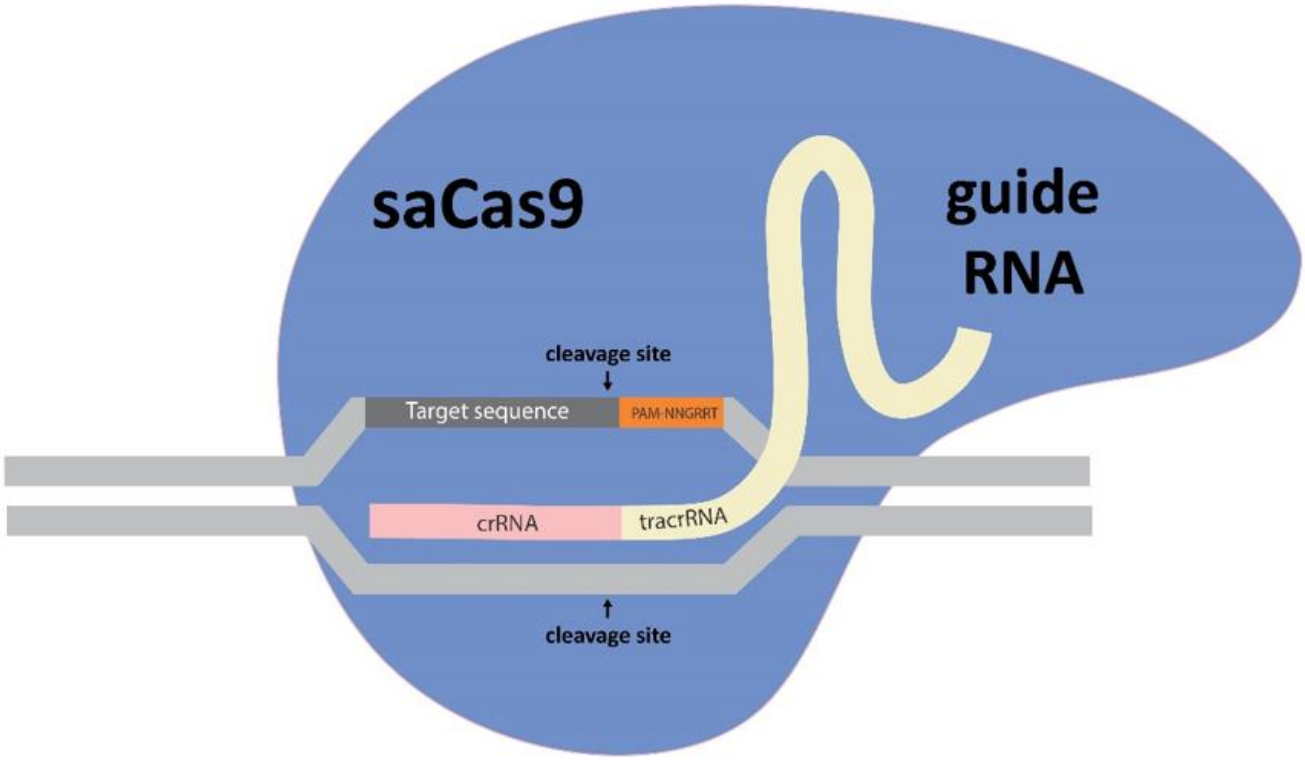


Figure 1.3: Schematic of the *Staphylococcus aureus* CRISPR/Cas9 system

The Cas9 nuclease (in blue) cleaves the genomic DNA targeted by the crRNA portion of the single guide RNA shown in pink. The tracrRNA scaffold is represented in yellow and this assists the Cas9 nuclease to bind to the DNA. The Cas9 creates DSBs indicated by the arrows upstream of the PAM sequence shown in orange 5'-NNGRRT-3' which is specific for *S. aureus.*

The most popular and well characterised nuclease is derived from *S. pyogenes* (SpCas9) however, due to its large size it does not make a suitable candidate for delivery as it is difficult to package. *S. aureus* Cas9 (SaCas9) is one of the smaller orthologues of Cas9 that has been characterised to be better suited for viral delivery. This is due to its size as it is approximately 1 kb smaller than SpCas9 (Ran et al., 2013). Size constraints are a very important aspect to consider during the development of potentially therapeutic vectors. Sequences encoding the SaCas9, regulatory elements as well as the sgRNA cassette has been successfully packaged into single stranded adeno-associated viruses (ssAAVs) (Scott et al., 2017). This "all in one system" has successfully been used to edit endogenous genes in the liver and has shown great promise for the treatment of HBV (Scott et al., 2017).

Various target sites in all ORFs of the HBV genome have been used to design HBV-specific sgRNAs using the SpCas9 nuclease system (Dong et al., 2015, Lin et al., 2014, Wang et al., 2015, Zhen et al., 2015). These studies have shown HBsAg and cccDNA has decreased significantly when using the CRISPR/Cas9 complex that utilise HBV-specific sgRNAs during *in vitro* and *in vivo* experiments. Dong et al designed sgRNAs against HBV genotype B targeting the X ORF. Their study revealed a decrease in the amount of cccDNA of 60% to 70% in transfected Huh7 cells. The CRISPR/Cas9 system may be manipulated to incorporate a dual-guide system. This has been demonstrated by Wang et al by creating dual-guide RNAs that targeted genotypes A-D of HBV (Wang et al., 2015). Their cccDNA analysis revealed successful targeted disruption across the HBV genotypes. The SpCas9 and sgRNA sequences may be packaged into lentiviral vectors for delivery *in vitro* and *in vivo* (Kennedy et al., 2015, Ramanan et al., 2015, Seeger and Sohn, 2014). Kennedy et al delivered their sgRNAs using lentiviral vectors against all ORFs and observed a 10-fold decrease in the formation of cccDNA.

Regulatory regions of the HBV genome may be targeted by SpCas9 and sgRNA sequences delivered by lentiviral vectors. This was successfully demonstrated by Seeger & Sohn, who tested HBV-specific guide RNAs to target the enhancer and core regions of the HBV genome. The sgRNA sequences and Cas9 nuclease were able to disrupt cccDNA (Seeger and Sohn, 2014). Other delivery systems that have been employed to deliver the SpCas9 system include adeno-viral vectors. Li et al successfully demonstrated the delivery of SaCas9 complex by AAVs into transgenic mice targeting the core region of the HBV genome (Li et al., 2018). The co-delivery of sgRNA expression cassettes was demonstrated successfully by Schiwon et al but utilising high-capacity adeno viral vectors (Schiwon et al., 2018). Transduction of these vectors into HBV infection models resulted in the degradation of cccDNA and inhibition of HBsAg (Schiwon et al., 2018). Non-viral vectors such as lipid nanoparticles have been employed to deliver the CRISPR/Cas9 system for the *in vivo* targeting of HBV DNA. This was successfully demonstrated by Jiang et al who employed the SpCas9 orthologue for this system. Their results confirmed the disruption of cccDNA and reduction of HBsAg (Jiang et al., 2017). However, lentiviral vectors may not be suited to anti-HBV gene therapies as they are poor transducers of hepatocytes (Rothe et al., 2012), and pre-existing immunity to adenoviral vectors may prevent delivery and expression of the CRISPR/Cas9 system [reviewed in (Kotterman and Schaffer, 2014)].

For gene editing purposes, the CRISPR/Cas9 system has been modified for target gene regulation (Zhao et al., 2017). This is accomplished by a catalytically dead Cas9 nuclease which is created by mutations, D10A and H557A in the nuclease domains. The dead Cas9 system requires the sgRNA sequence and PAM, like the wild type system. When the dead Cas9 system binds to its target, cleavage will not occur due to the mutations in the nuclease. The dead Cas9 nuclease may either be inert and in some cases it may act as a gene silencer/repressor as it blocks RNA polymerase from binding to the promoter.

This type of system, may be used to silence the genes expressed by HBV or it may be used as a negative control if its function is inert (Scott et al., 2017, Zhao et al., 2017).

1.6 Mechanism of action of sequence-specific designer nucleases

A single unrepaired DSB is sufficient to cause apoptosis making DSBs one of the most critical damages to the cell (Sonoda et al., 2006). DSBs can be created by environmental factors such as ionising radiation, cellular metabolic products as well as recombination intermediates (Sonoda et al., 2006). Sequence-specific designer nucleases have been exploited to edit DNA through repair pathways which are induced by creating a DSB.

DSBs in eukaryotes are most likely repaired by one of two pathways, either the NHEJ or HDR pathway (Takata et al., 1998) (Figure 1.4). DSB repair by HDR is the primary mechanism employed in yeast species. This pathway results in the precise repair of the DNA and it requires homologous sequences, a sister chromatid or a homologous chromosome to serve as the template for repair (Takata et al., 1998, Liang et al., 1998). It is a conservative process which results in very little to no sequence loss during the repair (Liang et al., 1998).

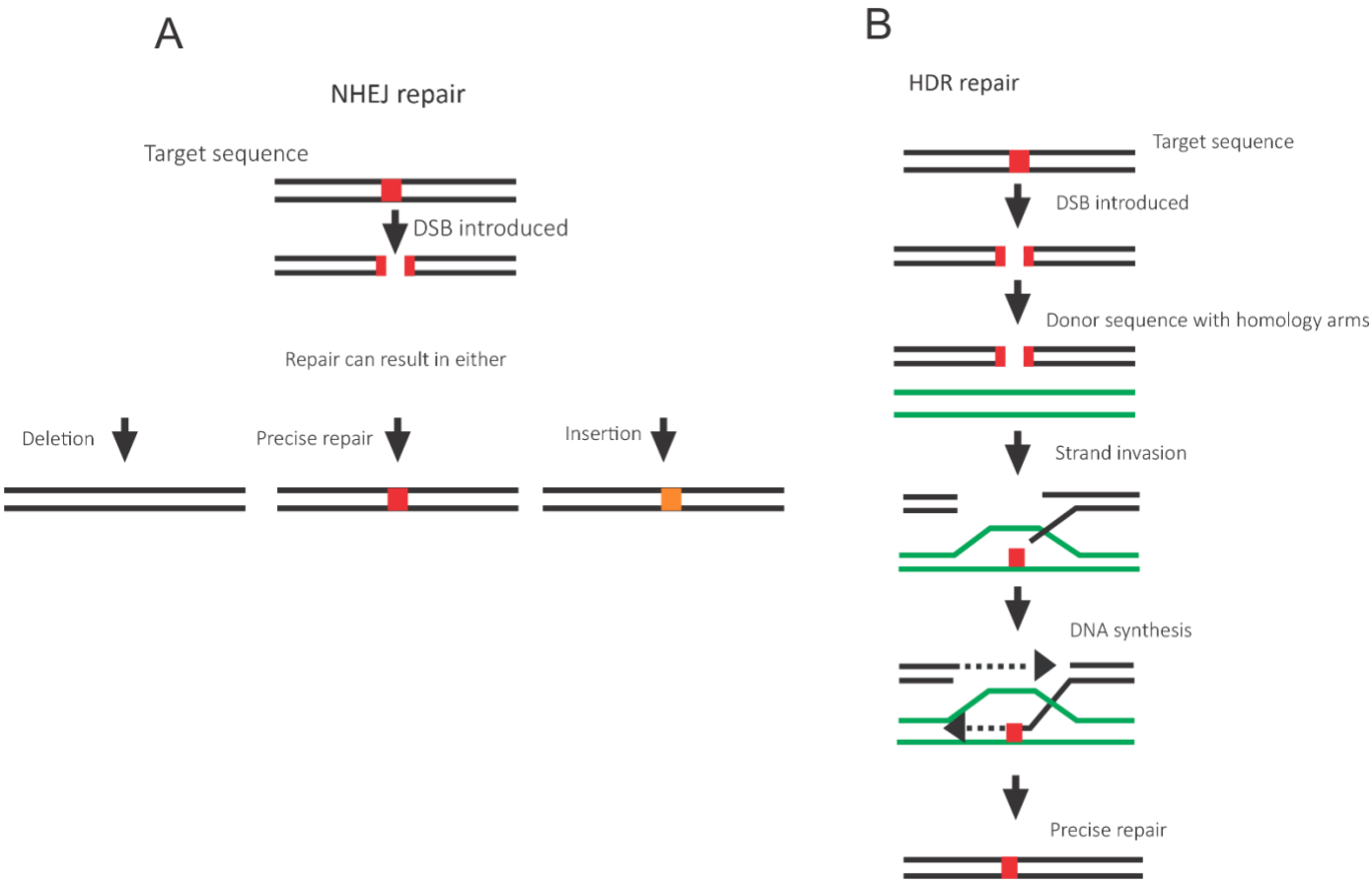


Figure 1. 4: Possible pathways of cellular DNA repair following DSB

(**A**) The error-prone NHEJ repair pathway ligates DSBs with blunt or complementary ends. DSBs that do not have complimentary overhangs are likely to generate indels as it will be filled or resected. The chances of indels increase as repeated cleavage occurs at the same site. The solid black lines represent the target DNA, the red box represents the DSB point and the orange box represents inserted DNA. (**B**) HDR which is less likely to be error-prone ensures that nucleotides are resected from each end of the DSB to produce 3' overhangs. One of the 3 ends from the break invades the donor DNA. The donor DNA serves as template and the 3'end of the break is extended. The extended strand hybridises to the other 3' overhang which also undergoes extension. The ligation of these two strands completes the HDR process. The solid black lines represent the target double-stranded DNA, solid green lines represent donor sequences, the red box represents repaired DNA. Adapted from (Dudáš and Chovanec, 2004).

Mammalian cells with DSBs can induce both pathways, however it is noticeable that the NHEJ pathway is favoured. NHEJ compared to HDR is a less accurate form of repair (Weterings and Chen, 2008). During NHEJ repair the two termini of the damaged DNA strands form compatible ends that can be ligated back together (Weterings and Chen, 2008). This can result in the loss or gain of nucleotides which compromises the genomic integrity of the cell (Weterings and Chen, 2008). It is not yet clear which factors determine the pathway the cell chooses when there is a DSB, however it is proposed that the cell cycle must play a crucial role in the decision (Nowsheen and Yang, 2012).

Gene editing technologies are used to take advantage of the cellular repair mechanisms. Repeated cleavage in the target DNA by the nucleases and repair by NHEJ will eventually lead to insertions and deletions (Schiffer et al., 2012). With this knowledge the use of CRISPR/Cas9 is an attractive approach for antiviral gene therapy. By using the RNA guided nuclease, it can create a DSB at a desired target site to cause mutation in the cccDNA.

1.7 Rationale of the study

Sequence-specific designer nucleases such as CRISPR/Cas9 can be exploited as they may be used to disable the cccDNA of HBV. This is based on the introduction of mutations at a target site in the viral genome. Cleaved DNA is typically repaired by the error prone NHEJ pathway, it leads to insertions and deletions within the target sequence. The modified dead Cas9 system may be employed to silence/repress genes instead of achieving targeted disruption. This presents the CRISPR/Cas9 system as an advantageous strategy to disrupt cccDNA by designing sgRNAs to target the viral genome with the aim to achieve a functional cure. Many *in vitro* studies have been conducted using CRISPR/Cas9 orthologues such as *S. pyogenes*, *Streptococcus thermophilus* and *S. aureus* which achieved targeted disruption of the cccDNA via the NHEJ pathway (Kostyushev et al., 2019, Scott et al., 2017, Ramanan et al., 2015).

Due to the size limitation of the more commonly used *S. pyogenes* CRISPR/Cas9 orthologue, the use of Cas9 orthologue from *S. aureus* is more favourable for packaging and delivery. A study done by Scott et al used the CRISPR/Cas9 orthologue from *S. aureus* with sgRNAs targeting the *S* ORF (Scott et al., 2017). These were efficiently packaged into ssAAVs for delivery in mice. Targeted mutation of viral DNA was observed in an *in vitro* model of infection and anti-HBV efficacy due to HBsAg knockdown, indicated that inactivation of cccDNA was successful (Scott et al., 2017). However, the *in vivo* efficacy of anti-HBV sgRNAs was not demonstrated successfully. Therefore, there is a need to optimise the CRISPR/Cas9 delivery system to *in vivo* models of HBV infection. One approach may be to employ the *S. aureus* Cas9 and designing guide RNAs against other regions of the HBV genome which may have a more potent effect *in vivo*.

1.8 Research Aims and Objectives

Aim: The aim of the study was to design and clone new crRNA sequences that target all ORFs of the HBV genome using the *S. aureus* Cas9 orthologue.

Objectives:

1. To identify cccDNA target binding sites for CRISPR/Cas9 cleavage using *in silico* prediction tools.
2. To clone the newly designed sgRNAs into plasmids encoding either wild type or dead Cas9.
3. To determine *in vitro* antiviral efficacy of newly designed sgRNAs using both the wildtype and dead Cas9 in mammalian cell culture.
4. To assess targeted disruption of cccDNA caused by the CRISPR/Cas9 complex.
5. To measure potential cell toxicity associated with the CRISPR/Cas9 complex.

CHAPTER 2-MATERIALS AND METHODS

2.1 Plasmids

2.1.1 HBV target plasmid (pCH-9/3091)

pCH-9/3091 is an HBV plasmid generated by Nassal and colleagues which was designed to be a replication-competent plasmid (Nassal et al., 1990). This plasmid was used as the target for *in vitro* assessments as it is able to model HBV replication. It comprises a greater-than-genome length HBV sequence (genotype D) that is controlled by the cytomegalovirus (CMV) immediate early promoter/enhancer. Transcription of the greater-than-genome-length sequence produces an RNA that resembles the pgRNA from which viral replication proceeds.

2.1.2 Reporter plasmid (pCMV-eGFP)

The pCMV-eGFP reporter plasmid contains the gene for the enhanced green fluorescent protein (eGFP) (Passman et al., 2000). This plasmid is under the control of a CMV promoter and was used to assess the transfection efficiency in *in vitro* studies. GFP expression was assessed using fluorescence microscopy.

2.1.3 Plasmids encoding SaCas9/dCas9 and HBV target sequences

The pAAV-SaCas9 and pAAV-dSaCas9 expression vectors were derived from a plasmid donated by Dr Feng Zhang (Ran et al., 2013). Each plasmid contains either the sequences for an active SaCas9 or dead (dSaCas9) nuclease expressed by a CMV promoter. The pAAV-dSaCas9 vector contains the D10A and H557A mutations in the nuclease domains and therefore expresses the catalytically inactive SaCas9 (dSaCas9). Both the SaCas9 and dSaCas9 plasmids have a U6sgRNA scaffold that allows the crRNA-encoding sequence to be cloned into the *Bbs*I sites of the plasmid (Figure 2.1).

Together the crRNA and tracrRNA scaffold code for a full sgRNA. The sgRNAs were designed to target various regions on the HBV genome (Figure 2.2).

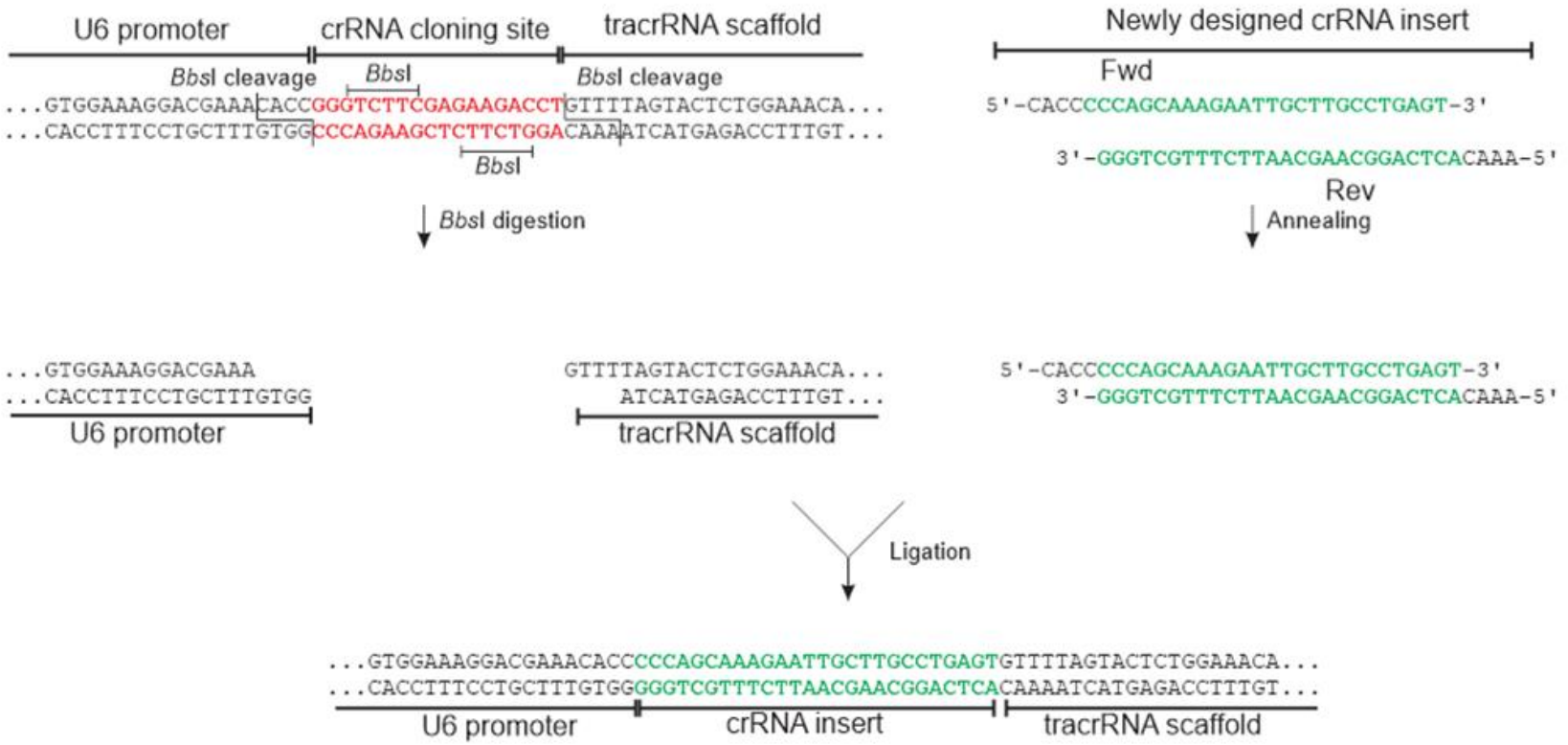


Figure 2.1: Oligonucleotide cloning of the crRNA insert into the pAAV expression vector

The pAAV expression vector has a U6 crRNA cloning site and tracrRNA scaffold with two *Bbs*I restriction sites to facilitate the insertion of the newly designed crRNA insert. The oligonucleotides designed *in silico* have forward and reverse strands that are annealed together and ligated into at the *Bbs*I site of the pAAV expression vector. The forward and reverse oligonucleotides, that make up the crRNA-encoding sequence, have sticky ends complimentary to the *Bbs*I cleavage sites. The resulting expression vector following ligation contains the U6 crRNA insert with the tracrRNA scaffold.

From the original plasmid Dr Feng Zhang designed, Dr Tristan Scott (T. Scott) used *Kpn*I and *Not*I restriction sites to remove the region that contains that U6 sgRNA scaffold with the two *Bbs*I sites (Scott et al., 2017). This was then sub cloned into the pTZ-saU6gRNA-*Bbs*I plasmid where the insertion of the crRNA at the *Bbs*I sites took place. The final cloning step used *Kpn*I and *Not*I to insert the U6 with crRNA insert into the pAAV expression vector which was used throughout this study. The crRNA portion of the sgRNA was designed using the *in silico* tools CRISPR RGEN Tools (http://www.rgenome.net/cas-designer/) and Design sgRNAs for CRISPRko (Broad Institute) (https://portals.broadinstitute.org/gpp/public/analysis-tools/sgrna-design). Based on the input sequence these in-silico tools predict possible crRNA sequences that can be used. Each tool has their own guidelines that are specified which explains the prediction scores. The HBV sequence contained in pCH-9/3091 was used as the input sequence for designing the crRNA. The sequences that were common to both online tools were chosen (Table 2.1). The crRNA-encoding sequences were synthesized as pairs of oligonucleotides (Inqaba Biotec, Pretoria, South Africa) (Table 2.2). When annealed the oligonucleotide pairs form overhangs allowing ligation into the pAAV vectors digested with *Bbs*I (Figure 2.1) (Figure 2.3). Equal amounts of both forward and reverse strands of each oligonucleotide pair, was annealed by denaturing at 95 °C for 5 minutes and allowing the strands to renature by cooling the samples at room temperature.

Table 2.1: Target sites of the selected sgRNAs from *in silico* tools

Target name	Target site (ORF)	Co-ordinates on the HBV genome
sgRNA A1	Core	162 - 187 bp
sgRNA A2	Core	190 - 215 bp
sgRNA A3	Core	199 - 224 bp
sgRNA A4	Core	352 - 377 bp
sgRNA A5	Polymerase	846 - 871 bp
sgRNA A6	Polymerase/Surface	983 - 1008 bp
sgRNA A7	Polymerase/Surface	1257 - 1282 bp
sgRNA A8	Polymerase/Surface	1258 - 1283 bp
sgRNA A9	Polymerase/Surface	1282 - 1307 bp
sgRNA A10	Polymerase/Surface	1764 - 1789 bp
sgRNA A11	Polymerase	2262 - 2287 bp
sgRNA A12	Polymerase	2477 - 2502 bp
sgRNA A13	Polymerase	2632 – 2657 bp
sgRNA A14	HBx	2952 – 2977 bp
sgRNA A15	Core/HBx	3182 - 3207 bp
sgRNA A16	Polymerase/HBx	2727 - 2752 bp
sgRNA A17	Core/HBx	3182 - 3207 bp
sgRNA A18	Core	3193 - 3218 bp
sgRNA A19	HBx	2944 - 2969 bp
sgRNA A20	Polymerase	2255 - 2280 bp
sgRNA-8	Surface	1504 – 1523 bp

*sgRNA-8 sequence designed by Dr Tristan Scott

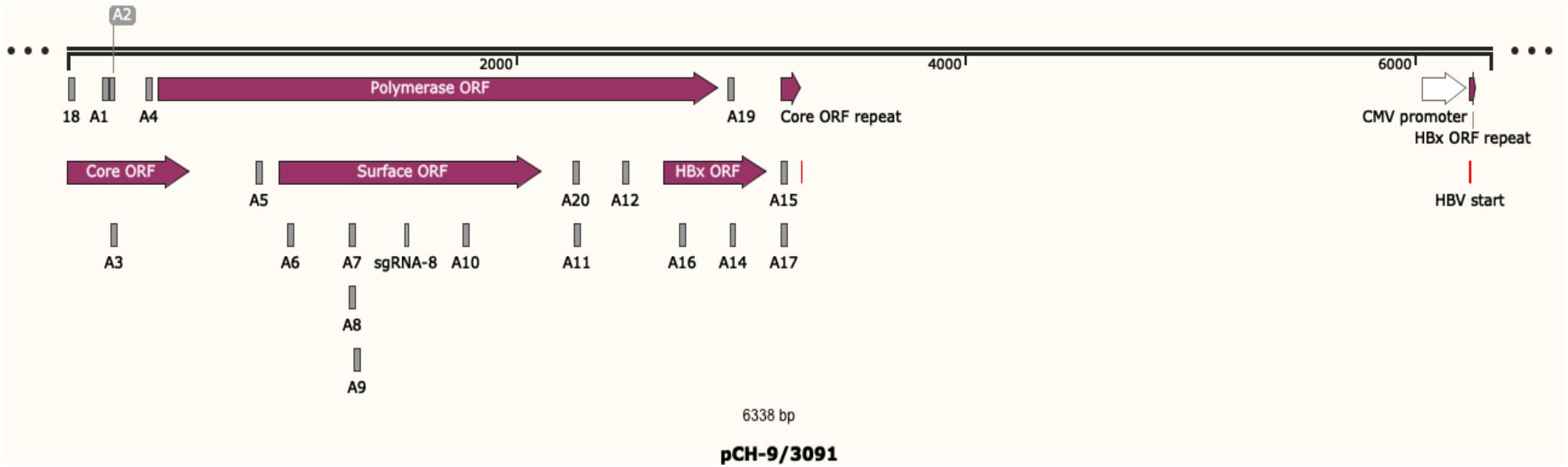


Figure 2.2: Binding sites of sgRNA sequences in the HBV replication-competent plasmid

Schematic representation of the target binding sites in the pCH-9/3091 plasmid. This plasmid was used as the input sequence for designing the panel of sgRNAs shown as A1-A20. These newly designed sgRNAs target all overlapping ORFs shown above. Target binding site for sgRNA-8 is represented in the schematic above.

Table 2.2: HBV sequences encoding the crRNA of sgRNA sequences

RGEN Target 5'-3'	Forward oligonucleotide	Reverse oligonucleotide
sgRNA A1	CACCCCCAGCAAAGAATTGCTTGC**CTGAGT**	AAACACTCAGGCAAGCAATTCTTTGCTGGG
sgRNA A2	CACCGAACTAATGACTCTAGCTAC**CTGGGT**	AAACACCCAGGTAGCTAGAGTCATTAGTTC
sgRNA A3	CACCTTAACACCCACCCAGGTAGC**TAGAGT**	AAACACTCTAGCTACCTGGGTGGGTGTTAA
sgRNA A4	CACCTATTTGGTGTCTTTCGGAGT**GTGGAT**	AAACATCCACACTCCGAAAGACACCAAATA
sgRNA A5	CACCATTTACACACTCTATGGAAG**GCGGGT**	AAACACCCGCCTTCCATAGAGTGTGTAAAT
sgRNA A6	CACCGATCCAACTGGTGGTCGGGA**AAGAAT**	AAACATTCTTTCCCGACCACCAGTTGGATC
sgRNA A7	CACCTTCCACTGCATGGCCTGAGG**ATGAGT**	AAACACTCATCCTCAGGCCATGCAGTGGAA
sgRNA A8	CACCCTCATCCTCAGGCCATGCAG**TGGAAT**	AAACATTCCACTGCATGGCCTGAGGATGAG
sgRNA A9	CACCCAGAGTTTGGTGGAAGGTTG**TGGAAT**	AAACATTCCACAACCTTCCACCAAACTCTG
sgRNA A10	CACCGTGCTGGTTGTTGAGGATCC**TGGAAT**	AAACATTCCAGGATCCTCAACAACCAGCAC
sgRNA A11	CACCGGAAAGTATGTCAACGAATT**GTGGGT**	AAACACCCACAATTCGTTGACATACTTTCC
sgRNA A12	CACCATGACCAAGCCCCAGCCAGT**GGGGGT**	AAACACCCCCACTGGCTGGGGCTTGGTCAT
sgRNA A13	CACCATGGAAACGATGTATATTTG**CGGGAT**	AAACATCCCGCAAATATACATCGTTTCCAT
sgRNA A14	CACCGGTCGGTCGTTGACATTGCT**GAGAGT**	AAACACTCTCAGCAATGTCAACGACCGACC
sgRNA A15	CACCCATGGACATCGACCCTTATA**AAGAAT**	AAACATTCTTTATAAGGGTCGATGTCCATG
sgRNA A16	CACCACCCCGAGAAGGGTCGTCCG**CAGGAT**	AAACATCCTGCGGACGACCCTTCTCGGGGT
sgRNA A17	CACCCATGGACATCGACCCTTATA**AAGAAT**	AAACATTCTTTATAAGGGTCGATGTCCATG
sgRNA A18	CACCAGTAGCTCCAAATTCTTTAT**AAGGGT**	AAACACCCTTATAAAGAATTTGGAGCTACT
sgRNA A19	CACCGTTGACATTGCTGAGAGTCC**AAGAGT**	AAACACTCTTGGACTCTCAGCAATGTCAAC
sgRNA A20	CACCATTGATTGGAAAGTATGTCA**ACGAAT**	AAACATTCGTTGACATACTTTCCAATCAAT
sgRNA-8	CACCGCAAGAATCCTCACAATACCG	AAACCGGTATTGTGAGGATTCTTGC

*Highlighted sequences represent the *Bbs*I overhangs, bold sequences represent the PAM sequence.
*sgRNA-8 oligonucleotides designed by Dr Tristan Scott. This was re-cloned into the linearized pAAV-SaCas9 and dSaCas9 backbone to serve as the positive control for *in vitro* assays in this study.

To linearize the pAAV backbone, all digests were carried out as 20 µl reactions containing 1 µg of plasmid DNA, 1 U of *Bbs*I and 2 µl of 10× Buffer (Thermofisher Scientific, MA, USA). The reaction was carried out at 37 °C for 1 hour. Following the 1 hour incubation, the digestion reactions were resolved on a 1% agarose gel (Appendix 5.2) containing ethidium bromide (0.5 µg/ml) and was imaged using a G:BOX transilluminator (Syngene, Cambridge, UK). The single linearised band of approximately 7000 bp was excised from the gel and purified using the QIAquick® Gel Extraction Kit (Qiagen, Hilden, Germany) (Appendix 5.3). The resulting backbone was subsequently used to ligate crRNA-encoding sequences. The sequences were ligated in a backbone to insert ratio of 1:3 at 22 °C overnight.

Thereafter chemically competent cells were transformed using the ligation mix (Appendix 5.1), plated on Luria Bertani agar (Appendix 5.1) and incubated overnight at 37 °C. A control plate of backbone ligation with no insert was included to check if any self-ligation occurred.

Selected colonies were inoculated in 10 ml of Luria Bertani medium (Appendix 5.1) and incubated overnight at 37 °C with shaking at 150 rpm. Small scale plasmid preparation (Appendix 5.4.1) was carried out on the bacterial cultures following overnight incubation. To confirm the successful ligation of the insert with the backbone, restriction digestions containing 1 µg of plasmid DNA, 1 U of *Not*I and 1 U *BamH*I with 2 µl of 10× Buffer (Thermo Scientific, CA, USA) in 20 µl reactions were carried out. The reaction was incubated at 37 °C for 1 hour then the DNA was resolved on a 1% agarose gel (Appendix 5.2) containing ethidium bromide (0.5 µg/ml) and was imaged using a G:BOX transilluminator (Syngene, Cambridge, UK). Samples (50 ng of each plasmid) that had the correct restriction profiles were sequenced (Inqaba Biotec, Pretoria, South Africa).

The primer 5'- GGTACCTGAGGGCCTATTTCCCATGATTC-3' was used to verify sequences. Sequencing data was analysed using SnapGene® software (from GLS Biotech; available at snapgene.com). For convenient naming purposes, the plasmids generated for this study are identified by either SaCas9 or dSaCas9 with the name of the sgRNA i.e. pSaCas9-A1 or pdSaCas9-A1.

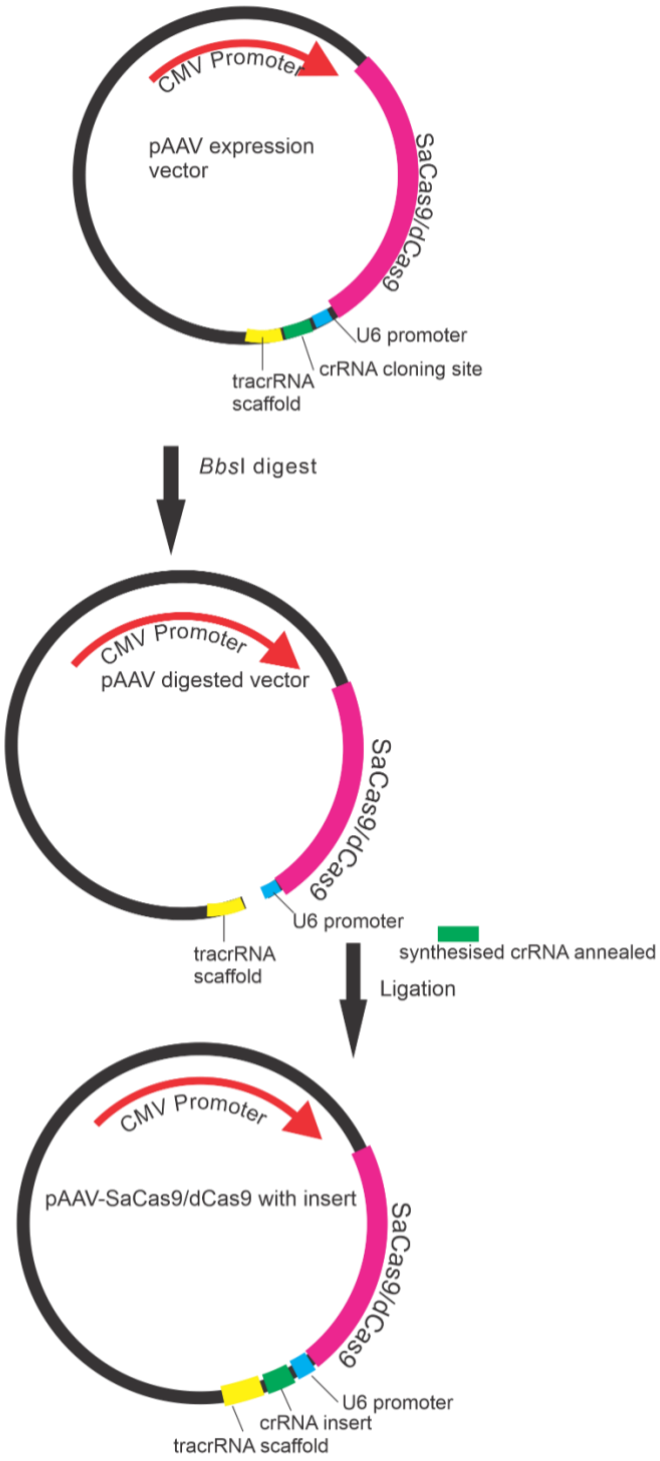


Figure 2.3: Cloning strategy for the generation of the pSaCas9-A1 to A20 and pdSaCas9-A1 to 20 plasmids.

Cloned pSaCas9-sgRNA and pdSaCas9-sgRNA plasmids were generated by digesting the backbone with *Bbs*I to remove a short fragment. This allowed ligation of the crRNA-encoding sequences into the backbone generating the final pAAV-SaCas9-sgRNA plasmid.

2.2 Large-scale plasmid preparations

All positive clones (pSaCas9-A1 to A20 and pdSaCas9-A1 to A20) plasmids, the HBV replication-competent plasmid pCH-9/3091 and reporter plasmid pCMV-GFP were prepared using the QIAGEN Plasmid Maxi Kit (Qiagen, Hilden, Germany) according to the manufacturer's instructions.

A single colony was inoculated into 150 ml of Luria Bertani supplemented with 100 µg/ml of ampicillin (Appendix 5.1). This was incubated overnight at 37 °C with shaking. Following incubation overnight, the bacterial culture was centrifuged at 6000 ×g at 4 °C for 20 minutes. The resulting pellet was re-suspended in 10 ml of buffer P1. Thereafter, 10 ml of buffer P2 was added and mixed gently by inverting the tube 4-6 times; it was then incubated at room temperature for 5 minutes.

Ten millilitres of pre-chilled buffer P3 was added and gently mixed by inverting the tube 4-6 times followed by incubation on ice for 20 minutes. Following this, the samples were centrifuged at 20 000 ×g at 4 °C for 40 minutes. During the centrifugation of the sample, the provided Qiagen-tip 500 column was equilibrated with 10 ml of buffer QBT and was emptied by gravity flow. After centrifugation, the supernatant was added to the column and allowed to enter the resin by gravity flow. The column was washed twice with 30 ml of buffer QC. The Qiagen-tip 500 column was transferred to a sterile 50 ml collection tube. Fifteen millilitres of buffer QF was added to the column to elute the DNA. To precipitate the DNA 10.5 ml of isopropanol was added to the solution that was mixed and centrifuged at 15 000 ×g for 30 minutes at 4 °C. The supernatant was discarded and the pellet washed with 5 ml of 70% ethanol and centrifuged at 15 000 ×g for 20 minutes at 4 °C. The supernatant was discarded and the pellet was allowed to air dry for 5 minutes.

The pellet was re-suspended in 100 µl of ddH_2O and stored at -20 °C. Plasmid concentrations were verified using spectrophotometry (NanoPhotometer® NP80, Implen, Munich, Germany).

2.3 Tissue culture conditions

Liver-derived Human hepatoma 7 (Huh7) and HepG2.2.15 cells were used to assess the efficacy of anti-HBV sgRNAs *in vitro*. Huh7 and HepG2.2.15 cells were cultured in a CellStar® 75cm_2 flask (Greiner Bio-One, Frickenhausen, Germany) using low glucose (1 g/L) for Huh7 and high glucose for HepG2.2.15 (4.5 g/L) Dulbecco's Modified Eagle's Medium (DMEM) (Gibco™, Thermo Scientific, CA, USA), supplemented with penicillin (100 000 U/mL), streptomycin (100 µg/ml) and 10% foetal bovine serum (FBS). Cells were maintained at 37 °C with 5% CO_2. All cells were maintained under these standard conditions for the duration of a study unless stated otherwise. Culturing and passaging of cells described in (Appendix 5.5).

HepG2.2.15 cells contain an integrated greater-than-genome-length HBV sequence. This means they have stable HBV replication and produce infectious virions.

2.4 Detection of anti-HBV sgRNAs and SaCas9 proteins

2.4.1.1 Transfection of Huh7 cells

Huh7 cells were seeded twenty-four hours prior to transfection in a 96-well CellStar® plate (Greiner Bio-One, Frickenhausen, Germany) at approximately 40 000 cells per well made up to 125 µl of complete DMEM (Appendix 5.5). Huh7 cells were transfected with 100 ng of each pSaCas9-sgRNA plasmid using a 1:1 ratio of Lipofectamine™ 3000 (Thermo Scientific, CA, USA) with Opti-MEM (Gibco®, BRL, UK) to DNA. The re-cloned sgRNA-8 plasmid (Scott et al., 2017) contains a guide that successfully targets the *S* ORF. This plasmid was used a positive control.

The pTZ plasmid was used as a negative control. Some wells were transfected with GFP only to determine the transfection efficiency. The transfection was maintained under standard conditions described previously. Transfections were performed in triplicate for each plasmid tested. Forty-eight hours after transfection, immunofluorescence staining was conducted to determine the expression of SaCas9. Transfection efficiency was analysed by GFP expression using a fluorescence microscope 20× magnification (EVOS® FL Cell Imaging System, Thermo Fisher Scientific).

2.4.1.2 Immunofluorescence staining of Cas9 nuclease

The medium was removed from each well and was replaced with 200 µl of 1× phosphate buffered saline (PBS) (Sigma-Aldrich, MO, USA). The PBS was removed and 200 µl of 4% paraformaldehyde (PFA) was used to fix the cells for 15 minutes at room temperature. The PFA was removed and the cells were washed twice with 200 µl of 1× PBS. The cells were then incubated with 200 µl of 0.1% Triton-X (Sigma-Aldrich, MO, USA) in 1× PBS for 10 minutes at room temperature. Triton-X was removed from the cells and washed twice with 200 µl of 1× PBS. The cells were then blocked in 100 µl of 1% bovine serum albumin (BSA) (Roche Applied Science, Mannheim, Germany) in 1× PBS at room temperature for 1 hour in a humidity chamber. One hundred microlitres of mouse anti-HA primary antibody (Abcam, Cambridge, UK) was prepared at a dilution of 1:200 in 1% BSA.

The primary antibody was added to each well and incubated in a humidity chamber for 1 hour at room temperature. The primary antibody was removed before washing the cells twice with 200 µl of 1× PBS. The fluorescently labelled secondary antibody (Alexa Fluor 488, Thermo Scientific, CA, USA), was diluted 1:200 in 1% BSA. This was added to each well and incubated in the dark for 40 minutes at room temperature in a humidity chamber. The secondary antibody was removed, and the cells were washed twice with 200 µl of 1× PBS.

The cells were stained with 100 µl of 1× 4, 6-diamidine-2-phenylindole chloride (DAPI) for 5 minutes at room temperature. DAPI was removed from the cells and washed twice with 200 µl of 1× PBS. To detect a signal from the transfected cells, FITC and DAPI filters were used to detect signal and were imaged using a fluorescence microscope 20× magnification (EVOS® FL Cell Imaging System, Thermo Fisher Scientific).

2.4.2 RNA extraction from transfected Huh7 cells

Twenty-four hours prior to transfection, Huh7 cells were seeded in a 12-well CellStar® plates (Greiner Bio-One, Frickenhausen, Germany) at approximately 80 000 cells per well made up to 500 µl of complete DMEM (Appendix 5.5). Each well was transfected in triplicate with 500 ng pSaCas9 plasmid using Lipofectamine™ 3000 and Opti-MEM (Gibco®, BRL, UK). An untreated pAAV-SaCas9 plasmid with no guide was used as the negative control. The cells were maintained under standard conditions.

Forty-eight hours later the medium was removed from the cells and 500 µl of TRIzol® Reagent (Thermo Scientific, CA, USA) was added to each well and incubated for 5 minutes. The homogenates were transferred to microcentrifuge tubes, 200 µl of chloroform added to each tube and mixed vigorously for 15 seconds. Thereafter the samples were incubated at room temperature for 5 minutes and centrifuged at 12 000 ×g for 15 minutes at 4 °C. Approximately 250 µl of the upper aqueous phase was transferred to a clean microcentrifuge tube. To that an equal amount of absolute isopropanol was added, mixed thoroughly and then incubated at room temperature for 5 minutes.

Following incubation, the samples were centrifuged at 12 000 ×g for 20 minutes at 4 °C. The supernatant was carefully discarded and the resulting pellet was washed in 500 µl of 75% ethanol which was followed by centrifugation at 8000 ×g for 5 minutes. The supernatant was carefully removed and the pellet briefly centrifuged to get rid of residual ethanol.

The pellet was left to air dry for approximately 5 minutes then re-suspended in 50 µl of nuclease-free water. The concentration of the extracted RNA samples was measured by spectrophotometry (NanoPhotometer® NP80, Implen, Munich, Germany).

2.4.3 Reverse transcription of RNA for quantification of anti-HBV sgRNA

Each sample was subjected to a DNase treatment prior to RT-qPCR and performed in triplicate. Each reaction consisted of approximately 1µg of RNA, Nuclease-free water, 10 ×$MgCl_2$ DNase I buffer and DNase I made up to 10 µl. This was incubated at 37 °C for 30 minutes. Following incubation, 1 µl of 50 mM EDTA was added and incubated at 65 °C for 10 minutes. This DNase treated RNA was used for setting up the RT-qPCR. The Luna® Universal One-Step RT-qPCR Kit (New England Biolabs, NJ, USA) was used to reverse transcribe 1 µg of DNase treated RNA extracted from Huh7 cells.

The reaction contained 1 µg of RNA, Luna Universal One-Step Reaction Mix (2X), Luna WarmStart® RT Enzyme Mix (20X), Forward primer (0.4 µM), Reverse primer (0.4 µM) and Nuclease-free water made up to 10 µl. The expression of each sgRNA was calculated relative to the human *glyceraldehyde-3-phosphate dehydrogenase* (h*GAPDH*) housekeeping gene.

The Bio-Rad CFX96™ Real Time System was used and the thermal cycling conditions were set up to be the following: initial denaturation at 95 °C for 10 minutes, 40 cycles of denaturation at 95 °C for 20 seconds, followed by annealing at 58 °C for 20 seconds, extension at 72 °C for 20 seconds. To analyse the results a melting curve was obtained by denaturation at 95 °C for 10 seconds followed by cooling at 65 °C for 1 minute and heating to 95 °C at a ramp rate of 0.1 °C/s with continuous signal acquisition. The data obtained allowed for the RNA expression of each sgRNA to be calculated relative to h*GAPDH*.

Table 2.3: Primers used for RT-qPCR

Target	Forward	Reverse
sgRNA A7	5'-CACCTTCCACTGCATGGC CTGAGGATGAGT-3'	5'AACAAGTTG ACGAGATAAAC-3'
sgRNA A8	5'-CACCCTCATCCTCAG GCCATGCAGTGGAAT-3'	
sgRNA A9	5'-CACCCAGAGTTTGGT GGAAGGTTGTGGAAT-3'	
sgRNA A14	5'-CACCGGTCGGTCG TTGACATTGCTGAGAGT-3'	
sgRNA A19	5'-CACCGTTGACATTGCTG AGAGTCCAAGAGT-3'	
sgRNA-8	5'CACCGCAAGAATCCT CACAATACCG-3'	
h*GAPDH*	5'- GAAGGTGAAGGTCGGAGT-3'	5'-GAAGATGGTGATGGGATTTC-3'

2.5 Assessment of anti-HBV efficacy of newly designed sgRNAs

To assess knockdown of viral replication, 24 hours prior to transfection, Huh7 cells were seeded at 40 000 cells per well in 48-well CellStar® plate (Greiner Bio-One, Frickenhausen, Germany), made up to 250 µl of complete DMEM (Appendix 5.5). Each of the tested SaCas9-sgRNA and dSaCas9-sgRNA plasmids was separately co-transfected with pCH-9/3091 and pCMV-GFP using a 3:1 ratio of PEI Max to DNA. The cells were transfected with 500 ng of sgRNA plasmid, 50 ng of pCH-9/3091 and 50 ng of pCMV-GFP. Twenty-five microlitres of transfection mix was added to the Huh7 cells and maintained under standard conditions. Twenty-four hours after transfection, the medium was removed from each well and replaced by fresh medium.

The transfection efficiency was assessed by analysing GFP expression using fluorescence microscopy at 20× magnification (EVOS® FL Cell Imaging System, Thermo Fisher Scientific). At least 50% transfection efficiency was achieved before moving onto the next assay. Forty-eight hours after transfection an HBsAg enzyme linked immunosorbent assay (ELISA) was carried out on the culture supernatant using the Monolisa™ HBs Ag ULTRA kit (Bio-Rad, CA, USA). One hundred microlitres of the culture supernatant were transferred into a microplate coated with monoclonal anti-HBsAg antibodies. Fifty microlitres of the conjugate solution was added to each well. The microplate was covered with adhesive film and incubated at 37 °C for 1 hour and 30 minutes. Following incubation, the microplate was washed with 1× Wash Buffer using the Immuno Wash™ 1575 Microplate Washer (Bio-Rad, CA, USA). After the wash, 100 µl of the development solution was added to each well and the plate was incubated in the dark for 30 minutes at room temperature. Thereafter the reaction was stopped by adding 100 µl of the stopping solution and incubated at room temperature for 4 minutes. The optical densities (OD) of each sample were measured at 490 and 655 nm using the iMark™ Microplate Reader (Bio-Rad, CA, USA).

2.6 Evaluation of toxicity associated with gene products of anti-HBV plasmids

A 3-(4,5-dimethylthiazol-2-yl)-2,5-diphenyltetrazolium bromide (MTT) assay was carried out to determine cell viability after treatment with pSaCas9 and pdSaCas9-sgRNA plasmids. Huh7 cells were seeded into a 96-well plate CellStar® plates (Greiner Bio-One, Frickenhausen, Germany) twenty-four hours prior to transfection. Each well was made up to 125 µl of complete DMEM (Appendix 5.5. The cells were transfected in triplicate with each pSaCas9 or pdSaCas9-sgRNA plasmid (80 ng), pCH-9/3091 (8 ng) and reporter plasmid pCMV-GFP (8 ng). Lipofectamine™ 3000 and Opti-MEM (Gibco®, BRL, UK) was used to co-transfect the cells.

Three controls were used in this assay. An untransfected control which consisted of cells that received no DNA, cells treated with 50% dimethyl sulfoxide (DMSO) as a positive control and a mock pTZ plasmid as negative control. Untreated cells should maintain cell viability while DMSO is known to cause toxicity in cells.

Forty-eight hours after transfection, the media was removed from the wells and 20 µl of 3-(4, 5-Dimethylthiazol-2-yl)-2, 5 diphenyltetrazolium Bromide (MTT) solution (5 mg/ml) in 1× Phosphate Buffered Saline (PBS) was added to each well. The plate was incubated at 37 °C and 5% CO_2 for 1 hour. The resulting purple formazan by-product was solubilised in 200 µl of DMSO. The optical density (OD) was measured using the iMark™ Microplate Reader (Bio-Rad, CA, USA) at 570 and 650 nm.

2.7 Assessment of targeted disruption with anti-HBV sgRNA and Cas9 complex

2.7.1 Transfection of HepG2.2.15 cells

Twenty-four hours prior to transfection, HepG2.2.15 cells were seeded in a 24-well CellStar® plate (Greiner Bio-One, Frickenhausen, Germany) at 40 000 cells per well made up to 500 µl of complete DMEM (Appendix 5.5). Two hours prior to transfection the culture supernatant was harvested. Lipofectamine™ 3000 and Opti-MEM (Gibco®, BRL, UK) was used to co-transfect the cells. The transfection mix included 250 ng of each sgRNA plasmid being tested and 50 ng of pCMV-GFP plasmid. The transfections were performed in triplicate. Twenty-four hours after transfection the growth medium was replaced. Medium (100 µl) was kept from the first (day 3), second (day 8) and third (day 14) transfections and used for ELISA. Five days post transfection the growth medium was removed, and cells were washed with 200 µl of saline/EDTA solution. This was removed and another 200 µl of saline/EDTA solution was added to each well.

The plate was incubated under standard conditions for 5 minutes after which the solution was removed and replaced with 100 µl of TrypLE Express (Gibco™, Thermo Scientific, CA, USA). The plate was incubated under standard conditions as before for 5 minutes. After the incubation period 900 µl of growth medium was added to the cells and re-suspended. From that, 500 µl of medium with re-suspended cells was transferred to a clean 1.5 ml microcentrifuge tube. The remaining cells were used to re-seed the 24 well plate. The harvested triple transfected cells were stored at -20 °C.

2.7.2 DNA Extraction from HepG2.2.15 cells

To confirm targeted disruption at the intended site, DNA was extracted from the transfected cells using the QIAamp® DNA Blood Mini Kit according to the manufacturer's instructions (Qiagen, Hilden, Germany). Triple transfected HepG2.2.15 cells were pelleted and re-suspended in 200 µl of saline. Twenty microlitres of proteinase K was added and the mixture was mixed vigorously by pulse vortexing for 15 seconds. Two hundred microlitres of buffer AL was added to each sample and pulse vortexed for 15 seconds. All samples were incubated at 56 °C for 10 minutes. Following incubation, the samples were centrifuged briefly. Two hundred microlitres of 98-100% ethanol was added to the mixture and pulse vortexed for 15 seconds. The mixture was transferred to the provided spin column and centrifuged at 6000 ×g for 1 minute and the flow-through discarded. Five hundred microlitres of buffer AW1 was added to each column and centrifuged at 6000 ×g for 1 minute.

The flow-through was discarded and 500 µl of buffer AW2 was added to each spin column and was centrifuged at 20 000 ×g for 3 minutes. The flow-through was discarded, the spin column was transferred to a new collection tube and centrifuged at 20 000 ×g for 1 minute. The spin column was placed into a clean 1.5 ml microcentrifuge tube and 200 µl of ddH_2O was added to the column and incubated for 5 minutes at room temperature.

The columns were centrifuged at 6000 ×g for 1 minute. DNA concentrations were measured spectrophotometrically (NanoPhotometer® NP80, Implen, Munich, Germany).

2.7.3 Surveyor assay

To determine whether targeted disruption was achieved by the CRISPR/Cas9 complex, a Surveyor assay was performed which employs a celery endonuclease I (Cel1 enzyme). This enzyme cleaves heteroduplexes formed during annealing reactions. These may be indicative of introduced mutations.

2.7.3.1 Preparation of the Cel1 enzyme

Cel1 enzyme was provided by Professor Patrick Arbuthnot and prepared using the following protocol: Store bought celery of approximately 0.5 kg was juiced at 4 °C and adjusted to a concentration of 1 M with Tris-HCl, pH 7.7, 100 µM Phenylmethylsulfonyl fluoride (PMSF). This was centrifuged at 2600 ×g. The resulting supernatant was saturated to 25% in $(NH_4)_2SO_4$ and mixed for 30 minutes at 4°C. This mixture was centrifuged at 13 000 – 16 200 ×g for 40 minutes at 4 °C. The supernatant was adjusted to 80% $(NH_4)_2SO_4$ and mixed for 30 minutes at 4°C. The mixture was centrifuged at 13 000 – 16 200 ×g for 1.5 hours. The resulting pellet was suspended in 0.1 M Tris-HCl, pH 7.7, 100 µM PMSF. The mixture was transferred to a dialysis tube with a 10 000 MW cut off. The mixture was dialysed against a total of 32 L of the same buffer with 4 changes over 4 hours. Extracted aliquots were stored at -80 °C (Till et al., 2004).

2.7.3.2 Amplification of sgRNA target site

Sequences approximately 300 bp upstream and downstream of the predicted target site for each sgRNA was amplified by PCR. This produced an amplicon of approximately 600 bp. The PCR mix included 12.5 µl of Taq DNA Polymerase 2× Master Mix (Ampliqon, Denmark), 10 pmol of forward and reverse primers, 5 µl of the template DNA and nuclease free water up to 25 µl.

The PCR was performed using the Bio-Rad T100™ Thermal Cycler with the following conditions: the initial denaturation at 95 °C for 15 s, annealing at 60 °C for 15 s, extension at 72 °C for 15 s, the final elongation at 72 °C for 5 minutes and cooling at 4 °C for 35 cycles. To the PCR products, 2 µl of 6 × orange loading dye was added.

The PCR products were then resolved on a 1.5% agarose gel (Appendix 5.2) containing 0.25% ethidium bromide. PCR products were imaged using the G: Box UV transilluminator (Syngene, Cambridge, UK) (Appendix 5.8). The PCR products were purified using the QIAquick® Gel Extraction Kit and eluted in 35 µl of ddH_2O. The concentration of DNA was determined using spectrophotometry (NanoPhotometer® NP80, Implen, Munich, Germany). The PCR amplicons were subjected to the Cel1 enzyme (Oleykowski et al., 1998, Till et al., 2004) .

2.7.3.3 Cel1 reaction

The Cel1 reaction consisted of 200 ng of PCR amplified DNA, 1× NEB Buffer 2 (New England Biolabs, NJ, USA) and ddH_2O to a final volume of 12 µl. The reaction was performed under the following conditions: denaturation at 95 °C followed by cooling to 35 °C at a ramp rate of -0.1 °C/s holding at 35 °C for 2 minutes. The samples were removed afterwards and 1 µl of Cel1 enzyme was added to the samples while 1 µl of ddH_2O was added to the control samples. The samples were returned to the thermocycler and incubated at 45 °C for 5 minutes then cooled to 4 °C. To the products, 2 µl of 6 × orange loading dye was added. The products were resolved on a 2% agarose gel (Appendix 5.2) containing 0.25% ethidium bromide and imaged using the G: Box UV transilluminator (Syngene, Cambridge, UK). Densitometry analysis was performed using ImageJ software.

Percentage targeted disruption was calculated using the following equation (Sentmanat et al., 2018):

$$\text{Targeted cleavage} = 100 \times \left[1 - \left(1 - \frac{Fraction\ cleaved}{Fraction\ uncleaved + Fraction\ cleaved}\right)^{\frac{1}{2}}\right]$$

Table 2.4: Primers used for Surveyor Assay

Target	Forward	Reverse
sgRNA A7, A8 & A9	5'- GGGGCAGAA TCTTTCCACCA-3'	5'- CCCGCCTGTA ACACGAGAAG-3'
sgRNA A14 &19	5'- GTTTACGTCC CGTCGGCGCT-3'	5'- GCGCAGACCA ATTTATGCCT-3'
sgRNA-8	5'- CCTCAGGCCAT GCAGTGGAA-3'	5'- GTAGTCATGC AGGTCCGGCA-3'

CHAPTER 3-RESULTS

3.1 Construction of wild type Cas9 anti-HBV sgRNA plasmids

Anti-HBV sgRNA plasmids were cloned using the wild type SaCas9 plasmid (Figure 3.1A) to insert the newly designed crRNA oligonucleotide sequences. The sgRNAs were designed to target various regions of the HBV genome (*S*, *C*, *P* and *HBx* ORF). The plasmid contains an open reading frame encoding the *S. aureus*-derived Cas9 nuclease which is expressed by the CMV promoter (Figure 3.1A). The wildtype SaCas9 plasmid was digested with *Bbs*I to remove a small fragment of approximately 22 bp to facilitate the insertion of the crRNA sequences. This digest yielded one visible band at approximately 7400 bp and another of 22 bp that was too small to be seen on the agarose gel (Figure 3.1B). This resulting band is a linearised plasmid backbone that still contains the sequences encoding SaCas9 and U6 promoter for the guide expression. The oligonucleotides (forward and reverse strands) that encode the crRNA were annealed and ligated into the plasmid backbone to form the complete pAAV vector with Cas9 as well as the guide sequence expressed by their respective promoters. Positive clones were identified by digestion with *Not*I and *Bam*HI which yielded two bands at approximately 7000 bp and 700 bp (Figure 3.1C). A total of 20 different crRNA sequences were cloned into plasmids with wild type SaCas9. Sequencing confirmed that the cloning was successful and that the inserted crRNAs had the correct sequences (Appendix 5.6).

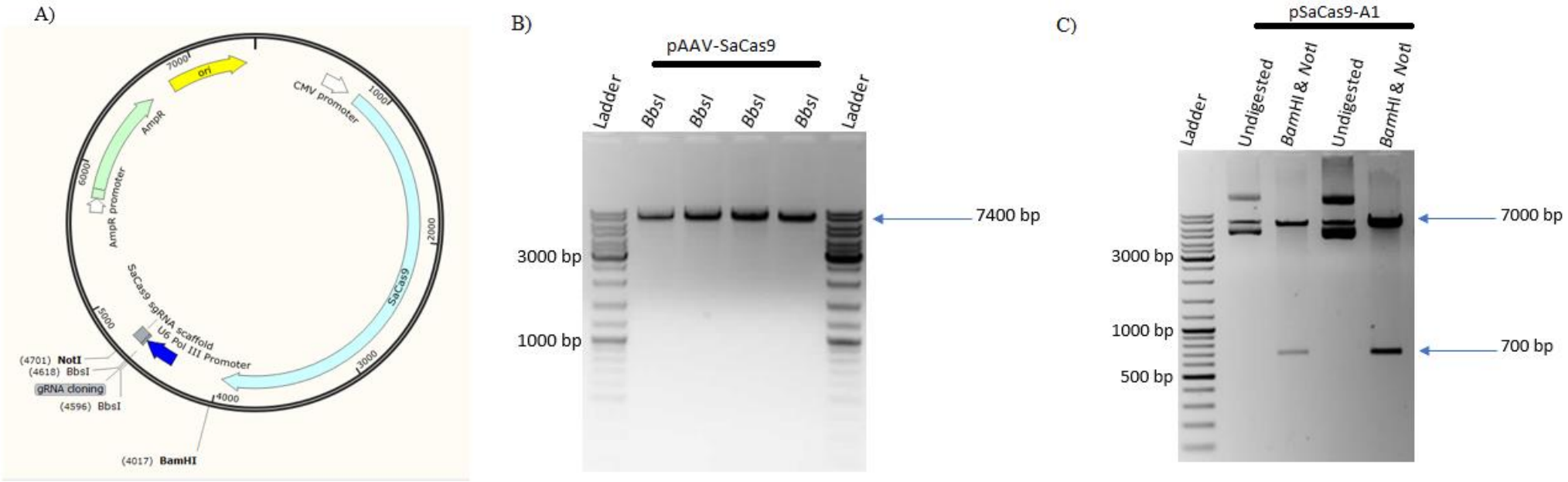


Figure 3.1: Generation of the wild type SaCas9 pAAV plasmid

A) The pAAV-SaCas9 plasmid map indicating the enzyme restriction sites that were used in the cloning process. In between the two *Bbs*I sites is the gRNA cloning site that was initially removed to ligate the newly designed crRNA. B) The vector was digested with *Bbs*I resulting in a linear backbone of approximately 7400 bp. Lane 1 represents the GeneRuler 10 kb DNA ladder, lane 2-5 represents the plasmid digested with *Bbs*I and lane 6 represents the GeneRuler 10 kb DNA ladder. C) Screening for positive clones was carried out by a digesting with *Bam*HI and *Not*I. The resulting bands were approximately 7000 bp and 700 bp. Lane 1 represents GeneRuler 10 kb DNA ladder, lane 2 and 4 represents the undigested plasmid, lane 3 and 5 plasmids the digested plasmid with *Bam*HI and *Not*I. This single gel is a representation of two different pSaCas9-A1 clones that were screened. All other cloned plasmids (pSaCas9-A2 to A20) produced the same result.

3.2 Construction of inactive Cas9 anti-HBV sgRNA plasmids

The inactive/dead SaCas9 (pdSaCas9) plasmid carries a Cas9 nuclease sequence with mutations in its catalytic domains to inactivate its cleaving capabilities. These are the D10A and H557A mutations in the nuclease. The Cas9 nuclease is guided by the sgRNA sequence however cleavage will not occur at the targeted site, it only binds. In this way there is no expectation of targeted disruption, however it may act as a silencer/repressor. To clone the dSaCas9 plasmids, the positively confirmed wild type SaCas9 plasmids and the dSaCas9 plasmid were both digested with *Not*I and *Bam*HI. As previously described the plasmids yielded two bands of approximately 7000 bp and 700 bp (Figure 3.2A). The 700 bp bands (that contain the guide sequences) from the wild type SaCas9 plasmid and the 7000 bp from the dSaCas9 (that contains the dead nuclease sequence) were gel extracted. The 700 bp fragments encoding the different sgRNAs were separately cloned into the dSaCas9 plasmid backbone to produce the catalytically inactive anti-HBV sgRNA plasmids. A total of 20 crRNA sequences were cloned with the inactive dSaCas9. Positive clones were identified by digest with *Not*I and *Bam*HI (Figure 3.2B). Sequencing data of positive clones with the correct sequence are attached (Appendix 5.6).

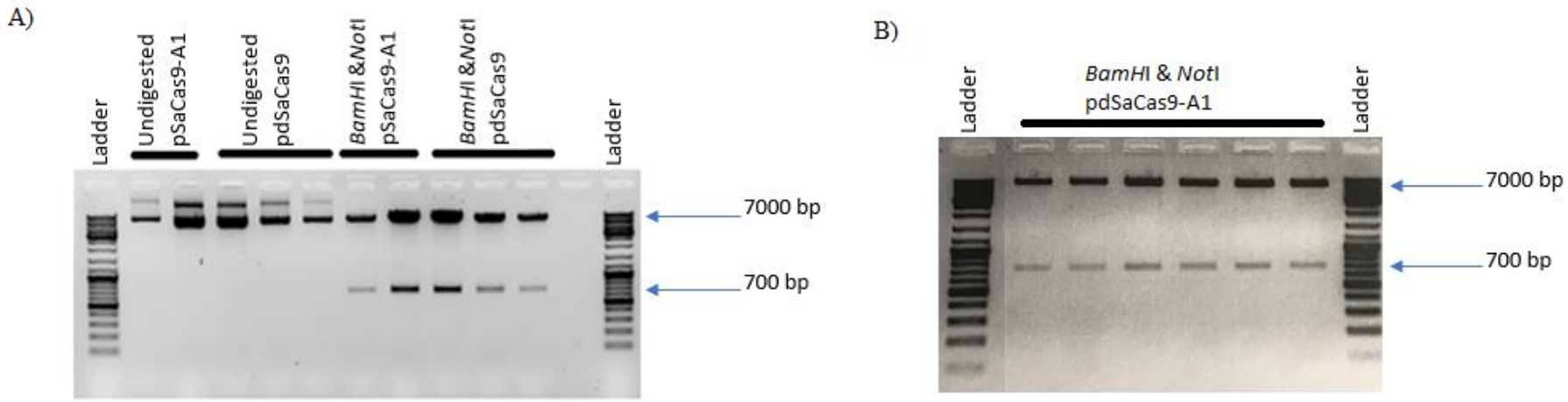


Figure 3.2: Enzymatic digestion of inactive dSaCas9 plasmid

A) A positive clone of the wild type SaCas9-A1 plasmids was digested with *Not*I and *Bam*HI, separated by agarose gel electrophoresis and the 700 bp fragment extracted. This fragment contains the correct crRNA sequence for ligation into the pdSaCas9 linearised plasmid (7000 bp gel extracted fragment), to create pdSaCas9-A1. The gel above is a single representation of how all the plasmids were generated. B) The pdSaCas9-A1 plasmid was digested with *Bam*HI and *Not*I to screen for positive clones. This single gel is a representation of 6 different pdSaCas9-A1 clones that were screened. All other cloned plasmids (pdSaCas9-A2 to A20) produced the same result. Ladder (GeneRuler 10 kb DNA ladder).

3.3 Expression of CRISPR/Cas9 system *in vitro*

3.3.1 SaCas9 nucleases are expressed efficiently in liver-derived cells

To examine the expression of the Cas9 nuclease, liver-derived Huh7 cells were transfected with wild type SaCas9 plasmids. Immunofluorescence detection of the HA tag was carried out using a primary antibody against the HA epitope as well as a fluorescently labelled secondary antibody (Alexa Fluor 488, Thermo Scientific, CA, USA) to stain the Huh7 cells. A mock transfection using the pTZ plasmid was used as a negative control and a separate pCMV-eGFP transfection was performed to confirm whether the transfection was successful. A plasmid that was prepared in our laboratory (sgRNA-8) was included as the positive control (Scott et al., 2017). The transfections were carried out in triplicate to confirm reproducibility. Detection of GFP expression by fluorescence microscopy confirmed the transfection was successful (Figure 3.3). Each of the tested SaCas9-sgRNA plasmids revealed expression of the Cas9 nuclease which was comparable to the positive control. Only a few SaCas9-sgRNA plasmids are represented in the figure below, as the pool of tested SaCas9 plasmids were narrowed. As expected, there was no expression seen in the negative control. The results (Figure 3.3) confirm that in each transfection that was conducted, the expression of the Cas9 nuclease was successful.

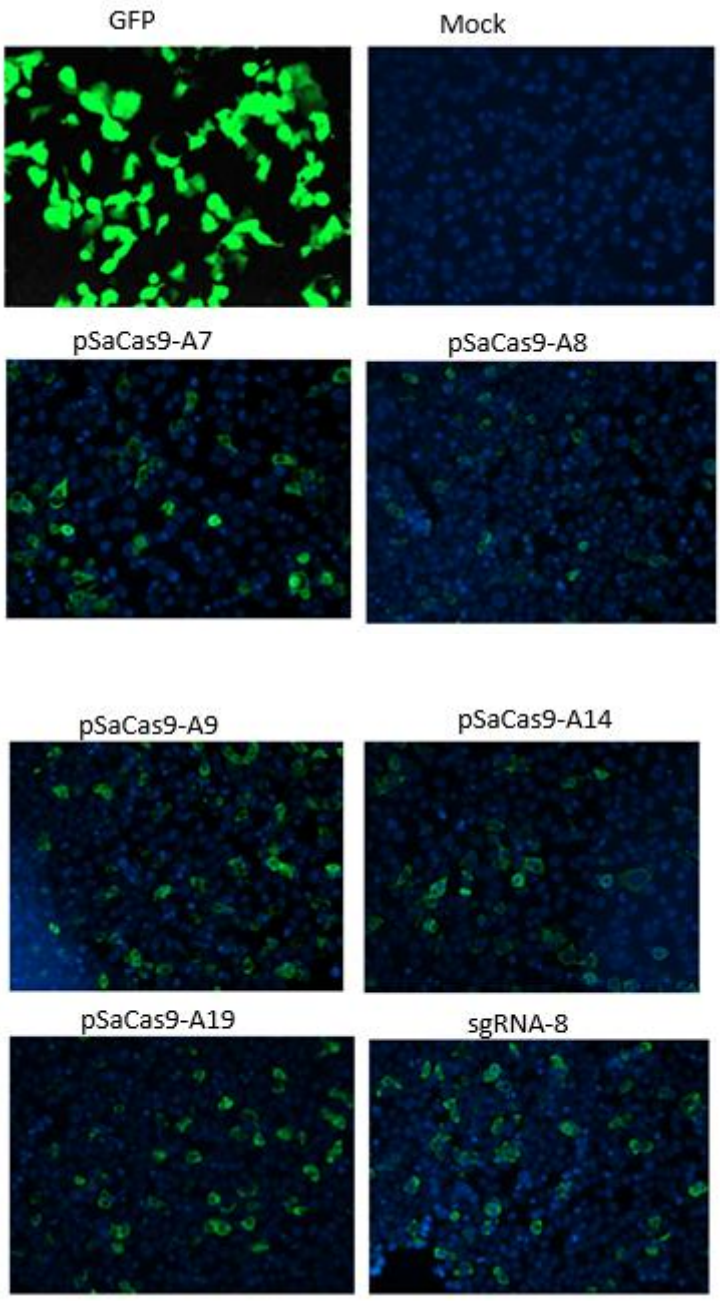


Figure 3.3: Detection of expressed Cas9 nuclease by immunofluorescence staining in Huh7 cells transfected with SaCas9 plasmids

Immunofluorescence staining was carried out to confirm the expression of the Cas9 nuclease from the SaCas9 plasmids. Huh7 cells were transfected with the indicated SaCas9 plasmids. A GFP transfection was included to confirm transfection efficiency. A mock transfection using pTZ was also included. The monoclonal anti-HA primary antibody together with a fluorescently labelled secondary antibody was used for Cas9 nuclease detection. DAPI was used to counterstain the nuclei. The cells were then visualised using fluorescence microscopy at 20× magnification.

3.3.2 Expression of pAAV-SaCas9 sgRNA sequences *in vitro*

To verify whether the sgRNA sequences are being expressed *in vitro*, RNA levels were measured using reverse transcription quantitative PCR (RT-qPCR). RT-qPCR was performed on RNA that was extracted from liver-derived Huh7 cells. The cells were transfected with the wild type SaCas9 plasmids expressing the different sgRNA sequences (A7, A8, A9, A14, A19). These sequences were chosen complimentary to the above experiment. A mock transfection using the pTZ plasmid was included. A transfection using the sgRNA-8 plasmid was included as a positive control. The RNA levels of each sgRNA was measured relative to the housekeeping gene human *glyceraldehyde-3phosphate dehydrogenase* (h*GAPDH*) mRNA (Figure 3.4). Expression of each sgRNA sequence was determined using different primer sets described in Table 2.3. As different primer sets were used to detect the different sgRNAs the expression levels cannot be compared. This is highlighted by sgRNA-8 levels which worked well but is expressed at the "lowest" levels.

The results show that each plasmid expressed its respective sgRNA sequences *in vitro*. Previous results have also confirmed the successful expression of the Cas9 nuclease. Together these results confirm that each component required for the CRISPR/Cas9 system was expressed in each *in vitro* assessment.

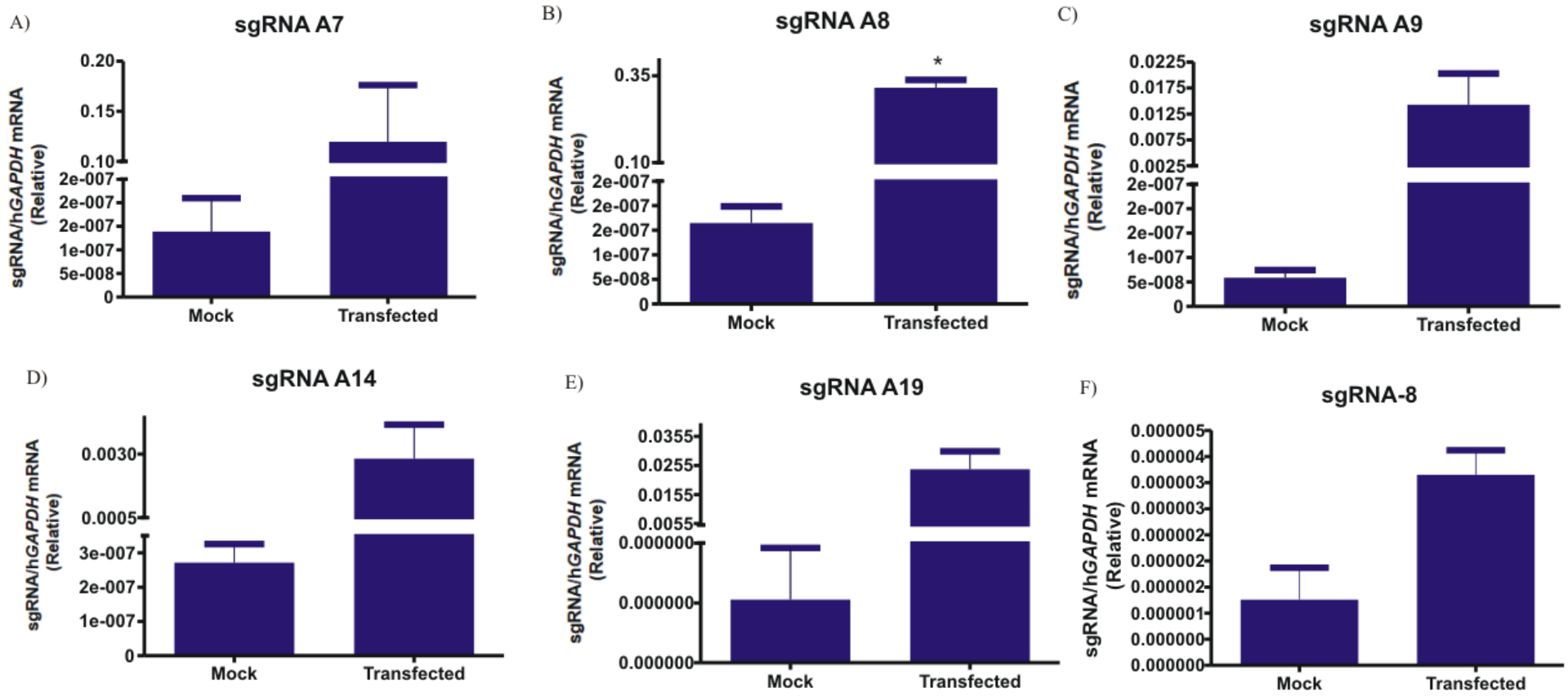


Figure 3.4: RNA expression profiles of sgRNAs relative to h*GAPDH*

To evaluate the expression of each sgRNA *in vitro*, Huh 7 cells were transfected with pAAV-SaCas9-sgRNA plasmids. A mock transfection was included (A-F). Expression of each sgRNA was calculated relative to h*GAPDH* mRNA. The error bars indicate SEM (n=3), * indicates $p < 0.05$.

3.4 Surface antigen knockdown assay to assess the efficacy of anti-HBV plasmids

Since the Cas9 nuclease and sgRNAs are expressed, the efficacy of CRISPR-mediated HBV surface antigen knockdown was tested in Huh7 cells. The Huh7 cells were co-transfected with each SaCas9 plasmid expressing the different sgRNA sequences as the effector. Each transfection also included the HBV replication-competent plasmid pCH-9/3091 which acts as the target for gene editing and the pCMV-GFP reporter plasmid to check whether the transfection was successful. A mock transfection was included where there is no knockdown expected and the plasmid sgRNA-8 was used as positive as it is known to cause significant knockdown (Scott et al., 2017). For reproducibility, each transfection of the different SaCas9 plasmids was carried out in triplicate. HBsAg knockdown was determined by performing an ELISA from the medium that was removed from the transfected cells. The optical densities (OD) of each sample were measured at 490 and 655 nm using the iMark™ Microplate Reader (Bio-Rad, CA, USA).

In the initial screening process of all the pSaCas9-sgRNA plasmids there was no significant knockdown of HBsAg observed in the transfected Huh7 cells (Figures 3.5-3.8). Since the ELISA measures HBsAg this result was expected for the sgRNA sequences which do not target the *S* ORF directly (Figure 3.5, 3.6, 3.8). The result was unexpected however, for the sgRNA sequences that did target the *S* ORF (Figure 3.7). Positive control sgRNA-8 which targets the *S* ORF exhibited significant knockdown of HBsAg ranging between 50-70 % reduction. Some of the transfected SaCas9 plasmids seem to increase HBsAg, however it is not statistically significant. Taken together the results show that the anti-HBV sgRNA plasmids were not efficient to cause knockdown of HBsAg in liver-derived cells.

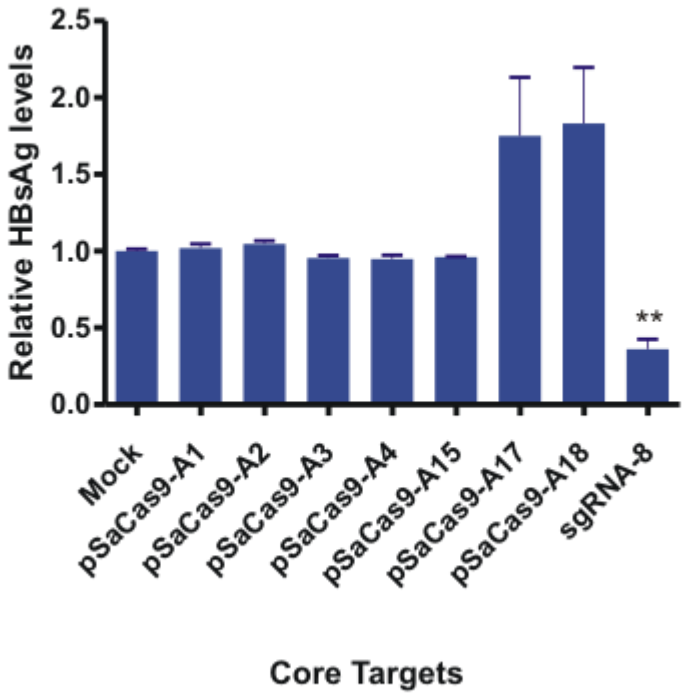


Figure 3.5: Assessment of core anti-HBV sgRNA-mediated knockdown of HBsAg in liver-derived cells

To assess the efficacy of the newly designed sgRNA sequences with the Cas9 system, Huh7 cells were co-transfected with pCH-9/3091, pCMV-GFP and the SaCas9 plasmids. Each sgRNA sequence targeting the *C* ORF was determine relative to a mock. A SaCas9 plasmid with no guide sequence served as the mock and sgRNA-8 as a positive control. ELISA was conducted on supernatants collected from cells 48 hours after transfection. Transfections were carried out in triplicate. The error bars indicate the standard error of the mean (SEM) (n=3), ** indicates $p < 0.01$.

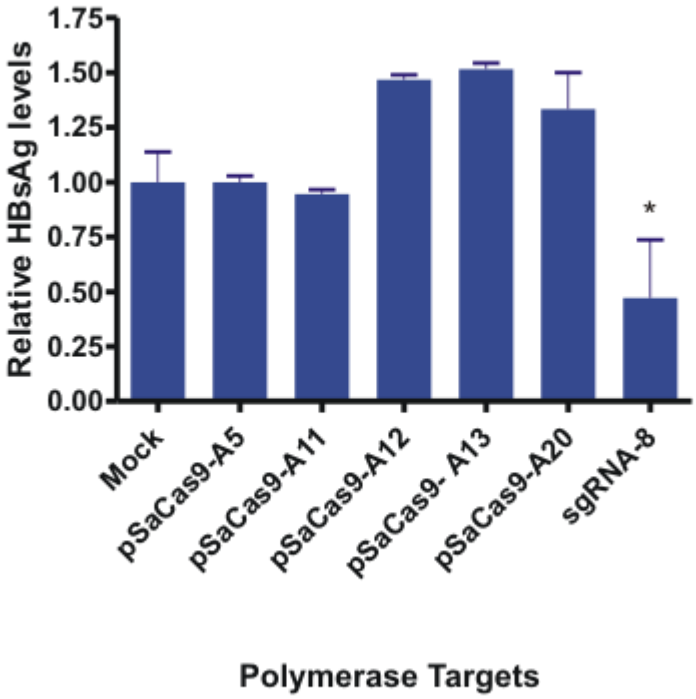


Figure 3.6: Assessment of polymerase anti-HBV sgRNA-mediated knockdown of HBsAg in liver-derived cells

To assess the efficacy of the newly designed sgRNA sequences with the Cas9 system, Huh7 cells were co-transfected with pCH-9/3091, pCMV-GFP and the SaCas9 plasmids. Each sgRNA sequence targeting the *P* ORF was determined relative to a mock. A SaCas9 plasmid with no guide sequence was used as the mock and sgRNA-8 plasmid used as a positive control. ELISA was conducted on supernatants collected from cells 48 hours after transfection. Transfections were performed in triplicate. The error bars indicate the standard error of the mean (SEM) (n=3), * indicates $p < 0.05$.

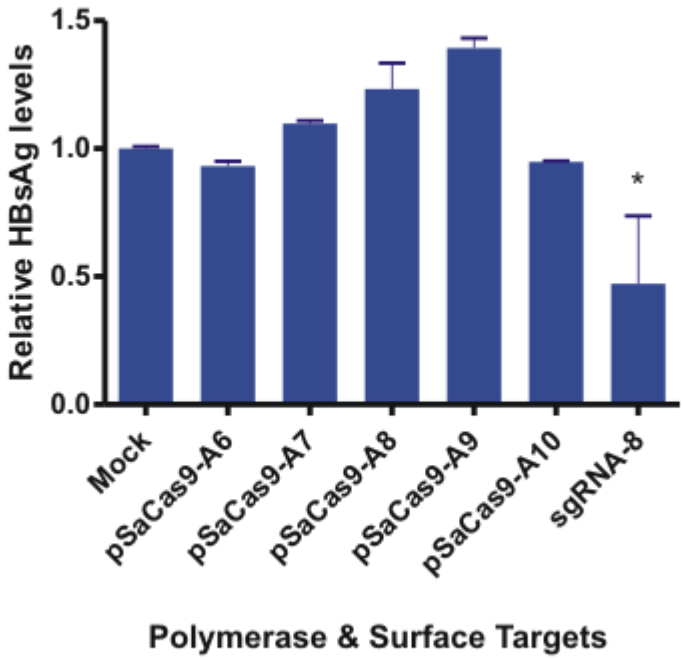


Figure 3.7: Assessment of polymerase/surface anti-HBV sgRNA-mediated knockdown of HBsAg in liver-derived cells

To assess the efficacy of the newly designed sgRNA sequences with the Cas9 system, Huh7 cells were co-transfected with pCH-9/3091, pCMV-GFP and the pSaCas9 plasmids. Each sgRNA sequence targeting the *P*/*S* ORF was determined relative to a mock. A SaCas9 plasmid with no guide sequence used as the mock and sgRNA-8 served as the positive control. ELISA was conducted on supernatants collected from cells 48 hours after transfection. Transfections were carried out in triplicate. The error bars indicate the standard error of the mean (SEM) (n=3), * indicates $p< 0.05$.

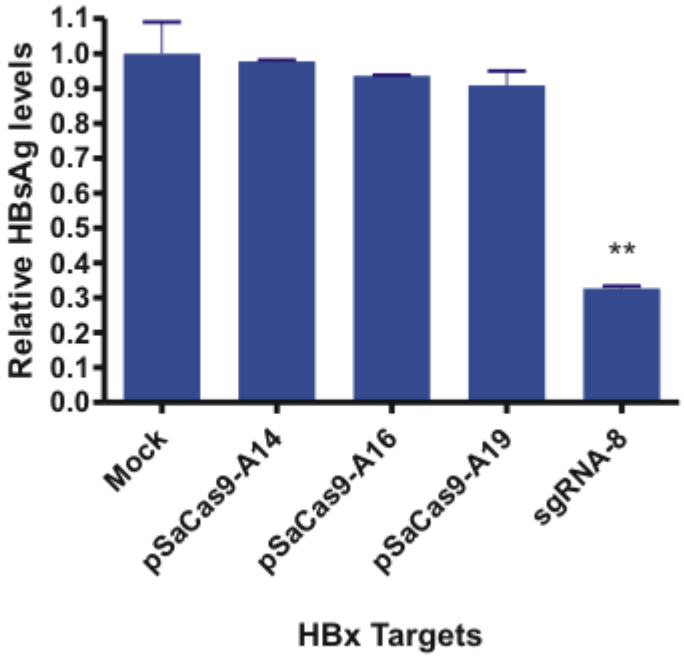


Figure 3.8: Assessment of HB*x* anti-HBV sgRNA-mediated knockdown of HBsAg in liver-derived cells

To assess the efficacy of the newly designed sgRNA sequences with the Cas9 system, Huh7 cells were co-transfected with pCH-9/3091, pCMV-GFP and the SaCas9 plasmids. Each sgRNA sequence targeting the *HBx* ORF was determined relative to a mock plasmid. The mock was a SaCas9 plasmid with no guide sequence and sgRNA-8 was used as the positive control. ELISA was conducted on supernatants collected from cells 48 hours after transfection. Transfections were performed in triplicate. The error bars indicate the standard error of the mean (SEM) (n=3), ** indicates $p< 0.01$.

3.5 Inactive SaCas9 anti-HBV sgRNA plasmid's effect on HBsAg secretion

The plasmid expressing a dead Cas9 (pdSaCas9) has no catalytic cleavage abilities. This is a result of the mutations that were introduced in the nuclease that disable catalytic cleavage. However, these plasmids exhibit the potential to inhibit viral transcription having a silencing effect without the introduction of mutations. Liver-derived Huh7 cells were co-transfected with pCH-9/3091, pCMV-GFP and a panel of the plasmids expressing an inactive Cas9 (pdSaCas9). A mock transfection was included using a dSaCas9 plasmid that has no guide sequence. The sgRNA-8 and inactive dSaCas9-sgRNA-8 were used as the positive control (Scott et al., 2017). Cells were also transfected with the active Cas9 plasmids for comparability purposes. For reproducibility each transfection for the different SaCas9 and dSaCas9 plasmids was performed in triplicate. HBsAg knockdown was determined by performing an ELISA from the medium that was removed from the transfected cells. The result observed in Figure 3.9 was similar to the previous results Figure 3.5-3.8 which showed that plasmids expressing an active Cas9 protein had no effect on HBsAg knockdown. As discussed before, this result is surprising as the nuclease in these plasmids does have catalytic cleavage capabilities. There was no HBsAg knockdown observed in the dSaCas9 plasmids which revealed that they do not have any transcriptional silencing effect on HBsAg expression. The positive sgRNA-8 plasmid achieved significant knockdown of approximately 80% while the dsgRNA-8 showed no transcriptional silencing effect on HBsAg expression.

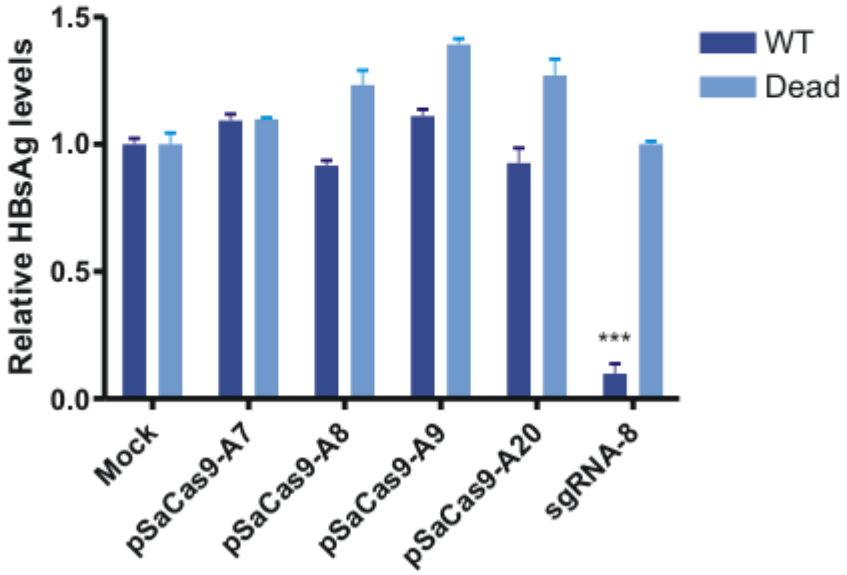


Figure 3.9: Assessment of active and inactive SaCas9-mediated knockdown of HBsAg in liver-derived cells

To assess the transcriptional silencing effect of the sgRNA sequences with the inactive Cas9 nuclease system, liver-derived Huh7 cells were co-transfected as described above. Each inactive Cas9 plasmid was compared to its active counterpart. These were calculated relative to the mock. The sgRNA-8 plasmid was used as a positive control. The mock was a SaCas9 and dSaCas9 plasmid with no guide sequence. An ELISA was conducted on supernatants collected from cells 48 hours after transfection. Transfections were carried out in triplicate. The error bars indicate the standard error of the mean (SEM) (n=3), *** indicates $p < 0.001$.

3.6 Targeted disruption of DNA by anti-HBV sgRNA and Cas9 complex *in vitro*

The previous ELISA data demonstrated that the newly designed anti-HBV sgRNA and Cas9 complex had no effect on HBsAg protein expression. All transfected plasmid displayed the same similar results in that none of caused any knockdown. It may therefore be assumed that these plasmids behave the same. To interrogate what was happening at the DNA level, a Surveyor assay was carried out to determine if there was any targeted disruption to the integrated HBV sequence in HepG2.2.15 cells. For these assays, a few effectors were chosen from the full panel of 20 and transfected into HepG2.2.15 cells three times consecutively. This cell line has the HBV sequence integrated; it requires more than one transfection as it produces a lot of viral DNA copies. Total DNA was extracted from HepG2.2.15 cells after the third consecutive transfection. DNA extracted from cells transfected with the pTZ plasmid was used as a negative control and sgRNA-8 used as the positive control (Scott et al., 2017). Primers were designed to amplify sequences approximately 300 bp upstream and 300 bp downstream of the Cas9 cleavage site. These sequences were amplified by PCR (Figure 3.10, Appendix 5.8). The PCR amplicons were denatured, annealed at room temperature to allow for heteroduplex and/or homoduplex formation before adding Cel1. The Cel1 enzyme is utilized in this assay as it able to cleave heteroduplexes that form as a result of mutations (Figure 3.10). Cleaved products are indicative of targeted disruption from the CRISPR/Cas9 complex. The Cel1 treated samples were resolved by agarose gel electrophoresis and the separated bands were used to calculate the percentage of targeted disruption. Wild type and mutant HBx amplicons annealed as heteroduplexes during the PCR. This was used as the positive control for cleavage. Equal concentrations of both wild type and mutant HBx sequences were combined after PCR. These sequences were subjected to the same PCR conditions as above.

The primers used to amplify the targeted region determined the expected band sizes if any cleavage occurred.

The expected band sizes would be 600 bp (uncleaved) and approximately 300 bp cleaved products. The results in Figure 3.11 indicate that the cells treated with the mock had no cleavage occurring which indicated the presence of homoduplexes only.

Positive control plasmid sgRNA-8 achieved approximately 15-17% targeted disruption (Figure 3.11C). In contrast the cells treated with the different SaCas9 plasmids showed very little cleavage all less than 5% (Figure 3.11A &B). These results confirm that although there may be some genomic cleavage occurring it is not sufficient to have any effect on HBsAg.

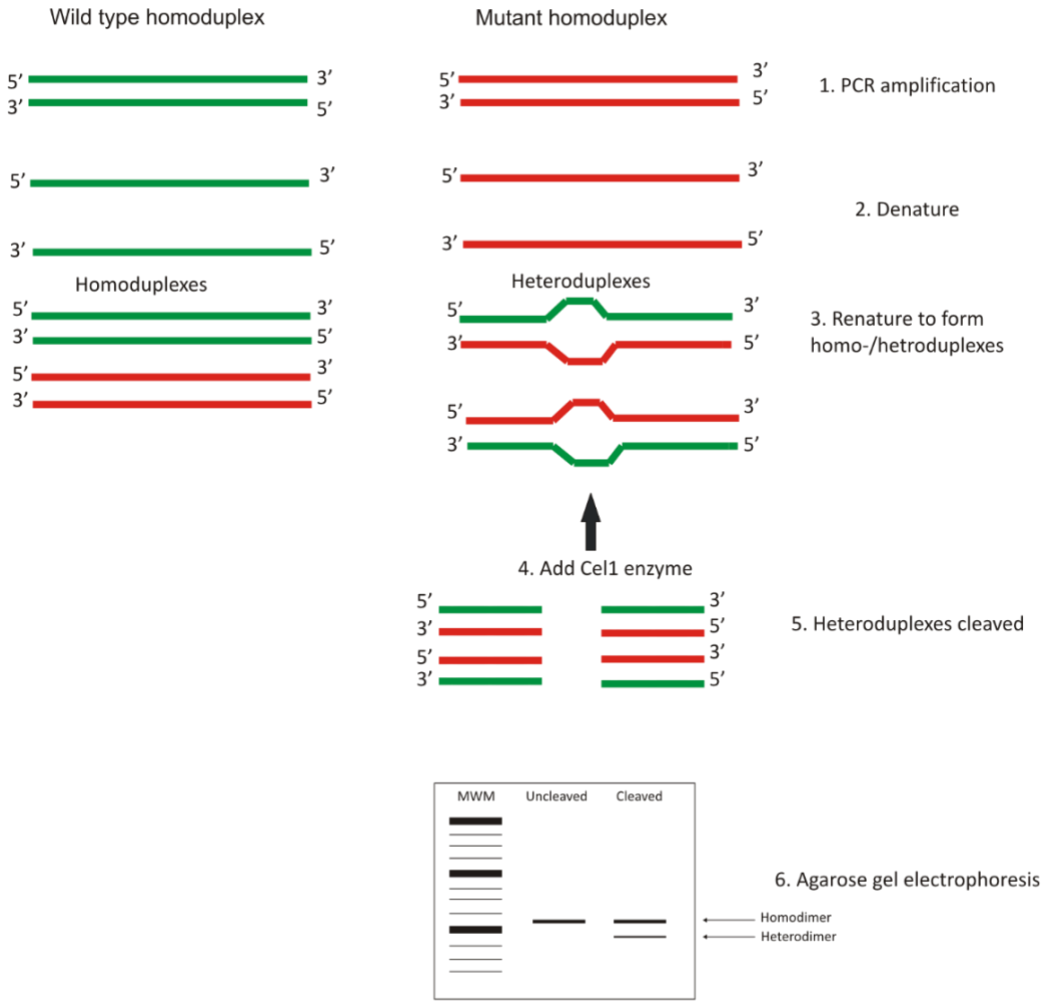


Figure 3.10: Schematic diagram depicting Cel1-mediated cleavage of heteroduplexes

Target sites are subjected to PCR amplification (1), followed by a denaturation step (2) that allows for homo/heteroduplex formation due to indels during the renaturation step (3). Cel1 enzyme is added to PCR products (4) which recognizes and cleaves heteroduplexes (5). Cleaved and uncleaved products are resolved by agarose gel electrophoresis and the density of separated bands are used to determine targeted disruption. Adapted from (Ehrke-Schulz et al., 2016).

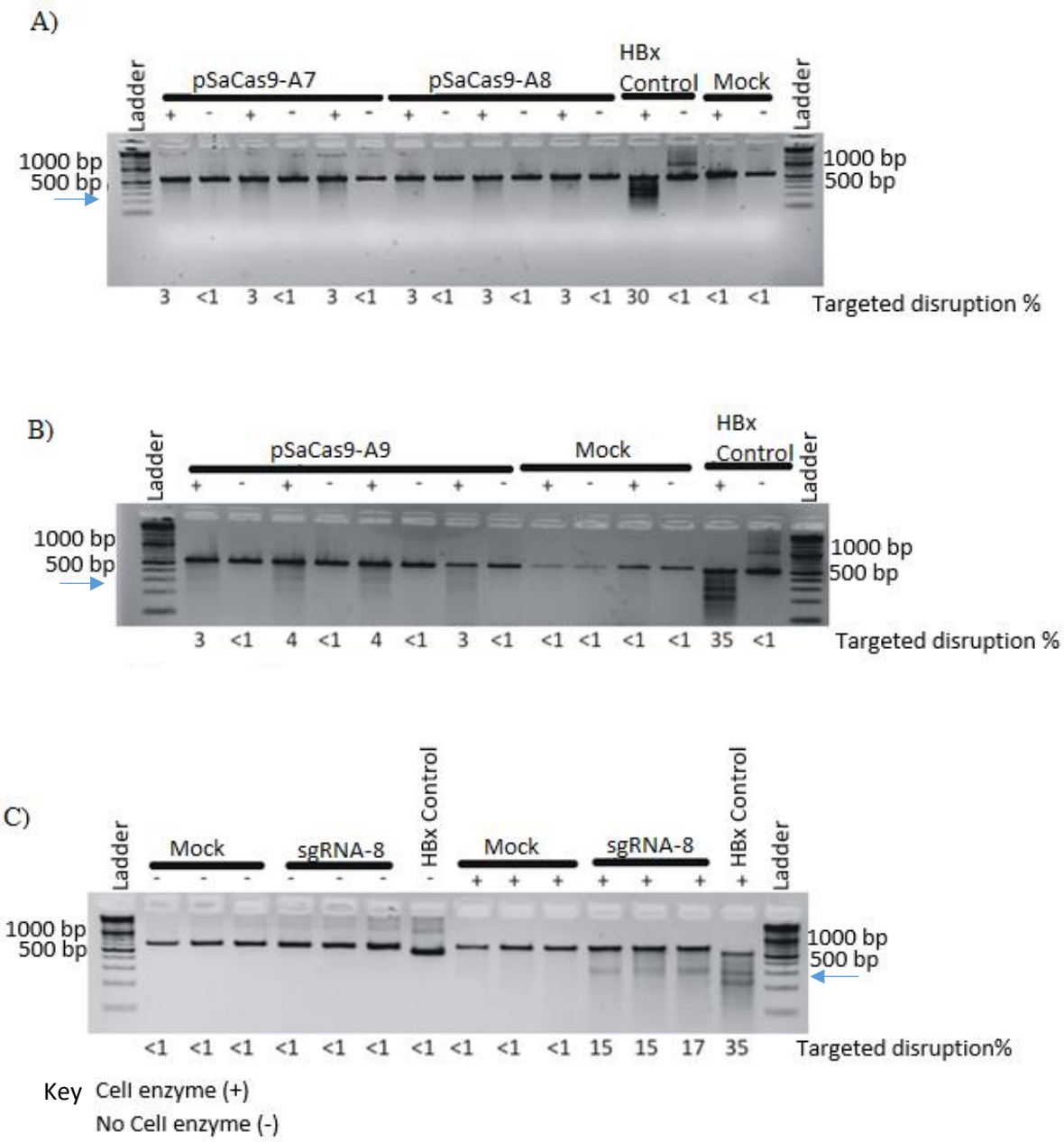


Figure 3.11: sgRNA and Cas9 mediated cleavage of HepG2.2.15 extracted DNA

HepG2.2.15 cells were transfected three times consecutively with the indicated SaCas9 vectors. Total DNA was extracted from these cells and used to amplify the sgRNA target sites for use in Cel1 assays. Cel1 assays were carried out on target sites for sgRNA-A7 and sgRNA-A8 (A), sgRNA-A9 (B) and sgRNA-8 (C). + indicates the Cel1 enzyme was added to the PCR amplicon, - indicates the absence of the Cel1 enzyme.

3.7 Anti-HBV sgRNA and Cas9 complex do not exhibit toxicity *in vitro*

To assess whether the SaCas9 plasmids encoding the different sgRNA were not toxic, an MTT assay was conducted on cells transfected with these effectors. This assay quantifies metabolic activity as a measure of live cells. In living cells mitochondrial succinate dehydrogenase reduces the MTT to an insoluble formazan product which can be solubilised by DMSO to produce a purple product. This assay is therefore colourimetric as the intensity of the purple colouration is indicative of metabolic activity and therefore of living cells. Huh7 cells were co-transfected with pCH-9/3091, pCMV-eGFP and the SaCas9 or dSaCas9 plasmids encoding different sgRNA sequences. Only a few plasmids were chosen as the pool of SaCas9 and dSaCas9 plasmids was narrowed. Three controls were included in this assay. The SaCas9 and dSaCas9 plasmids carrying no guide sequence were used as controls. Cells were treated with 50% DMSO as a positive control for toxicity while untreated cells were used as a negative control. For reproducibility the transfections were carried out in triplicate.

While DMSO-treated cells exhibited significant toxicity, cells treated with the pSaCas9/dSaCas9 plasmids did not exhibit a significant decrease in OD reading compared to the untreated cells (Figure 3.12). This result confirms that the gene products from these plasmids are not causing any toxicity to the cells.

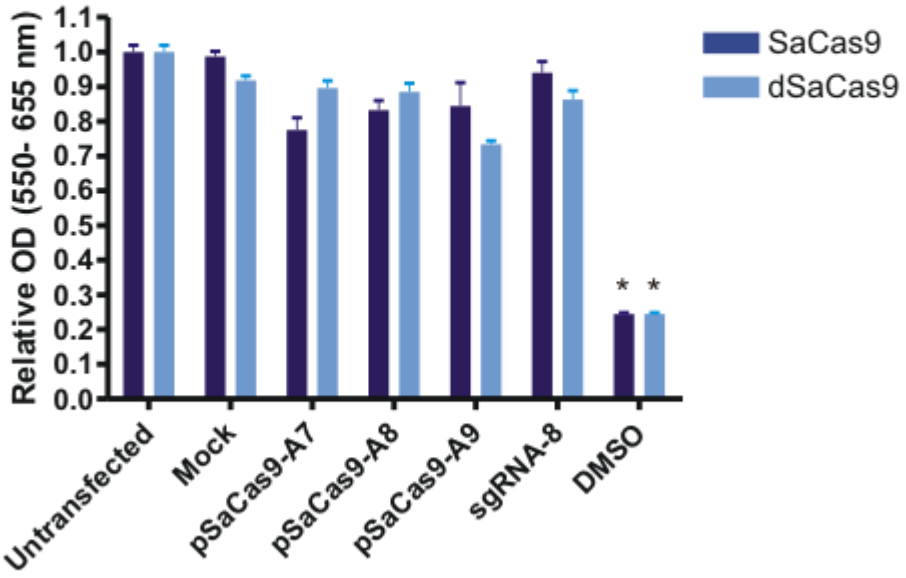


Figure 3.12: *In vitro* assessment of CRISPR/Cas9 complex mediated cytotoxicity in cultured cells by MTT assay

An MTT assay was conducted 48 hours following transfection of Huh7 cells with SaCas9 dSaCas9 plasmids encoding the different sgRNAs as indicated above. For reproducibility the transfections were performed in triplicate. The error bars indicate the SEM (n=3) (* $p < 0.05$).

3.8 Anti-HBV sgRNA plasmids do not exhibit self-cleavage of plasmid DNA

The above results have shown that the SaCas9 plasmids do not efficiently exhibit inhibition of HBsAg expression. The plasmids have shown very low targeted disruption despite all components of the CRISPR/Cas9 complex being sufficiently expressed *in vitro*. Upon further evaluation of the designed sequences it was discovered that the sgRNAs were designed with a PAM sequence. This suggested that the SaCas9 plasmids could be targeted by the very sgRNAs that they express and might explain why the system is so inefficient. To assess this, Cel1 assays were carried out on the sgRNA expressing plasmid (Figure 3.13). The assay was set up as previously described having designed primers against each SaCas9 plasmid expressing the different sgRNAs. Uncleaved products should yield band sizes of approximately 400 bp.

The results shown in Figure 3.13 show there was no targeted disruption occurring in the SaCas9 plasmid. Despite the sgRNA sequences having a PAM sequence, the Cas9 nuclease did not cleave its own plasmid DNA. Although *in silico* tools were used to design the sgRNA sequences, the chosen sequences are not good candidates. This confirms that the designed sgRNA sequences are inefficient at directing the Cas9 nuclease to achieve sufficient targeted disruption.

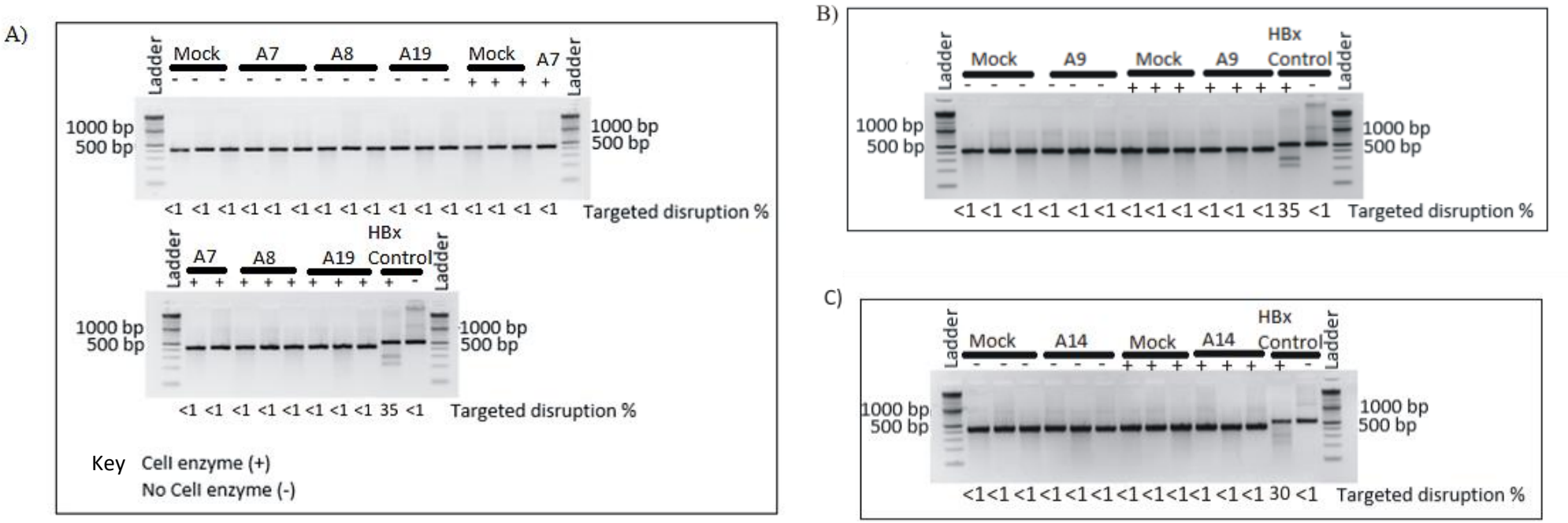


Figure 3.13: Cel1 assay to assess self-cleavage of the SaCas9 plasmid

The Cel1 assay was performed on HepG2.2.15 cells that were transfected three times consecutively with each SaCas9 plasmid. A) Cel1 assay performed on cells transfected with pSaCas9 expressing sgRNA-A7, A8 and A19. B) Cel1 assay preformed on cells transfected with pSaCas9 expressing sgRNA-A9. C) Cel1 assay performed on cells transfected with pSaCas9 expressing sgRNA A14. + indicates the Cel1 enzyme was added to the PCR amplicon, - indicates the absence of the Cel1 enzyme.

CHAPTER 4-DISCUSSION

The cccDNA of HBV can be described as a stable non-integrated minichromosome. This cccDNA utilises the host cell's transcriptional machinery to produce the viral RNA required for viral protein production and replication (Levrero et al., 2009). A major source of cccDNA in infected hepatocytes is from recycling of newly synthesised nucleocapsids. If the nucleocapsid is not enveloped and secreted from the cell, it will instead be redirected back to the nucleus where it accumulates and maintains the pool of cccDNA (Levrero et al., 2009). This promotes the persistence of the cccDNA which is a challenge to existing therapies that are not yet able to achieve a sterilising cure for chronic HBV. Current drugs are able to supress viral replication and slow the progression that leads to cirrhosis and hepatocellular carcinoma (Ayoub and Keeffe, 2011). However, they are unable to eliminate or disable the pool of cccDNA. Elimination or inactivation of cccDNA from infected hepatocytes without causing hepatotoxicity is an absolute requirement to achieve a cure for chronic HBV infection (Yang and Kao, 2014). Therefore, the goal of this project was to adapt the *S. aureus* CRISPR/Cas system to inactivate the cccDNA. The rationale for using the *S. aureus* orthologue versus the most used *S. pyogenes*, is based on their size differences which is an important factor for potential gene delivery.

4.1 Successful generation of pAAV-SaCas9 and pAAV-dSaCas9 plasmids expressing the newly designed anti-HBV sgRNA sequences

The purpose of this study was to assess the use of the CRISPR/Cas9 system to target the cccDNA of HBV. This complex requires the Cas9 nuclease which is guided by an RNA sequence to its target. For the current study a panel of sgRNAs were designed to target various regions of the HBV genome in the hopes to achieve greater targeted disruption or transcriptional inhibition of cccDNA.

Previous studies by Scott et al demonstrated the antiviral efficacy of the small Cas9 nuclease derived from *S.aureus* with sgRNAs targeting the *S* ORF (Scott et al., 2017). The plasmid was efficient *in vitro* as cccDNA levels was reduced in a cell line that mimics viral infection, the same HBsAg knockdown effects were not observed *in vivo*. Only a few sgRNA sequences were designed, only 1 sgRNA sequence out of 10 worked best. In contrast when using the Cas9 orthologue from *S. pyogenes*, a study by Ramanan et al successfully demonstrated that a large panel of guides can be used and most were able to work efficiently when targeting all the ORFs against HBV genotype D. These results were demonstrated *in vitro* and *in vivo* (Ramanan et al., 2015). This study included Surveyor Assays and ELISA assays.

The sgRNAs used in this project were successfully cloned into the SaCas9 and dSaCas9 plasmid. RT-qPCR studies were performed to confirm the expression of the sgRNAs required to identify and bind to the target. There are some drawbacks associated with the experimental design. There is a possibility that the primers designed for this experiment may not be optimal. Currently there is no indication of how much expression constitutes a good sgRNA which is another limitation of this experiment. Future studies may be required to validate expression of sgRNAs such as a semi-quantitative gel. Immunofluorescence staining was performed to confirm the expression of the SaCas9 nuclease, the other essential component of the CRISPR/Cas9 complex. The HA epitope within the SaCas9 plasmid by immunodetection validated the expression of the SaCas9 nuclease in liver-derived Huh7 cells.

4.2 Targeting of cccDNA of HBV using CRISPR/Cas

Repeated cleavage caused by a gene editing tool which leads to NHEJ activation will eventually lead to indels at the target site (Schiffer et al., 2012). There is evidence to show that the cccDNA may be mutated or even eradicated in a few cases by using the CRISPR/Cas9 system (Kennedy et al., 2015, Li et al., 2017, Zhen et al., 2015).

In vitro assessments of the SaCas9 and dSaCas9 plasmids in this study demonstrated an inability of their gene products to inhibit HBsAg expression. Gene products of SaCas9 plasmids demonstrated insufficient targeted disruption to be detected by the surveyor assay and underlies why knockdown of HBsAg was not observed.

In contrast the positive sgRNA-8 plasmid achieved at least 10% targeted disruption and was able achieve up to 80% HBsAg knockdown (Scott et al., 2017). Other studies designed sgRNAs for genotypes A-D targeting various regions of the HBV genome using the Cas9 orthologue from *S. aureus* which demonstrated successful inhibition of HBsAg both *in vitro* and *in vivo* (Lin et al., 2014, Liu et al., 2018). These studies confirm that the CRISPR/Cas9 system can be used to disrupt HBV gene expression and suggests that the absence of knockdown in this study can be attributed to the panel of sgRNAs. The bioinformatics tools that were used to design the sgRNAs in this project may not be good predicators of what constitutes an effective guide.

4.3 Safety of the gene products from pAAV-SaCas9 plasmids

A major concern regarding the use of gene editing tools is the possibility of the designer nuclease causing non-specific cleavage at sites that resemble the on-target sequence. This type of cleavage at an undesired site can cause cellular toxicity by disrupting the functionality of host genes (Stone et al., 2016). Although the CRISPR/Cas9 system specificity is controlled by the sgRNA sequence and site specific cleavage by the PAM, there is still a possibility of having off target effects (Zhang et al., 2015).

Although the sgRNA sequences that were designed and used were not efficient in causing knockdown they did not elicit any toxic effects to the Huh7 cells that were treated with the SaCas9 plasmids. The cells remained viable following treatment and confirmed that the SaCas9 plasmids expressing the different sgRNAs are not associated with cytotoxicity.

Although the MTT assay is a standard test for cell viability that is widely used, there are drawbacks associated with the assay. The reduction of tetrazolium dye is assumed to be proportional to the number of viable cells in the exponential growth phase. However, it has been shown that the newer dyes are not taken up by cells and so their reduction is not an indication of metabolically active cells [reviewed in (Berridge et al., 2005)]. Despite the drawbacks, the MTT assay is still a widely accepted method to test for cytotoxicity.

Taken together the results have shown that the *S. aureus* Cas9 nuclease and the sgRNA are not associated with extensive cytotoxicity. Like other gene editing nucleases, the CRISPR/Cas9 system is associated with off-target effects which could lead to serious complications. In addition to the MTT assay, off target sites may be predicted by using bioinformatics with Off-spotter tool (https://cm.jefferson.edu/Off-Spotter/). This analysis would verify if the newly designed sgRNAs are associated with more off-target effects than on-target effects.

4.4 The design of the sgRNA sequences is important for the efficiency of the CRISPR/Cas9 system

The efficiency of the CRISPR/Cas9 system relies on the sgRNA binding to the target sequence as well as the PAM sequence for cleavage to occur. In many of the CRISPR/Cas9 studies, the observation is that not all sgRNA sequences in a panel have the same efficiency, some are more efficient than others. This is due to the molecular features of the sgRNA sequence which plays an important role in the efficiency of the Cas9 nuclease (Moreno-Mateos et al., 2015). An sgRNA comprises the crRNA sequence which is complimentary to the targeted DNA sequence (Xu et al., 2015).

A study done by Ran et al. found that in mammalian cells SaCas9 nuclease achieves a higher editing efficiency in mammalian cells with crRNAs that are between 21 and 23 nucleotides long (Ran et al., 2013).

In contrast the Cas9 orthologue from *S. pyogenes* works efficiently with the natural 20 nucleotide crRNA length or truncated to 17 nucleotides without compromising the nuclease efficiency. In addition, it is found that by replacing the first base of the crRNA sequence with a guanine base improved the expression of sgRNAs (Ran et al., 2013). Phenotypic selection studies conducted by Moreno et al suggested that a guanine base adjacent to the PAM also favours cleavage (Moreno-Mateos et al., 2015). Findings by Wang et al demonstrated that the sequence composition of purines are preferred near the 3' end of the crRNA which is crucial to Cas9 loading (Wang et al., 2014). Due to the many factors that need to be considered when designing the crRNA sequences, predictive sgRNA-scoring algorithms are available to assess the efficiency of a potential sgRNA (Moreno-Mateos et al., 2015).

The efficiency of the Cas9 nuclease also relies on the recognition of the 5'-NNGRRT-3' PAM located immediately downstream of the target DNA sequence (Nishimasu et al., 2015). Since the target sequence contains the PAM, the sgRNA should not include the PAM sequence. A study done by Liu et al designed guides that facilitate Cas9 binding to the initiating 5'G and the downstream PAM sequence to facilitate the Cas9 cleavage (Liu et al., 2018). This study including others that have detailed their guide sequences, confirm that the PAM should not be included in the sgRNA (Karimova et al., 2015, Seeger and Sohn, 2014).

There may be a number of reasons why the sgRNAs in this study were not efficient. Although most of the sgRNAs that were designed for this study did not have the initiating 5' guanine base, expression of each guide *in vitro* was observed (Figure 3.4). Due to experimental limitations of the RT-qPCR, other experiments may be needed to confirm the link between sgRNA expression and cleavage efficacy. These guides mistakenly included the PAM which was meant for the target sequence. This led to the assumption that self-cleavage of the vector could occur, however, the results in Figure 3.13 have shown that self-cleavage did not occur.

If self-cleavage of the vector had occurred it could have ruled out that the sgRNA sequences do not work. The extra bases in the sgRNA sequence may result in a non-functional sgRNA, affect RNA folding, or create a new target site. Therefore, it cannot be unequivocally stated exactly why the sgRNA sequences are non-functional without re-designing guides without a PAM in it.

4.5 Future work to address the challenges faced for a successful HBV gene therapy

Like other gene editing nucleases, the CRISPR/Cas9 system is associated with off-target effects which could lead to serious complications (Yang and Chen, 2018). In addition to the MTT assay, off target sites may be predicted by using bioinformatics tools such as Off-spotter tool (https://cm.jefferson.edu/Off-Spotter/). This analysis would verify if the newly designed sgRNAs are associated with more off-target effects than on-target effects. This tool has been demonstrated successfully by Scott et al by using the tools prediction to amplify possible off target sites followed by the surveyor assay to observe any targeted disruption (Scott et al., 2017).

HBV gene therapy is delivered *in vivo* therefore tissue specificity is an important aspect to consider. It is vital that an engineered nuclease system such as the CRISPR/Cas9 only targets the affected cells. Such is the case with HBV which affects hepatocytes, the gene therapy should only be delivered to the liver. Future work that addresses the tissue specificity concern is the replacement of the constitutively active CMV promoter with the liver-specific modified mouse transthyretin (MTTR) promoter. This has been successfully demonstrated with the incorporation of the MTTR promoter into primary microRNA expression cassettes (Mowa et al., 2014). These were then used to counter HBV replication by harnessing the RNA interference pathway (Mowa et al., 2014).

A similar study done by Bloom et al., used transcriptional repressor TALEs to inhibit HBV replication under the control of the MTTR promoter (Bloom et al., 2019). To date there is no analysis of the SaCas9 nuclease efficacy when expressed under the control of the MTTR promoter and would be worthwhile to test.

Another important challenge regarding gene therapy is the use of an appropriate delivery vector. Characteristics of a good delivery mechanism include safety, no known pathogenicity and long-lasting enough to carry out its intended effects. The delivery of a transgene must overcome many obstacles to reach the nucleus for expression. Obstacles faced by transgene delivery include degradation by cellular enzymes and the difficulty passing through the plasma membrane to the nucleus. Hence it is necessary to use a gene delivery system that protects the transgene (Ibraheem et al., 2014). Viral vectors such as recombinant single stranded adeno-associated viruses (ssAAVs) have been widely used as they are attractive vectors for liver diseases (Kattenhorn et al., 2016).

They have a good safety profile and they mediate transgene delivery efficiently. These vectors demonstrate low immunogenicity while persisting in human cells for months (Mali, 2013). The use of these vectors is appropriate for HBV gene therapy delivery, as HBV replication in infected hepatocytes make the cells more susceptible to transduction by AAVs (Chen et al., 2009). However, size constraints do need to be considered when using AAVs. The smaller size of sequences encoding *S.aureus* Cas9 allows for easy packaging and delivery using ssAAVs and was successfully demonstrated *in vitro* (Scott et al., 2017). However, studies have shown that there may be pre-existing antibodies to AAV capsids that may affect the duration of the delivered transgene (Li et al., 2007).

Pre-existing antibodies prevent the vectors from reaching their intended target cells. A future study that may overcome immunogenicity challenges is the use of a non-viral vector delivery system to deliver the SaCas9 and sgRNA sequences. There are a few studies that suggest the use of nanoparticles for the safe delivery of CRISPR/Cas9. Miller et al., described a lipid-like material that is suitable for the co-delivery of Cas9 mRNA and sgRNA sequences both *in vitro* and *in vivo* (Miller et al., 2017).

This study confirmed the successful co-delivery of Cas9 and sgRNA sequences using this delivery system both *in vitro* and *in vivo*. Following *in vitro* studies, an appropriate animal model for preclinical testing is vital. Transgenic mouse models are a popular choice for *in vivo* studies (Chisari et al., 1985, Marion et al., 2003). This model is analogous to HBV infection at the stage when replication has ceased and the viral DNA has integrated into host genome as it occurs in chronic infection (Chisari et al., 1985). Although this model stimulates replication of HBV *in vivo*, it does lack an infection step which may not be optimal for anti-HBV gene therapy testing. Another animal model that has been used for HBV studies are the chimpanzees (Dandri et al., 2005). Chimpanzees are susceptible to human HBV however, there are ethical concerns regarding their use (Dandri et al., 2005).

Since there are *in silico* tools that allow for the easy design of crRNA sequences, it may be worthwhile designing sgRNA sequences that target genotype A1 which is more relevant to the South African context. In this study the sgRNA sequences were designed to target the replication-competent plasmid pCH-9/3091 which falls under genotype D that is more commonly distributed worldwide (Nassal et al., 1990).

4.6 Conclusion

The development of a functional cure for chronic hepatitis B virus is crucial to alleviate this global health burden. The current treatments for HBV are not able to eliminate cccDNA which is responsible for the persistence of the virus. To achieve a functional cure, the CRISPR/Cas9 gene editing system is being widely explored to disable the cccDNA. Since the HBV genome has four overlapping reading frames it was worthwhile to test whether sgRNA sequences that target various regions of the genome could inhibit HBV replication and disable the cccDNA. Unfortunately, in this study the anti-HBV sgRNAs designed showed little targeted disruption of the viral DNA and no reduction in the levels of HBsAg.

The system is worthy of further investigation as the results did confirm that the CRISPR/Cas9 system is not associated with any cytotoxic effects. Therefore, close attention is needed when designing the sgRNA sequences as they play a vital role to the success of the CRISPR/Cas9 system.

CHAPTER 5-APPENDIX

5.1 Bacterial culturing: Preparation and transformation of chemically competent cells

Materials:

- **Luria Bertani media**

To prepare Luria Bertani medium, 10 grams of Bacto-tryptone, 5 g yeast extract and 5 g NaCl were made up to 1 litre with ddH_2O and autoclaved for 20 minutes at 121 °C and 1 kg/cm_2.The medium was stored at room temperature.

- **1000× Ampicillin**

One hundred milligrams of ampicillin was dissolved in 10 ml of 50% ethanol. The mixture was filter sterilised and stored at -20 °C.

- **Luria Bertani agar plates**

To prepare plates, agar was added to Luria Bertani medium at a final concentration of 1 %(w/v). This was autoclaved for 20 minutes at 121 °C and 1 kg/cm_2 and then cooled down to 50 °C. Ampicillin was added to a final concentration of 100 µg/ml to the agar. The agar solution was poured into petri dishes and allowed to solidify at room temperature. The plates were stored at 4 °C.

- **Transformation buffer**

To prepare transformation buffer, 1.4702 g $CaCl_2$,0.3024 g PIPES-HCl and 15 ml of Glycerol were mixed together with 80 ml of ddH_2O. The pH was adjusted to 7.0with NaOH and ddH_2O was added to a total volume of 100 ml. The buffer was autoclaved for 20 minutes at 121 °C and 1 kg/cm_2 and stored at -20 °C.

5.1.1 Bacterial transformation

Materials:

- **Transformation buffer**
- **1000× Ampicillin**
- **DH5-α *Escherichia coli* (*E. coli*) cells**

Preparation of chemically competent cells

To prepare chemically competent cells, 20 µl of DH5-α *Escherichia coli* (*E. coli*) cells was inoculated into 10 ml of Luria Bertani medium used to prepare the bacterial pre-culture. In addition, a negative control included 20 µl of *E. coli* cells into 10 ml of Luria Bertani medium containing antibiotic (ampicillin).

Cultures were grown overnight at 37 °C with shaking at 150 rpm. Ten millilitres of the overnight culture was inoculated into 150 ml of fresh Luria Bertani medium and incubated at 37 °C with shaking at 150 rpm until OD at 600 nm was between 0.4-0.6. Following incubation, the bacterial culture was transferred to 50 ml tubes and centrifuged for 15 minutes at 3000 ×g (4 °C). The three pellets were pooled and made up to 35 ml with transformation buffer. The tube was incubated on ice for 30 minutes followed by centrifugation for 10 minutes at 1000 ×g (4 °C). The supernatant was poured off and the pellet re-suspended in 2 ml of transformation buffer. One hundred microlitres of chemically competent DH5-α *E. coli* was aliquoted into approximately 20 microcentrifuge tubes under sterile conditions on ice. Chemically competent bacteria were stored at -80 °C.

Transformation of chemically competent cells

Ampicillin resistant plasmid DNA (10 µl) was added to 100 µl of chemically competent cells in a micro-centrifuge tube and mixed gently. The mixture was incubated on ice for 30minutes then heat shocked at 42 °C for 90 seconds and placed back onto ice for 5minutes. The bacteria was spread onto pre-warmed ampicillin containing Luria Bertani agar plates and incubated overnight at 37 °C.

5.2 Agarose gel electrophoresis

Materials

- 50× Tris Acetate EDTA (TAE) Buffer
- Agarose
- Ethidium bromide (10 mg/ml)

Method

-50× Tris Acetate EDTA (TAE) Buffer

Two hundred and forty-two grams of Tris base, 57.1 ml glacial acetic acid, 100 ml of 0.5 M EDTA (pH 8.0) were made up to a total volume of 1 litre with ddH_2O and autoclaved for 20 minutes at 121 °C and 1 kg/cm_2. The buffer was stored at room temperature.

- Agarose gel

To prepare a 1% agarose gel, 1 g of agarose was added to 100 ml of 1× TAE buffer. The mixture was heated in a microwave until the agarose dissolved. The mixture was cooled to 60 °C before adding ethidium bromide to a final concentration of 0.5 µg/ml. The mixture was poured into a casting chamber with a comb and allowed to set at room temperature.

Once the gel was set it was transferred to a running chamber containing 1× TAE buffer and subjected to electrophoresis at 100 volts for 45 minutes. Thereafter, the gel was visualised using a G:BOX UV transilluminator (Syngene, Cambridge, UK).

5.3 Gel extraction (extraction of DNA from agarose gel)

Materials

- MinElute Gel Extraction kit (Qiagen, Hilden, Germany)
- Isopropanol

Method

The fragment containing the DNA of interest was excised from the agarose gel. Each agarose gel slice was placed into a microcentrifuge tube and weighed. To each tube containing the gel slice, 3 volumes of Buffer QG to 1 volume of gel (100 µl ~ 100 mg of gel) was added. The tubes were incubated at 50 °C for 10 minutes with periodic vortexing to dissolve the gel. One gel volume of isopropanol was added to the samples and mixed. The samples were transferred to a QIAquick spin column that was inserted into a 2 ml collection tube and centrifuged for 1 minute at 10 000 ×g using a standard bench-top microcentrifuge. The flow-through was discarded and the QIAquick spin column was placed back into the collection tube. Five hundred microlitres of Buffer QG was added to the column and centrifuged at 10 000 ×g for 1 minute. The flow-through was discarded, 750 µl of Buffer PE of was added to the QIAquick spin column to wash the DNA and centrifuged at 10 000 ×g for 1 minute. The samples were centrifuged at 10 000 ×g for an additional 2 minutes to remove excess ethanol from the column. The column was transferred into a clean 1.5 ml centrifuge tube and 30 µl of ddH_2O was added to the column and incubated for 5 minutes at room temperature. Following incubation, the samples were centrifuged at 10 000 ×g to elute the DNA. Concentrations of DNA were analysed using spectrophotometry and was stored at -20 °C.

5.4 Plasmid preparations

5.4.1 Small-scale plasmid preparation

Materials

- Luria-Bertani media
- Ampicillin
- EconoSpin™ All-in-One Mini Spin Columns (Epoch Life Sciences, MO, USA)

Method

A single colony was inoculated into 10 ml of Luria Bertani media supplemented with 100 µg/ml of ampicillin. The bacterial culture was incubated overnight at 37 °C with shaking at 150 rpm. Following incubation, the bacterial culture was centrifuged at 4000 ×g for 20 minutes. The pellet was re-suspended in 250 µl of MX1 Buffer. The pellet was re-suspended completely by vortexing. This mixture was transferred into a 1.5 ml microcentrifuge tube. Two hundred and fifty microlitres of MX2 Buffer was added and mixed gently by inverting the tube 4-6 times. The tubes were incubated at room temperature for 1-5 minutes until the solution became clear. Three hundred and fifty microlitres of MX3 Buffer was added to the mixture and gently inverted 4-6 times. The tubes were incubated on ice for 10 minutes. The tubes were then centrifuged at 14 000 ×g for 10 minutes. The supernatant was transferred to EconoSpin™ columns and centrifuged at 14 000 ×g for 1 minute. The flow-through was discarded.

Five hundred microlitres of WS Buffer was added to the spin column and centrifuged at 14 000 ×g for 1 minute and the flow-through discarded. An additional 500 µl of WS Buffer was added to the spin column and centrifuged at 14 000 ×g for 1 minute and the flow-through discarded. The spin column was centrifuged at 14 000 ×g for an additional 2 minutes to remove residual buffer.

The spin column was transferred to a clean 1.5 ml microcentrifuge tube and 50 µl of ddH_2O was added to the column and centrifuged at 12 000 rpm for 1 minute. Concentrations of eluted plasmid DNA was measured using spectrophotometry and stored at -20 °C.

5.5 Tissue culture (Culturing of mammalian cells)

Materials

- Complete DMEM

-1000×penicillin/streptomycin (100 000 U/mL; 100 000 µg/mL)

-Saline with 0.01% EDTA

The penicillin/streptomycin antibiotic was prepared by dissolving 0.9 g of penicillin and 15 g of streptomycin in 15 ml of PBS. The solution was filter sterilised and stored in 1 ml aliquots at -20 °C.

To prepare complete DMEM (high and low glucose), 50 ml of 10% heat inactivated FBS and 500 µl of Pen/Strep (penicillin 100 U/ml; streptomycin 100 µg/ml) was added to the medium. The medium was stored at 4 °C.

5.5.1 Culturing and passaging of cells

The Huh7 and HepG2.2.15 cells were grown in 75 cm_2 CellStar® cell culture flasks (Greiner Bio-One, Frickenhausen, Germany) and maintained in low(1 g/L) or high (4.5 g/L) glucose complete DMEM (Gibco™, Thermo Scientific, CA, USA) respectively. The cells were incubated at 37 °C in an atmosphere containing 5% CO_2 in a humidified incubator. All cells were incubated in these conditions unless stated otherwise. Upon reaching confluency the medium was discarded and the cells were washed with 10 ml of saline with EDTA which was incubated at 37 °C and 5% CO_2 for 10 minutes. Following the incubation, the saline was discarded.

Three millilitres of TrypLE™ Express was added to the cells and incubated under conditions specified above for 3 minutes. Following incubation, the flask was gently tapped to lift off the cells. Seven millilitres of complete DMEM was added and the cell suspension was transferred to a 15ml tube and centrifuged at 800 rpm for 3 minutes. The supernatant was carefully discarded, the resulting pellet re-suspended in 1 ml complete DMEM and thoroughly mixed.

The cells were split into new 75 cm^2 flasks with a total volume of 15 ml of complete DMEM. The cells were kept under conditions specified above and monitored under a light microscope (Olympus CKX31, Tokyo, Japan).

5.5.2 Transfection mixes

- Lipofectamine® 3000 and Opti-MEM Protocol

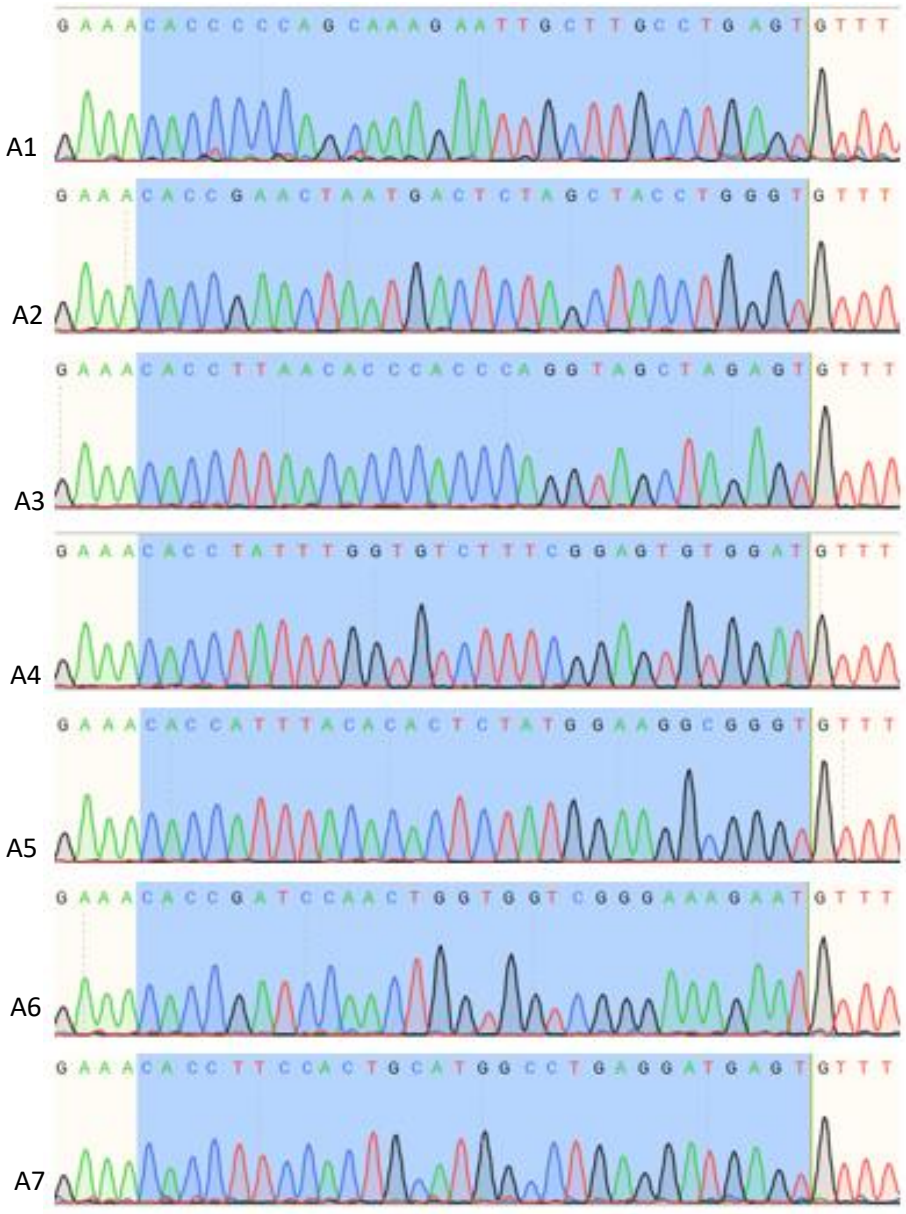
Cells were transfected 24 hours after seeding. For a 24-well plate a maximum of 1250 ng of DNA was used and up to 100 ng for a 96-well plate. Lipofectamine® 3000 and Opti-MEM (Gibco®, BRL, UK) was to make the DNA-Lipid complex according to the volumes specific to each plate. The DNA-Lipid complex was incubated at room temperature for 15 minutes. Following the incubation, 100 µl of the transfection mix was added dropwise to each well for a 24-well plate and 12.5 µl for a 96-well plate. The plates were gently swirled to ensure transfection mix was equally distributed in each well. Transfections were maintained under specified conditions.

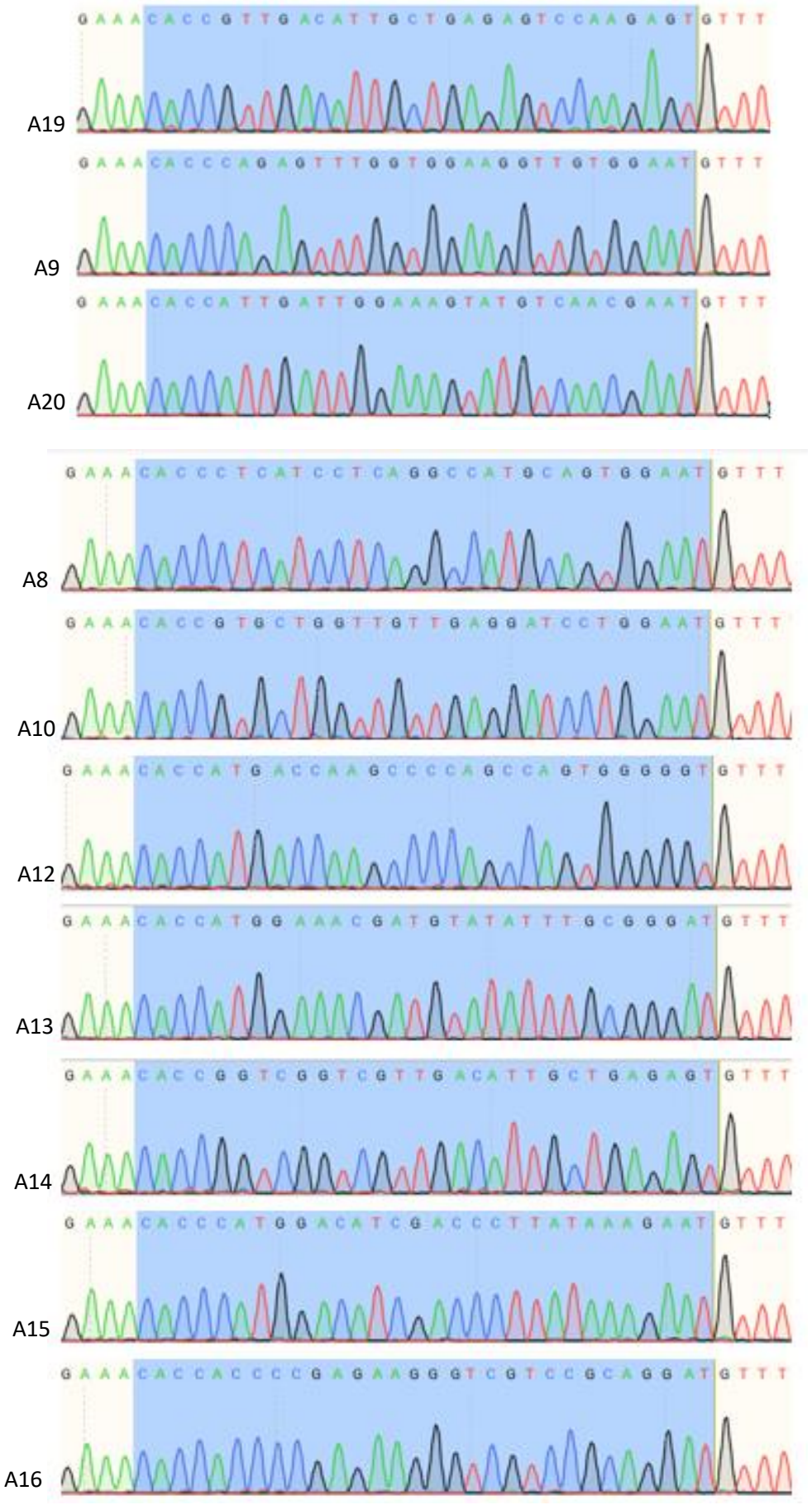
- Polyethyleneimine Max (PEI Max) and Opti-MEM Protocol

Cells were transfected 24 hours after seeding using a 48-well plate with a maximum of 600 ng of DNA per well. PEI Max was mixed with DNA at 3:1 ratio. Opti-MEM (Gibco®, BRL, UK) was used to dilute PEI Max before adding this mix to the DNA. The mixture was vortexed and incubated at room temperature for 15 minutes.

Following incubation, 25 µl of the transfection mix was added dropwise and equally distributed in the wells. Transfections were maintained under standard conditions.

5.6 Sequence analysis of the anti-HBV sgRNA plasmids




A19
A9
A20
A8
A10
A12
A13
A14
A15
A16

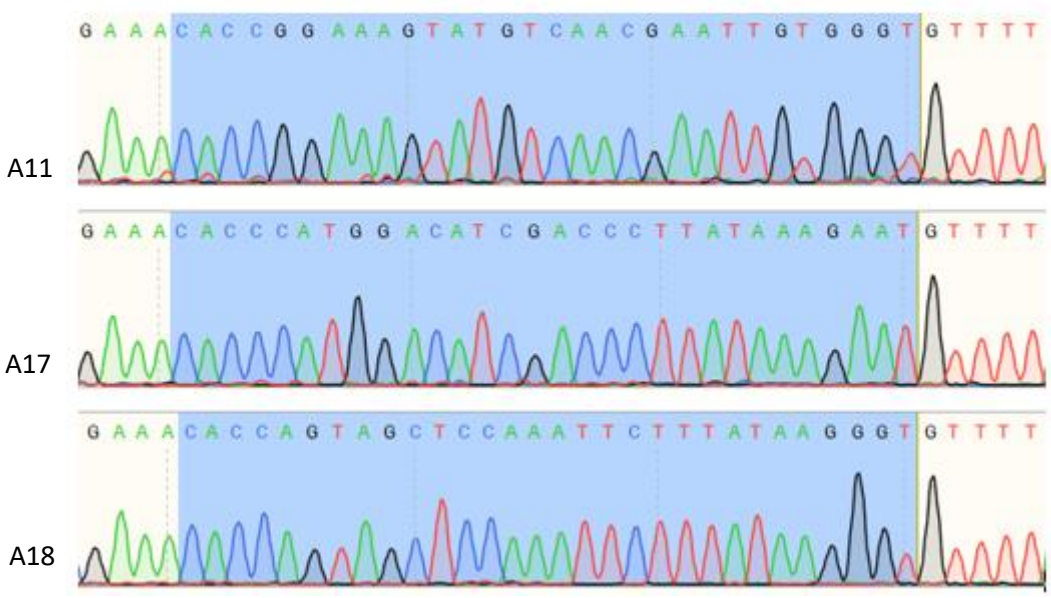


Figure 5.1: Chromatograms of the cloned crRNA sequences into the SaCas9 plasmids

The chromatograms represent the sequencing data for each cloned crRNA sequence, highlighted in blue, into the SaCas9 plasmids used throughout the *in vitro* assessments.

5.7 Transfection efficiency of anti-HBV sgRNA plasmids

5.7.1 Huh7 transfection efficiency for RT-qPCR studies

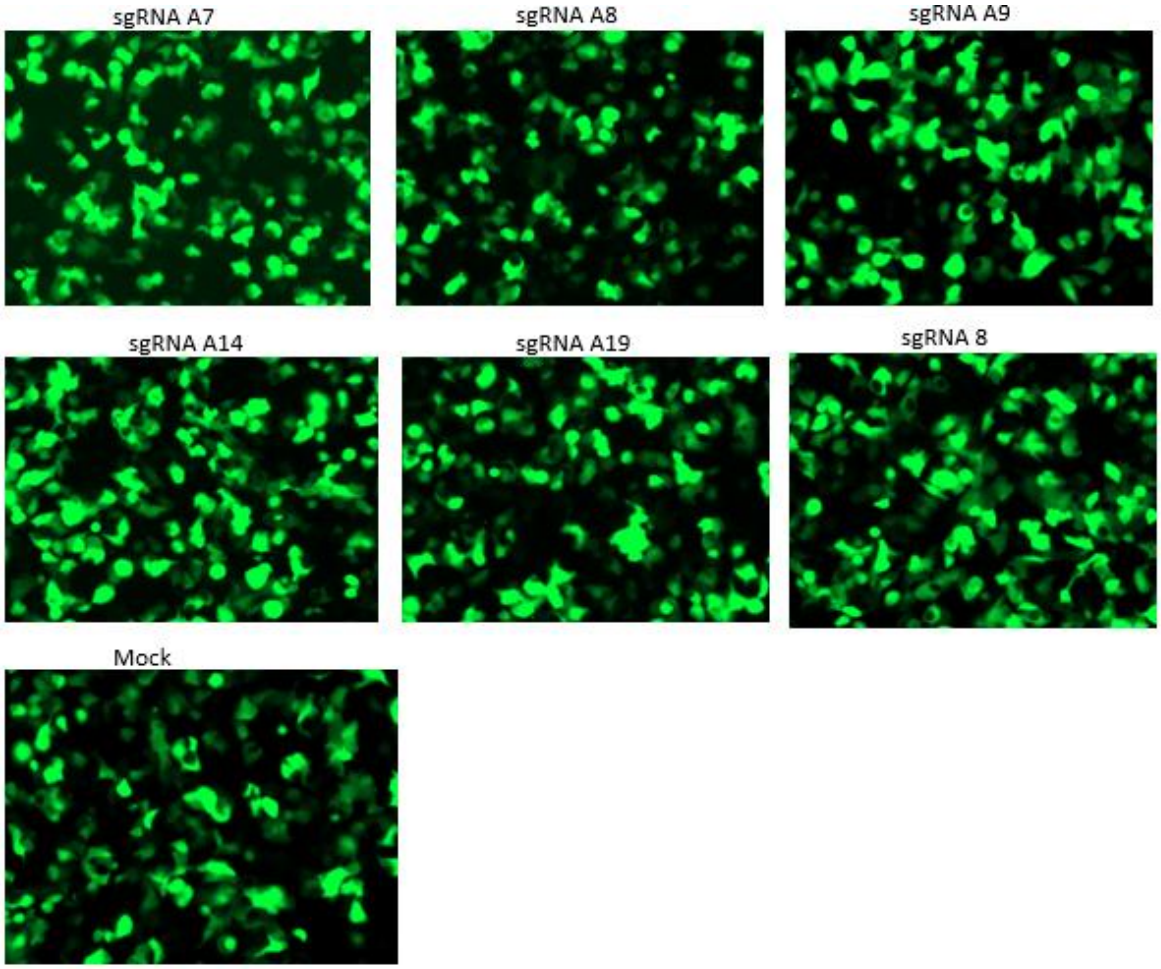
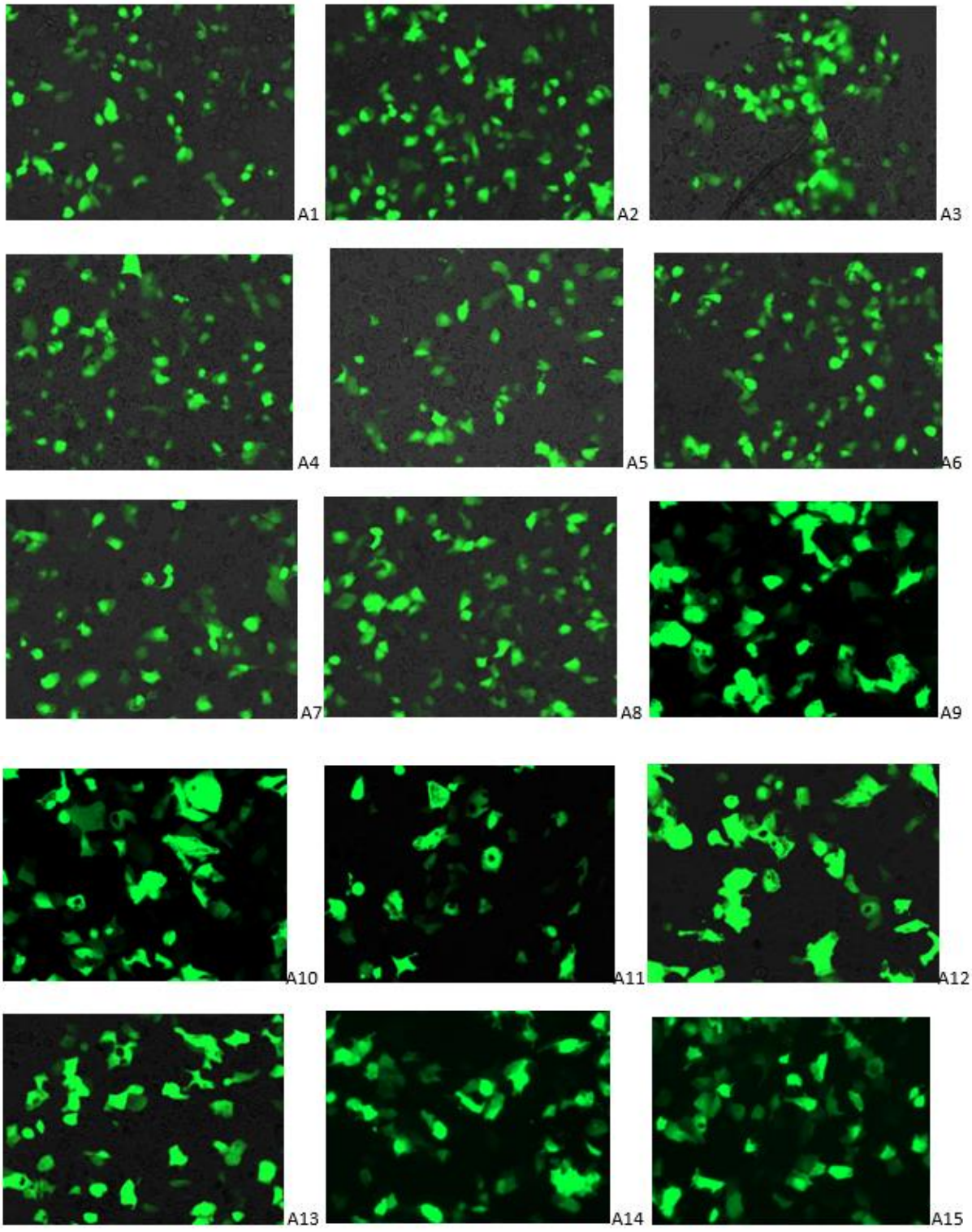


Figure 5.2: Transfection efficiency of pSaCas9-plasmids in Huh7 cells

Assessment of transfection efficiency for RT-qPCR studies evaluated using the pCMV-GFP plasmid. Fluorescence microscopy was used at 20× magnification.

5.7.2 Huh7 transfection efficiency of pSaCas9-sgRNA plasmids



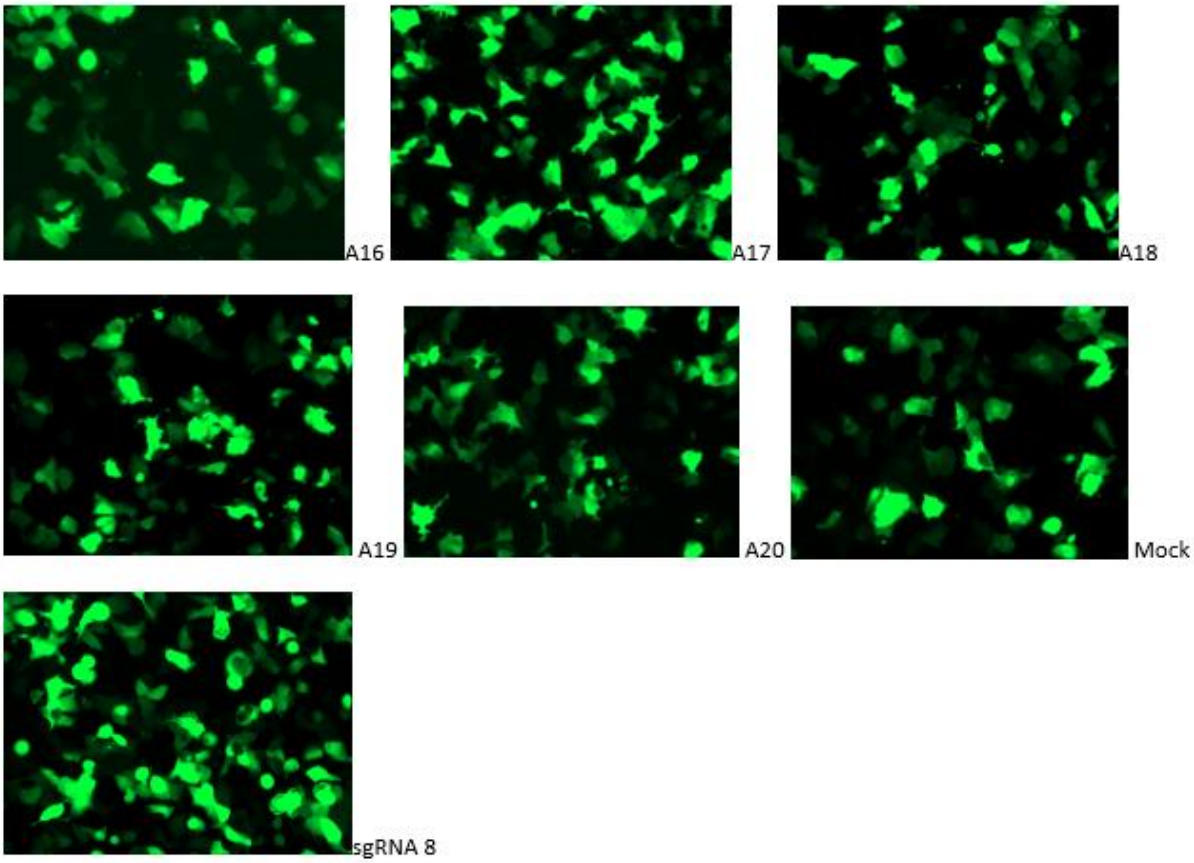


Figure 5.3: Transfection efficiency of pSaCas9-plasmids in Huh7 cells

Assessment of transfection efficiency for *in vitro* assays was evaluated using the pCMV-GFP plasmid. Fluorescence microscopy was used at 20× magnification.

5.7.3 Huh7 transfection efficiency of pdSaCas9-sgRNA plasmids

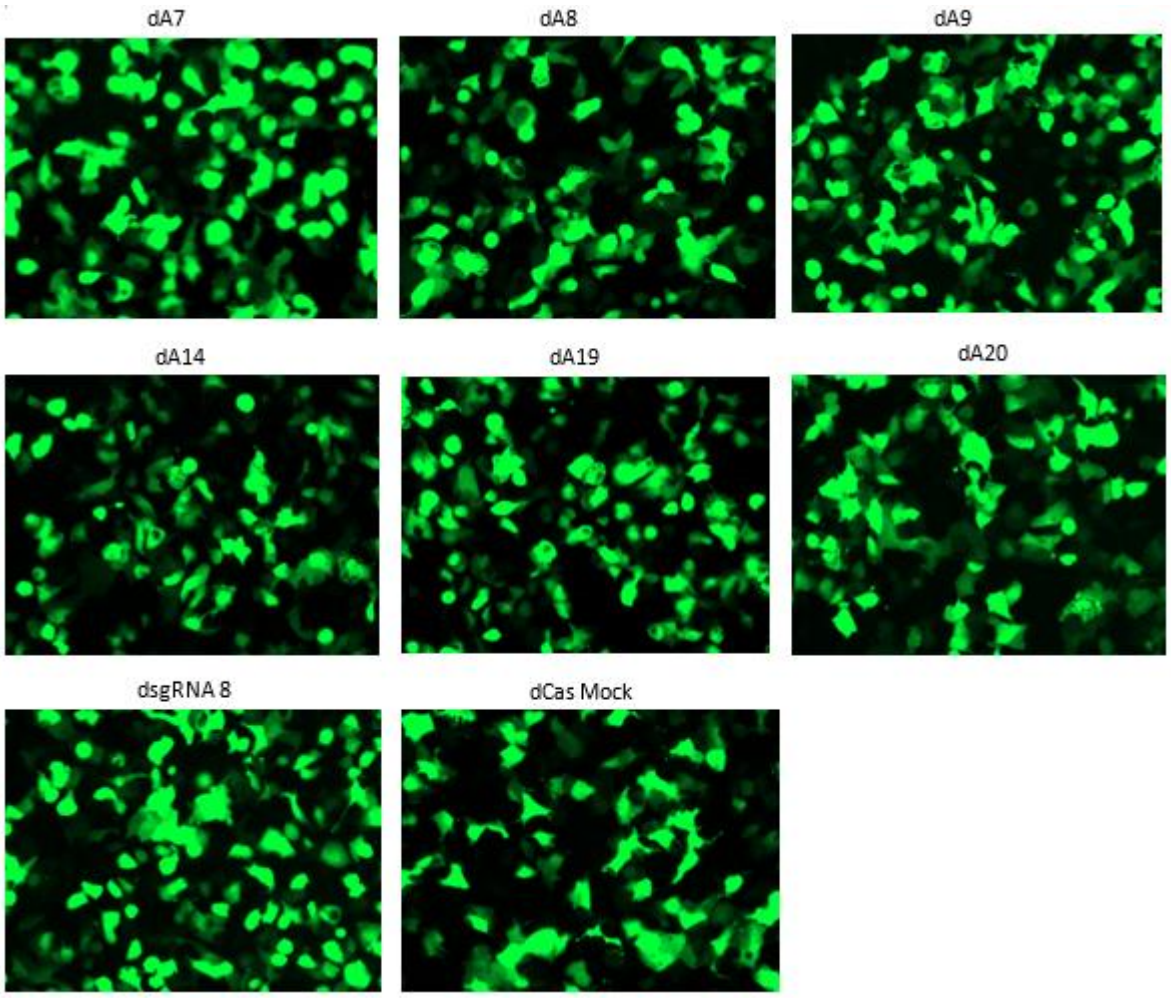


Figure 5.4: Transfection efficiency of pSaCas9-plasmids in Huh7 cells

Assessment of transfection efficiency in Huh7 cells transfected with pdSaCas9-sgRNA plasmids using the pCMV-GFP plasmid. Fluorescence microscopy was used at 20× magnification.

5.7.4 HepG2.2.15 transfection efficiency for surveyor assay

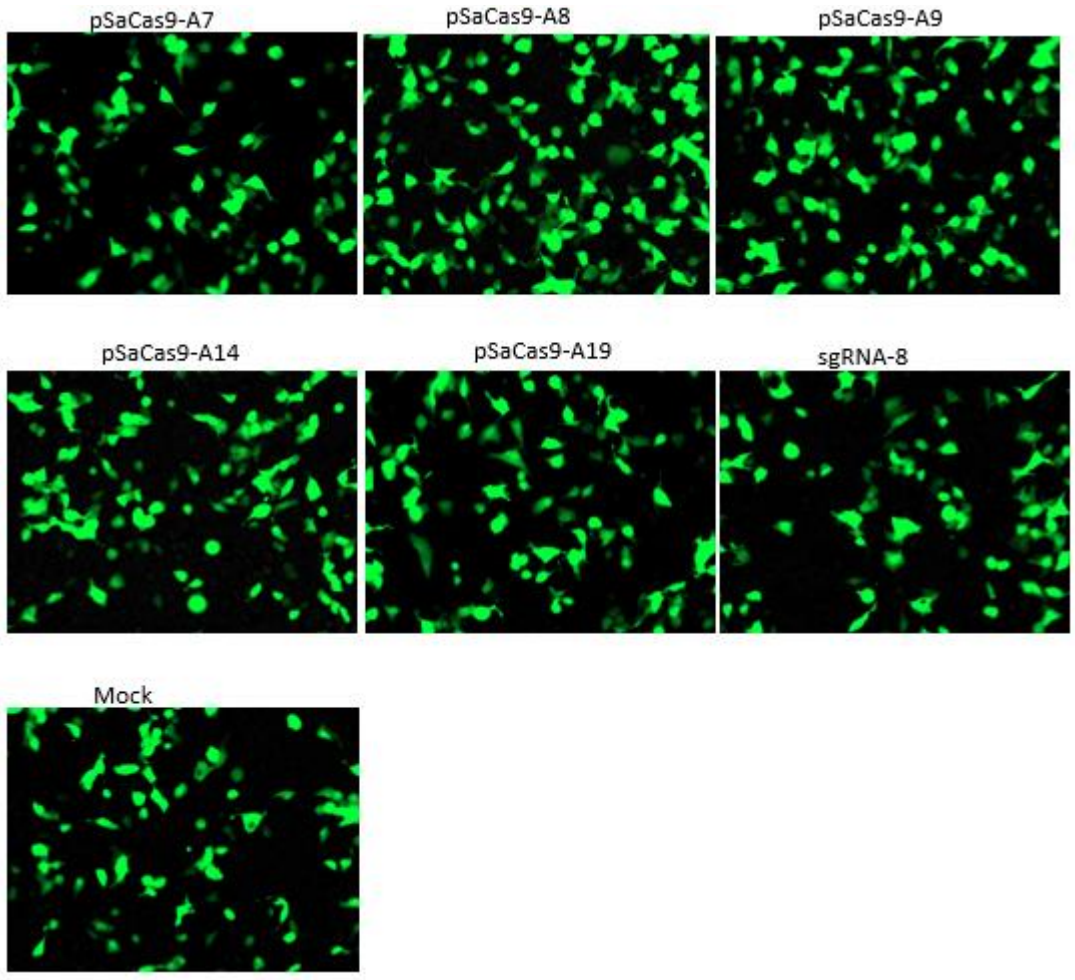


Figure 5.5: Transfection efficiency of pSaCas9-plasmids in HepG2.2.15 cells

Assessment of transfection efficiency for *in vitro* assays was evaluated using the pCMV-GFP plasmid. Fluorescence microscopy was used at 20× magnification.

5.8 PCR amplification for Surveyor assays

5.8.1 PCR amplification of HepG2.2.15 transfected cells for targeted disruption

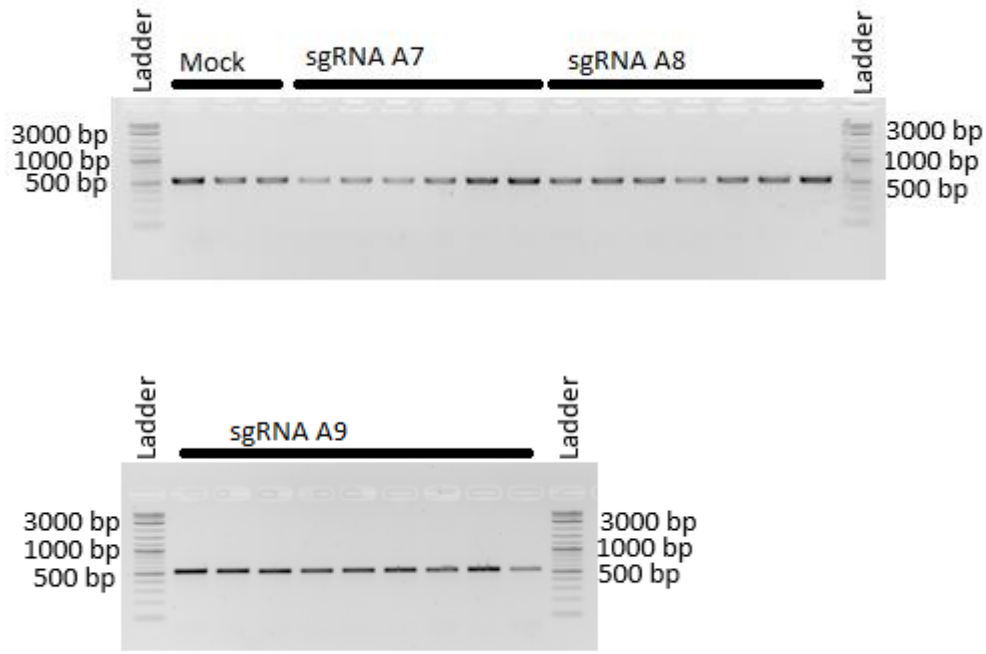


Figure 5.6: PCR amplification of the sgRNA target sites

PCR amplification of the target sites used to determine targeted disruption of each newly designed sgRNA. PCR amplicons were approximately 600 bp.

5.8.2 PCR amplification of HepG2.2.15 transfected cells to test possible self-cleavage of plasmid DNA

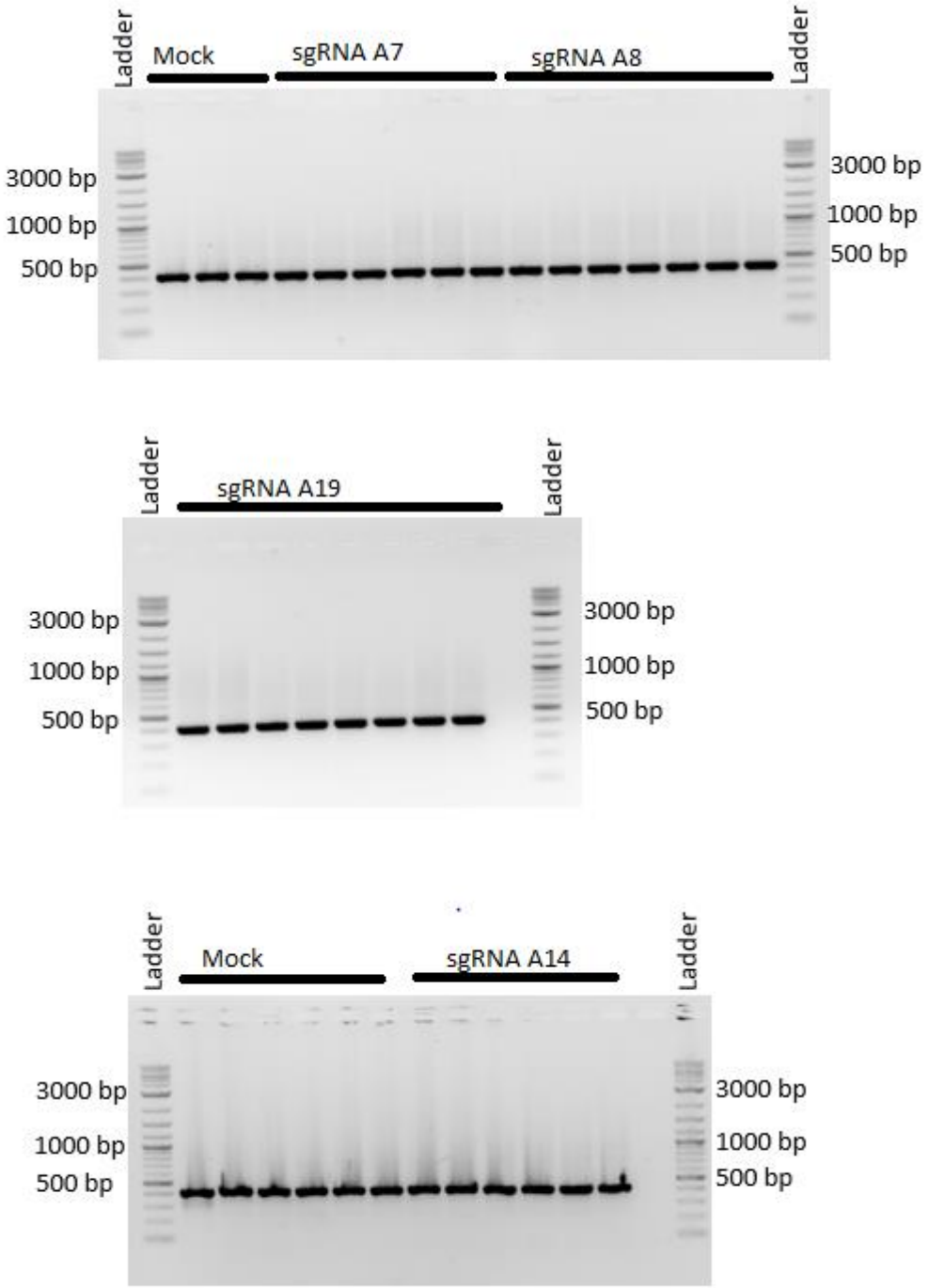


Figure 5.7: PCR amplification of sgRNA target sites from HepG2.2.15 transfections

HepG2.2.15 cells were transfected with pSaCas9-sgRNA plasmids in triplicate. Total DNA from the transfected cells were extracted and amplified. The PCR amplicons were approximately 400 bp.

5.9 Ethics certificate

UNIVERSITY OF THE WITWATERSRAND, JOHANNESBURG

HUMAN RESEARCH ETHICS COMMITTEE (MEDICAL

Human Research Ethics Committee (Medical)

Research Office Secretariat:
Faculty of Health Sciences, Phillip Tobias Building, 3rd Floor, Office 301/2/4, 29 Princess of Wales Terrace, Parktown, 2193
Tel +27 (0)11-717-1252 /1234/2656/2700
Private Bag 3, Wits 2050
Office email: HREC-Medical.ResearchOffice@wits.ac.za
Website: www.wits.ac.za/research/about-our-research/ethics-and-research-integrity/

Ref: W-CBP-190927-1 27/09/2019

TO WHOM IT MAY CONCERN:

Waiver: This certifies that the following research does not require clearance from the Human Research Ethics Committee (Medical)

Investigator: Bongiwe Sibiya et al (Student number: 1430582)

Supervisor: Abdullah Ely

Department: Molecular Medicine and Haematology

Project title: Adapting the Bacterial CRISPR/cas9 gene editing system to target the core promoter and enhancer sequences of the hepatitis B virus

Reason: *in vitro* lab study. Information used will be in the public domain.

Doctor CB Penny

Chairperson: Human Research Ethics Committee (Medical)

Copy – HREC (Medical) Secretariat: Rhulani Mkansi and Zanele Ndlovu.

REFERENCES

ABDUL, F., FILLETON, F., GEROSSIER, L., PATUREL, A., HALL, J., STRUBIN, M. & ETIENNE, L. 2018. Smc5/6 antagonism by HBx is an evolutionarily conserved function of hepatitis B virus infection in mammals. *Journal of virology,* 92**,** e00769-18.

ANTONUCCI, T. K. & RUTTER, W. J. 1989. Hepatitis B virus (HBV) promoters are regulated by the HBV enhancer in a tissue-specific manner. *Journal of virology,* 63**,** 579-583.

AYOUB, W. & KEEFFE, E. 2011. current antiviral therapy of chronic hepatitis B. *Alimentary pharmacology & therapeutics,* 34**,** 1145-1158.

BARRANGOU, R., FREMAUX, C., DEVEAU, H., RICHARDS, M., BOYAVAL, P., MOINEAU, S., ROMERO, D. A. & HORVATH, P. 2007. CRISPR provides acquired resistance against viruses in prokaryotes. *Science,* 315**,** 1709-1712.

BECK, J. & NASSAL, M. 2007. Hepatitis B virus replication. *World journal of gastroenterology: WJG,* 13**,** 48.

BELFORT, M. & ROBERTS, R. J. 1997. Homing endonucleases: keeping the house in order. *Nucleic acids research,* 25**,** 3379-3388.

BELLONI, L., ALLWEISS, L., GUERRIERI, F., PEDICONI, N., VOLZ, T., POLLICINO, T., PETERSEN, J., RAIMONDO, G., DANDRI, M. & LEVRERO, M. 2012. IFN-α inhibits HBV transcription and replication in cell culture and in humanized mice by targeting the epigenetic regulation of the nuclear cccDNA minichromosome. *The Journal of clinical investigation,* 122**,** 529-537.

BERRIDGE, M. V., HERST, P. M. & TAN, A. S. 2005. Tetrazolium dyes as tools in cell biology: new insights into their cellular reduction. *Biotechnology annual review,* 11**,** 127-152.

BLOOM, K., ELY, A., MUSSOLINO, C., CATHOMEN, T. & ARBUTHNOT, P. 2013. Inactivation of hepatitis B virus replication in cultured cells and in vivo with engineered transcription activator-like effector nucleases. *Molecular Therapy,* 21**,** 1889-1897.

BLOOM, K., KALDINE, H., CATHOMEN, T., MUSSOLINO, C., ELY, A. & ARBUTHNOT, P. 2019. Inhibition of replication of hepatitis B virus using transcriptional repressors that target the viral DNA. *BMC infectious diseases,* 19**,** 1-10.

BLOOM, K., MUSSOLINO, C. & ARBUTHNOT, P. 2015. Transcription activator-like effector (TALE) nucleases and repressor TALEs for antiviral gene therapy. *Current Stem Cell Reports,* 1**,** 1-8.

BOCH, J., SCHOLZE, H., SCHORNACK, S., LANDGRAF, A., HAHN, S., KAY, S., LAHAYE, T., NICKSTADT, A. & BONAS, U. 2009. Breaking the code of DNA binding specificity of TAL-type III effectors. *Science,* 326**,** 1509-1512.

BOCK, C.-T., SCHRANZ, P., SCHRÖDER, C. H. & ZENTGRAF, H. 1994. Hepatitis B virus genome is organized into nucleosomes in the nucleus of the infected cell. *Virus genes,* 8**,** 215-229.

CHEN, C.-C., SUN, C.-P., MA, H.-I., FANG, C.-C., WU, P.-Y., XIAO, X. & TAO, M.-H. 2009. Comparative study of anti-hepatitis B virus RNA interference by double-stranded adeno-associated virus serotypes 7, 8, and 9. *Molecular Therapy,* 17**,** 352-359.

CHEUNG, P. & LAU, P. 2005. Epigenetic regulation by histone methylation and histone variants. *Molecular Endocrinology,* 19**,** 563-573.

CHEVALIER, B. S. & STODDARD, B. L. 2001. Homing endonucleases: structural and functional insight into the catalysts of intron/intein mobility. *Nucleic acids research,* 29**,** 3757-3774.

CHISARI, F., PINKERT, C., MILICH, D., FILIPPI, P., MCLACHLAN, A., PALMITER, R. & BRINSTER, R. 1985. A transgenic mouse model of the chronic hepatitis B surface antigen carrier state. *Science,* 230**,** 1157-1160.

CHRISTIAN, M., CERMAK, T., DOYLE, E. L., SCHMIDT, C., ZHANG, F., HUMMEL, A., BOGDANOVE, A. J. & VOYTAS, D. F. 2010. Targeting DNA double-strand breaks with TAL effector nucleases. *Genetics,* 186**,** 757-761.

CLARK, D. N. & HU, J. 2015. Hepatitis B virus reverse transcriptase–Target of current antiviral therapy and future drug development. *Antiviral research,* 123**,** 132-137.

CONG, L., RAN, F. A., COX, D., LIN, S., BARRETTO, R., HABIB, N., HSU, P. D., WU, X., JIANG, W. & MARRAFFINI, L. A. 2013. Multiplex genome engineering using CRISPR/Cas systems. *Science,* 339**,** 819-823.

CRADICK, T. J., KECK, K., BRADSHAW, S., JAMIESON, A. C. & MCCAFFREY, A. P. 2010. Zinc-finger nucleases as a novel therapeutic strategy for targeting hepatitis B virus DNAs. *Molecular Therapy,* 18**,** 947-954.

CUMMINGS, I. W., BROWNE, J. K., SALSER, W. A., TYLER, G. V., SNYDER, R. L., SMOLEC, J. M. & SUMMERS, J. 1980. Isolation, characterization, and comparison of recombinant DNAs derived from genomes of human hepatitis B virus and woodchuck hepatitis virus. *Proceedings of the National Academy of Sciences,* 77**,** 1842-1846.

DANDRI, M., VOLZ, T., LÜTGEHETMANN, M. & PETERSEN, J. 2005. Animal models for the study of HBV replication and its variants. *Journal of clinical virology,* 34**,** S54-S62.

DECORSIÈRE, A., MUELLER, H., VAN BREUGEL, P. C., ABDUL, F., GEROSSIER, L., BERAN, R. K., LIVINGSTON, C. M., NIU, C., FLETCHER, S. P. & HANTZ, O. 2016. Hepatitis B virus X protein identifies the Smc5/6 complex as a host restriction factor. *Nature,* 531**,** 386-380.

DONG, C., QU, L., WANG, H., WEI, L., DONG, Y. & XIONG, S. 2015. Targeting hepatitis B virus cccDNA by CRISPR/Cas9 nuclease efficiently inhibits viral replication. *Antiviral research,* 118**,** 110-117.

DUDÁŠ, A. & CHOVANEC, M. 2004. DNA double-strand break repair by homologous recombination. *Mutation Research/Reviews in Mutation Research,* 566**,** 131-167.

EHRKE-SCHULZ, E., BERGMANN, T., SCHIWON, M., DOERNER, J., SAYDAMINOVA, K., LIEBER, A. & EHRHARDT, A. 2016. Quantification of designer nuclease induced mutation rates: a direct comparison of different methods. *Molecular Therapy-Methods & Clinical Development,* 3**,** 16047.

GRIMM, D., THIMME, R. & BLUM, H. E. 2011. HBV life cycle and novel drug targets. *Hepatology international,* 5**,** 644-653.

HEALTH, N. I. O. 2017. Livertox: clinical and research information on drug-induced liver injury. *Nih. gov https://livertox. nih. gov*.

HUANG, J. F., GUO, Y. J., ZHAO, C. X., YUAN, S. X., WANG, Y., TANG, G. N., ZHOU, W. P. & SUN, S. H. 2013. Hepatitis B virus X protein (HBx)-related long noncoding RNA (lncRNA) down-regulated expression by HBx (Dreh) inhibits hepatocellular carcinoma metastasis by targeting the intermediate filament protein vimentin. *Hepatology,* 57**,** 1882-1892.

IBRAHEEM, D., ELAISSARI, A. & FESSI, H. 2014. Gene therapy and DNA delivery systems. *International journal of pharmaceutics,* 459**,** 70-83.

JEAN-JEAN, O., LEVRERO, M., HANS, W., PERRICAUDET, M. & ROSSIGNOL, J.-M. 1989. Expression mechanism of the hepatitis B virus (HBV) C gene and biosynthesis of HBe antigen. *Virology,* 170**,** 99-106.

JIANG, C., MEI, M., LI, B., ZHU, X., ZU, W., TIAN, Y., WANG, Q., GUO, Y., DONG, Y. & TAN, X. 2017. A non-viral CRISPR/Cas9 delivery system for therapeutically targeting HBV DNA and pcsk9 in vivo. *Cell research,* 27**,** 440-443.

JINEK, M., JIANG, F., TAYLOR, D. W., STERNBERG, S. H., KAYA, E., MA, E., ANDERS, C., HAUER, M., ZHOU, K. & LIN, S. 2014. Structures of Cas9 endonucleases reveal RNA-mediated conformational activation. *Science,* 343**,** 1247997.

KARIMOVA, M., BESCHORNER, N., DAMMERMANN, W., CHEMNITZ, J., INDENBIRKEN, D., BOCKMANN, J.-H., GRUNDHOFF, A., LÜTH, S., BUCHHOLZ, F. & ZUR WIESCH, J. S. 2015. CRISPR/Cas9 nickase-mediated disruption of hepatitis B virus open reading frame S and X. *Scientific reports,* 5**,** 13734.

KATTENHORN, L. M., TIPPER, C. H., STOICA, L., GERAGHTY, D. S., WRIGHT, T. L., CLARK, K. R. & WADSWORTH, S. C. 2016. Adeno-associated virus gene therapy for liver disease. *Human gene therapy,* 27**,** 947-961.

KENNEDY, E. M., BASSIT, L. C., MUELLER, H., KORNEPATI, A. V., BOGERD, H. P., NIE, T., CHATTERJEE, P., JAVANBAKHT, H., SCHINAZI, R. F. & CULLEN, B. R. 2015. Suppression of hepatitis B virus DNA accumulation in chronically infected cells using a bacterial CRISPR/Cas RNA-guided DNA endonuclease. *Virology,* 476**,** 196-205.

KLEINSTIVER, B. P., PREW, M. S., TSAI, S. Q., NGUYEN, N. T., TOPKAR, V. V., ZHENG, Z. & JOUNG, J. K. 2015. Broadening Staphylococcus aureus Cas9 targeting range by modifying PAM recognition. *Nature biotechnology,* 33**,** 1293.

KOSTYUSHEV, D., BREZGIN, S., KOSTYUSHEVA, A., ZARIFYAN, D., GOPTAR, I. & CHULANOV, V. 2019. Orthologous CRISPR/Cas9 systems for specific and efficient degradation of covalently closed circular DNA of hepatitis B virus. *Cellular and Molecular Life Sciences,* 76**,** 1779-1794.

KOTTERMAN, M. A. & SCHAFFER, D. V. 2014. Engineering adeno-associated viruses for clinical gene therapy. *Nature Reviews Genetics,* 15**,** 445-451.

KRAMVIS, A., ARAKAWA, K., YU, M. C., NOGUEIRA, R., STRAM, D. O. & KEW, M. C. 2008. Relationship of serological subtype, basic core promoter and precore mutations to genotypes/subgenotypes of hepatitis B virus. *Journal of medical virology,* 80**,** 27-46.

KRAMVIS, A., KEW, M. & FRANÇOIS, G. 2005. Hepatitis B virus genotypes. *Vaccine,* 23**,** 2409-2423.

KRAMVIS, A. & PARASKEVIS, D. 2013. Subgenotype A1 of HBV–tracing human migrations in and out of Africa. *Antivir Ther,* 18**,** 513-21.

LEVRERO, M., POLLICINO, T., PETERSEN, J., BELLONI, L., RAIMONDO, G. & DANDRI, M. 2009. Control of cccDNA function in hepatitis B virus infection. *Journal of hepatology,* 51**,** 581-592.

LI, H., MURPHY, S. L., GILES-DAVIS, W., EDMONSON, S., XIANG, Z., LI, Y., LASARO, M. O., HIGH, K. A. & ERTL, H. C. 2007. Pre-existing AAV capsid-specific CD8+ T cells are unable to eliminate AAV-transduced hepatocytes. *Molecular Therapy,* 15**,** 792-800.

LI, H., SHENG, C., LIU, H., WANG, S., ZHAO, J., YANG, L., JIA, L., LI, P., WANG, L. & XIE, J. 2018. Inhibition of HBV expression in HBV transgenic mice using AAV-delivered CRISPR-SaCas9. *Frontiers in immunology,* 9**,** 2080.

LI, H., SHENG, C., WANG, S., YANG, L., LIANG, Y., HUANG, Y., LIU, H., LI, P., YANG, C. & YANG, X. 2017. Removal of integrated hepatitis B virus DNA using CRISPR-Cas9. *Frontiers in cellular and infection microbiology,* 7**,** 91.

LIANG, F., HAN, M., ROMANIENKO, P. J. & JASIN, M. 1998. Homology-directed repair is a major double-strand break repair pathway in mammalian cells. *Proceedings of the National Academy of Sciences,* 95**,** 5172-5177.

LIANG, T. J. 2009. Hepatitis B: the virus and disease. *Hepatology,* 49**,** S13-S21.

LIN, S.-R., YANG, H.-C., KUO, Y.-T., LIU, C.-J., YANG, T.-Y., SUNG, K.-C., LIN, Y.-Y., WANG, H.-Y., WANG, C.-C. & SHEN, Y.-C. 2014. The CRISPR/Cas9 system facilitates clearance of the intrahepatic HBV templates in vivo. *Molecular Therapy-Nucleic Acids,* 3**,** e186.

LIU, Y., ZHAO, M., GONG, M., XU, Y., XIE, C., DENG, H., LI, X., WU, H. & WANG, Z. 2018. Inhibition of hepatitis B virus replication via HBV DNA cleavage by Cas9 from Staphylococcus aureus. *Antiviral research,* 152**,** 58-67.

LOK, A. S., ZOULIM, F., DUSHEIKO, G. & GHANY, M. G. 2017. Hepatitis B cure: from discovery to regulatory approval. *Journal of hepatology,* 67**,** 847-861.

LUCIFORA, J. & PROTZER, U. 2016. Attacking hepatitis B virus cccDNA–The holy grail to hepatitis B cure. *Journal of hepatology,* 64**,** S41-S48.

MAKAROVA, K. S., HAFT, D. H., BARRANGOU, R., BROUNS, S. J., CHARPENTIER, E., HORVATH, P., MOINEAU, S., MOJICA, F. J., WOLF, Y. I., YAKUNIN, A. F., VAN DER OOST, J. & KOONIN, E. V. 2011. Evolution and classification of the CRISPR–Cas systems. *Nature Reviews Microbiology,* 9**,** 467.

MALI, S. 2013. Delivery systems for gene therapy. *Indian journal of human genetics,* 19**,** 3.

MARION, P., SALAZAR, F., LIITTSCHWAGER, K., BORDIER, B., SEEGER, C., WINTERS, M., COOPER, A. & CULLEN, J. 2003. A transgenic mouse lineage useful for testing antivirals targeting hepatitis B virus. *Frontiers in Viral Hepatitis.* Elsevier.

MILLER, J., MCLACHLAN, A. & KLUG, A. 1985. Repetitive zinc-binding domains in the protein transcription factor IIIA from Xenopus oocytes. *The EMBO journal,* 4**,** 1609-1614.

MILLER, J. B., ZHANG, S., KOS, P., XIONG, H., ZHOU, K., PERELMAN, S. S., ZHU, H. & SIEGWART, D. J. 2017. Non-viral CRISPR/Cas gene editing in vitro and in vivo enabled by synthetic nanoparticle co-delivery of Cas9 mRNA and sgRNA. *Angewandte Chemie International Edition,* 56**,** 1059-1063.

MOJICA, F. J., GARCÍA-MARTÍNEZ, J. & SORIA, E. 2005. Intervening sequences of regularly spaced prokaryotic repeats derive from foreign genetic elements. *Journal of molecular evolution,* 60**,** 174-182.

MORENO-MATEOS, M. A., VEJNAR, C. E., BEAUDOIN, J.-D., FERNANDEZ, J. P., MIS, E. K., KHOKHA, M. K. & GIRALDEZ, A. J. 2015. CRISPRscan: designing highly efficient sgRNAs for CRISPR-Cas9 targeting in vivo. *Nature methods,* 12**,** 982-988.

MOWA, M. B., CROWTHER, C., ELY, A. & ARBUTHNOT, P. 2014. Inhibition of hepatitis B virus replication by helper dependent adenoviral vectors expressing artificial anti-HBV pri-miRs from a liver-specific promoter. *BioMed research international,* 2014.

MURPHY, C. M., XU, Y., LI, F., NIO, K., RESZKA-BLANCO, N., LI, X., WU, Y., YU, Y., XIONG, Y. & SU, L. 2016. Hepatitis B virus X protein promotes degradation of SMC5/6 to enhance HBV replication. *Cell reports,* 16**,** 2846-2854.

MURRAY, K., BRUCE, S., HINNEN, A., WINGFIELD, P., VAN ERD, P., DE REUS, A. & SCHELLEKENS, H. 1984. Hepatitis B virus antigens made in microbial cells immunise against viral infection. *The EMBO journal,* 3**,** 645-650.

NASSAL, M., JUNKER-NIEPMANN, M. & SCHALLER, H. 1990. Translational inactivation of RNA function: discrimination against a subset of genomic transcripts during HBV nucleocapsid assembly. *Cell,* 63**,** 1357-1363.

NISHIMASU, H., CONG, L., YAN, W. X., RAN, F. A., ZETSCHE, B., LI, Y., KURABAYASHI, A., ISHITANI, R., ZHANG, F. & NUREKI, O. 2015. Crystal structure of Staphylococcus aureus Cas9. *Cell,* 162**,** 1113-1126.

NOWSHEEN, S. & YANG, E. 2012. The intersection between DNA damage response and cell death pathways. *Experimental oncology,* 34**,** 243.

OLEYKOWSKI, C. A., BRONSON MULLINS, C. R., GODWIN, A. K. & YEUNG, A. T. 1998. Mutation detection using a novel plant endonuclease. *Nucleic acids research,* 26**,** 4597-4602.

PASSMAN, M., WEINBERG, M., KEW, M. & ARBUTHNOT, P. 2000. In situ demonstration of inhibitory effects of hammerhead ribozymes that are targeted to the hepatitis Bx sequence in cultured cells. *Biochemical and biophysical research communications,* 268**,** 728-733.

PAUDEL, D. & SUVEDI, S. 2019. Hepatitis B Genotyping and Clinical Implication. *Hepatitis B and C.* IntechOpen.

POURCEL, C., SALVIGNOL, G. & VERGNAUD, G. 2005. CRISPR elements in Yersinia pestis acquire new repeats by preferential uptake of bacteriophage DNA, and provide additional tools for evolutionary studies. *Microbiology,* 151**,** 653-663.

RAMANAN, V., SHLOMAI, A., COX, D. B., SCHWARTZ, R. E., MICHAILIDIS, E., BHATTA, A., SCOTT, D. A., ZHANG, F., RICE, C. M. & BHATIA, S. N. 2015. CRISPR/Cas9 cleavage of viral DNA efficiently suppresses hepatitis B virus. *Scientific reports,* 5**,** 10833.

RAN, F. A., HSU, P. D., WRIGHT, J., AGARWALA, V., SCOTT, D. A. & ZHANG, F. 2013. Genome engineering using the CRISPR-Cas9 system. *Nature protocols,* 8**,** 2281.

REVILL, P. A., CHISARI, F. V., BLOCK, J. M., DANDRI, M., GEHRING, A. J., GUO, H., HU, J., KRAMVIS, A., LAMPERTICO, P., JANSSEN, H. L., LEVRERO, M., LI, W., LIANG, J. T., LIM, S., LU, F., PENICAUD, C. M., TRAVIS, J. E. & THIMME, R. 2019. A global scientific strategy to cure hepatitis B. *The Lancet Gastroenterology & Hepatology,* 4**,** 545-558.

ROTHE, M., RITTELMEYER, I., IKEN, M., RÜDRICH, U., SCHAMBACH, A., GLAGE, S., MANNS, M., BAUM, C., BOCK, M., OTT, M. & MODLICH, U. 2012. Epidermal growth factor improves lentivirus vector gene transfer into primary mouse hepatocytes. *Gene therapy,* 19**,** 425-434.

SARAVOLATZ, L. D., BHATTACHARYA, D. & THIO, C. L. 2010. Review of Hepatitis B Therapeutics. *Clinical Infectious Diseases,* 51**,** 1201-1208.

SCHAEFER, S. 2007. Hepatitis B virus taxonomy and hepatitis B virus genotypes. *World journal of gastroenterology: WJG,* 13**,** 14.

SCHIFFER, J. T., AUBERT, M., WEBER, N. D., MINTZER, E., STONE, D. & JEROME, K. R. 2012. Targeted DNA mutagenesis for the cure of chronic viral infections. *Journal of virology,* 86**,** 8920-8936.

SCHIWON, M., EHRKE-SCHULZ, E., OSWALD, A., BERGMANN, T., MICHLER, T., PROTZER, U. & EHRHARDT, A. 2018. One-vector system for multiplexed CRISPR/Cas9 against hepatitis B virus cccDNA utilizing high-capacity adenoviral vectors. *Molecular Therapy-Nucleic Acids,* 12**,** 242-253.

SCHWEITZER, A., HORN, J., MIKOLAJCZYK, R. T., KRAUSE, G. & OTT, J. J. 2015. Estimations of worldwide prevalence of chronic hepatitis B virus infection: a systematic review of data published between 1965 and 2013. *The Lancet,* 386**,** 1546-1555.

SCOTT, T., MOYO, B., NICHOLSON, S., MAEPA, M. B., WATASHI, K., ELY, A., WEINBERG, M. S. & ARBUTHNOT, P. 2017. ssAAVs containing cassettes encoding SaCas9 and guides targeting hepatitis B virus inactivate replication of the virus in cultured cells. *Scientific reports,* 7**,** 1-11.

SEEGER, C. & MASON, W. S. 2000. Hepatitis B virus biology. *Microbiol. Mol. Biol. Rev.,* 64**,** 51-68.

SEEGER, C. & SOHN, J. A. 2014. Targeting hepatitis B virus with CRISPR/Cas9. *Molecular Therapy-Nucleic Acids,* 3**,** e216.

SENTMANAT, M. F., PETERS, S. T., FLORIAN, C. P., CONNELLY, J. P. & PRUETT-MILLER, S. M. 2018. A survey of validation strategies for CRISPR-Cas9 editing. *Scientific reports,* 8**,** 1-8.

SHAUL, Y., RUTTER, W. & LAUB, O. 1985. A human hepatitis B viral enhancer element. *The EMBO Journal,* 4**,** 427-430.

SHEPARD, C. W., SIMARD, E. P., FINELLI, L., FIORE, A. E. & BELL, B. P. 2006. Hepatitis B Virus Infection: Epidemiology and Vaccination. *Epidemiologic Reviews,* 28**,** 112-125.

SHIH, C., BURKE, K., CHOU, M., ZELDIS, J., YANG, C.-S., LEE, C.-S., ISSELBACHER, K., WANDS, J. & GOODMAN, H. 1987. Tight clustering of human hepatitis B virus integration sites in hepatomas near a triple-stranded region. *Journal of virology,* 61**,** 3491-3498.

SILVA, G., POIROT, L., GALETTO, R., SMITH, J., MONTOYA, G., DUCHATEAU, P. & PÂQUES, F. 2011. Meganucleases and other tools for targeted genome engineering: perspectives and challenges for gene therapy. *Current gene therapy,* 11**,** 11-27.

SMITH, S., HARMANCI, H., HUTIN, Y., HESS, S., BULTERYS, M., PECK, R., REWARI, B., MOZALEVSKIS, A., SHIBESHI, M. & MUMBA, M. 2019. Global progress on the elimination of viral hepatitis as a major public health threat: An analysis of WHO Member State responses 2017. *JHEP Reports*.

SONODA, E., HOCHEGGER, H., SABERI, A., TANIGUCHI, Y. & TAKEDA, S. 2006. Differential usage of non-homologous end-joining and homologous recombination in double strand break repair. *DNA repair,* 5**,** 1021-1029.

SPEARMAN, C. & SONDERUP, M. W. 2014. Preventing hepatitis B and hepatocellular carcinoma in South Africa: The case for a birth-dose vaccine. *SAMJ: South African Medical Journal,* 104**,** 610-612.

STANAWAY, J. D., FLAXMAN, A. D., NAGHAVI, M., FITZMAURICE, C., VOS, T., ABUBAKAR, I., ABU-RADDAD, L. J., ASSADI, R., BHALA, N., COWIE, B., FOROUZANFOUR, M. H., GROEGER, J., HANAFIAH, K. M., JACOBSEN, K. H., JAMES, S. L., MACLACHLAN, J., MALEKZADEH, R., MARTIN, N. K. & COOKE, G. S. 2016. The global burden of viral hepatitis from 1990 to 2013: findings from the Global Burden of Disease Study 2013. *The Lancet,* 388**,** 1081-1088.

STODDARD, B. L. 2011. Homing endonucleases: from microbial genetic invaders to reagents for targeted DNA modification. *Structure,* 19**,** 7-15.

STONE, D., NIYONZIMA, N. & JEROME, K. R. 2016. Genome editing and the next generation of antiviral therapy. *Human genetics,* 135**,** 1071-1082.

TAKATA, M., SASAKI, M. S., SONODA, E., MORRISON, C., HASHIMOTO, M., UTSUMI, H., YAMAGUCHI-IWAI, Y., SHINOHARA, A. & TAKEDA, S. 1998. Homologous recombination and non-homologous end-joining pathways of DNA double-strand break repair have overlapping roles in the maintenance of chromosomal integrity in vertebrate cells. *The EMBO journal,* 17**,** 5497-5508.

TERRAULT, N. A. 2009. Benefits and risks of combination therapy for hepatitis B. *Hepatology,* 49**,** S122-S128.

TILL, B. J., BURTNER, C., COMAI, L. & HENIKOFF, S. 2004. Mismatch cleavage by single-strand specific nucleases. *Nucleic acids research,* 32**,** 2632-2641.

TRANSY, C., FOUREL, G., ROBINSON, W. S., TIOLLAIS, P., MARION, P. L. & BUENDIA, M.-A. 1992. Frequent amplification of c-myc in ground squirrel liver tumors associated with past or ongoing infection with a hepadnavirus. *Proceedings of the National Academy of Sciences,* 89**,** 3874-3878.

URNOV, F. D., MILLER, J. C., LEE, Y.-L., BEAUSEJOUR, C. M., ROCK, J. M., AUGUSTUS, S., JAMIESON, A. C., PORTEUS, M. H., GREGORY, P. D. & HOLMES, M. C. 2005. Highly efficient endogenous human gene correction using designed zinc-finger nucleases. *Nature,* 435**,** 646-651.

VITIELLO, A., ISHIOKA, G., GREY, H. M., ROSE, R., FARNESS, P., LAFOND, R., YUAN, L., CHISARI, F. V., FURZE, J. & BARTHOLOMEUZ, R. 1995. Development of a lipopeptide-based therapeutic vaccine to treat chronic HBV infection. I. Induction of a primary cytotoxic T lymphocyte response in humans. *The Journal of clinical investigation,* 95**,** 341-349.

WADE, M. 2015. High-throughput silencing using the CRISPR-Cas9 system: a review of the benefits and challenges. *Journal of biomolecular screening,* 20**,** 1027-1039.

WANG, J., XU, Z.-W., LIU, S., ZHANG, R.-Y., DING, S.-L., XIE, X.-M., LONG, L., CHEN, X.-M., ZHUANG, H. & LU, F.-M. 2015. Dual gRNAs guided CRISPR/Cas9 system inhibits hepatitis B virus replication. *World journal of gastroenterology: WJG,* 21**,** 9554.

WANG, T., WEI, J. J., SABATINI, D. M. & LANDER, E. S. 2014. Genetic screens in human cells using the CRISPR-Cas9 system. *Science,* 343**,** 80-84.

WETERINGS, E. & CHEN, D. J. 2008. The endless tale of non-homologous end-joining. *Cell research,* 18**,** 114-124.

WHO 2017. *Global hepatitis report 2017,* World Health Organization.

WIELAND, S. F., EUSTAQUIO, A., WHITTEN-BAUER, C., BOYD, B. & CHISARI, F. V. 2005. Interferon prevents formation of replication-competent hepatitis B virus RNA-containing nucleocapsids. *Proceedings of the National Academy of Sciences,* 102**,** 9913-9917.

WU, X., KRIZ, A. J. & SHARP, P. A. 2014. Target specificity of the CRISPR-Cas9 system. *Quantitative biology,* 2**,** 59-70.

XU, H., XIAO, T., CHEN, C.-H., LI, W., MEYER, C. A., WU, Q., WU, D., CONG, L., ZHANG, F. & LIU, J. S. 2015. Sequence determinants of improved CRISPR sgRNA design. *Genome research,* 25**,** 1147-1157.

YANG, H.-C. & CHEN, P.-J. 2018. The potential and challenges of CRISPR-Cas in eradication of hepatitis B virus covalently closed circular DNA. *Virus research,* 244**,** 304-310.

YANG, H.-C. & KAO, J.-H. 2014. Persistence of hepatitis B virus covalently closed circular DNA in hepatocytes: molecular mechanisms and clinical significance. *Emerging microbes & infections,* 3**,** 1-7.

ZHANG, X.-H., TEE, L. Y., WANG, X.-G., HUANG, Q.-S. & YANG, S.-H. 2015. Off-target effects in CRISPR/Cas9-mediated genome engineering. *Molecular Therapy-Nucleic Acids,* 4**,** e264.

ZHAO, C., SHU, X. & SUN, B. 2017. Construction of a gene knockdown system based on catalytically inactive ("dead") Cas9 (dCas9) in Staphylococcus aureus. *Appl. Environ. Microbiol.,* 83**,** e00291-17.

ZHEN, S., HUA, L., LIU, Y., GAO, L., FU, J., WAN, D., DONG, L., SONG, H. & GAO, X. 2015. Harnessing the clustered regularly interspaced short palindromic repeat (CRISPR)/CRISPR-associated Cas9 system to disrupt the hepatitis B virus. *Gene therapy,* 22**,** 404-412.

ZOULIM, F. & LOCARNINI, S. 2009. Hepatitis B virus resistance to nucleos (t) ide analogues. *Gastroenterology,* 137**,** 1593-1608. e2.

ZOULIM, F. & PERRILLO, R. 2008. Hepatitis B: reflections on the current approach to antiviral therapy. *Journal of hepatology,* 48**,** S2-S19.